

REPORT DOCUMENTATION P.

AD-A261 687

1188

Public reporting burden for this collection of information is estimated to average 1 hour per gathering and maintaining the data needed, and completing and reviewing the collection of collection of information, including suggestions for reducing this burden, to Washington, DC, Davis Highway, Suite 1204, Arlington, VA 22202-4302, and to the Office of Management and



ing data sources
per aspect of this
1215 Jefferson
03

1. AGENCY USE ONLY (Leave blank) 2. REPORT DATE January 1993 3. REPORT TYPE AND DATES COVERED Final Report 9/15/88 - 11/14/92

4. TITLE AND SUBTITLE Electrochemical and Spectroscopic Studies of Molten Halides 5. FUNDING NUMBERS

6. AUTHOR(S) Gleb Mamantov 61102F 2303 AS

7. PERFORMING ORGANIZATION NAME(S) AND ADDRESS(ES) Univ of Tennessee 404 Andy Holt Tower Knoxville, TN 37996-0140 8. PERFORMING ORGANIZATION REPORT NUMBER AFOSR-TR-93 0-01

9. SPONSORING / MONITORING AGENCY NAME(S) AND ADDRESS(ES) AFOSR/NC Building 410, Bolling AFB DC 20332-6448 10. SPONSORING / MONITORING AGENCY REPORT NUMBER AFOSR-88-0307

11. SUPPLEMENTARY NOTES

12a. DISTRIBUTION / AVAILABILITY STATEMENT APPROVED FOR PUBLIC RELEASE; DISTRIBUTION IS UNLIMITED. 12b. DISTRIBUTION CODE

13. ABSTRACT (Maximum 200 words) See Attached

93-04810
 160PX

14. SUBJECT TERMS 15. NUMBER OF PAGES 74 16. PRICE CODE

17. SECURITY CLASSIFICATION OF REPORT UNCLASSIFIED 18. SECURITY CLASSIFICATION OF THIS PAGE UNCLASSIFIED 19. SECURITY CLASSIFICATION OF ABSTRACT UNCLASSIFIED 20. LIMITATION OF ABSTRACT

13. This program deals with chemistry and electrochemistry in molten halides, media which are used in the production of several important elements, such as aluminum, magnesium and fluorine, in some high energy battery systems, as well as in other applications. The emphasis was placed on simple and complex chlorides and fluorides, for example the LiCl-KCl eutectic, the LiF-NaF-KF eutectic (FLINAK), alkali metal and organic tetrachloroaluminates, and cryolite. Pure fluorides usually have high melting points, for example cryolite, Na_3AlF_6 , melts at 1000°C compared to NaAlCl_4 which melts at 156°C . The use of molten mixtures of fluorides and chlorides can result in solute chemistry which is quite different from that observed in pure chlorides. One complication which cannot be entirely avoided is caused by atmospheric contaminants. Even the parent alkali chloroaluminates contain millimolar quantities of complexed oxide which may result from the interaction of some melts with Pyrex glass. Therefore, studies of solute species at typical electrochemical or spectroscopic concentrations should take into account the presence of oxide species wherever possible.

The electrochemistry and metallurgy of the transition metals of groups IV-B, V-B, and VI-B (the refractory metals) are important to the aerospace industry and in the construction of electrical and electronic devices. Studies of refractory metals were performed in alkali chloroaluminates. Specifically, the reduction of tantalum (V), niobium (V), and tungsten(VI), in acidic (AlCl_3 -rich) alkali chloroaluminates show that low oxidation state cluster species, such as $\text{Ta}_6\text{Cl}_{14}$ and W_6Cl_{12} , are formed which, due to high stability and/or insolubility in the melt, prevent further reduction to the metal. Although the cluster species may not be stable in basic (usually AlCl_3 - NaCl_{sat}) melts, problems can arise because of small amounts of oxide-containing species. Fluoride-containing chloroaluminate melts are a possible compromise between the use of fluoride melts, which require somewhat severe conditions, and low-temperature chloroaluminate melts. Raman spectroscopic studies of chloroaluminate melts containing varied amounts of fluoride indicated the existence of fluorochloroaluminate species of the form $\text{AlCl}_{11}\text{F}_{4-n}$ with n dependent on the ratio of fluoride to aluminum. All three refractory metals can be deposited from either basic NaAlCl_4 or in sodium fluorochloroaluminates (NAFCAL) at temperatures lower than those required for deposition from FLINAK. The phase diagram of the pseudo-binary system NaAlCl_4 -NaF has been determined using differential thermal analysis.

UV-visible, Raman and electron spin resonance (ESR) spectroelectrochemistry of chloranil reduction showed two closely spaced electron steps to the radical anion and the dianion in the acidic AlCl_3 -NaCl melts. In basic melts no IR evidence for the formation of a radical anion was obtained. Application of several spectroelectrochemistry approaches provides evidence for an intermediate which could not be detected by solely electrochemical measurements.

Ultramicroelectrodes were used to obtain useful cyclic voltammograms for the reduction of metal ions in polycrystalline NaAlCl_4 at temperatures much lower than the melting point. The advantages of ultramicroelectrodes, such as reduced IR drop and rapidly established steady states of mass transfer, were observed in these studies.

FINAL TECHNICAL REPORT

AFOSR Grant 88-0307

Department of Chemistry
University of Tennessee, Knoxville

UNCLASSIFIED

Accession For	
NTIS GFA&I	<input checked="" type="checkbox"/>
DTIC TAB	<input type="checkbox"/>
Unannounced	<input type="checkbox"/>
Justification	
By _____	
Distribution/	
Availability Codes	
Dist	Avail and/or Special
A-1	

Gleb Mamantov
Principal Investigator

January 8, 1993

Approved for public release;
distribution unlimited.

The following is a summary of research accomplishments and progress made during the period September 15, 1988 through December 31, 1992 under AFOSR Grant #88-0307.

A. List of Publications Resulting from this Grant

P. A. Flowers and G. Mamantov, "Infrared Spectroscopic and Spectroelectrochemical Investigation of Chloranil in Molten Sodium Chloroaluminates", *J. Electrochem. Soc.*, 136, 2944 (1989).

S. W. Orchard, Y. Sato, J.-P. Schoebrechts, and G. Mamantov, "The Use of Sodium Ion Conducting Glasses in Na/S(IV) Molten Chloroaluminate Electrochemical Cells", *J. Electrochem. Soc.*, 137, 2194 (1990).

G. Mamantov, L. J. Tortorelli, P. A. Flowers, B. L. Harward, D. S. Trimble, E. M. Hondrogiannis, J. E. Coffield, A. G. Edwards, and L. N. Klatt, "Investigations of Some Aspects of Chemistry in Alkali Chloroaluminate Melts", in Proceedings of the Seventh International Symposium on Molten Salts, C. L. Hussey, S. N. Flengas, J. S. Wilkes, and Y. Ito, eds., The Electrochemical Society, Inc., Pennington, NJ, 1990, pp. 794-804.

G. Mamantov, C. L. Hussey, and R. Marassi, "An Introduction to Electrochemistry in Molten Salts", in Techniques for Characterization of Electrodes and Electrochemical

Processes, R. Varma and J. R. Selman, eds., John Wiley and Sons, New York, 1991, pp. 471-513.

J. E. Coffield, S. P. Zingg, K. D. Sienerth, S. Williams, C. Lee, G. Mamantov and G. P. Smith, "Spectroscopic and Electrochemical Investigations of Selected Aromatic and Heteroaromatic Compounds in Ambient Temperature Chloroaluminate Melts", *Materials Science Forum*, 73-75, 25 (1991).

V. Taranenko, K. D. Sienerth, N. Sato, A. G. Edwards and G. Mamantov, "Studies of the Electroreduction of Tantalum and Niobium in Fluorochloroaluminate Melts", *Materials Science Forum*, 73-75, 595 (1991).

I.-Wen Sun, K. D. Sienerth, and G. Mamantov, "The Use of Phosgene for the Removal of Oxide Impurities from a Sodium Chloroaluminate Melt Saturated with Sodium Chloride", *J. Electrochem. Soc.*, 138, 2850 (1991).

J. H. von Barner, L. E. McCurry, C. A. Jorgensen, N.J. Bjerrum, and G. Mamantov, "Electrochemical and Spectroscopic Studies of Tantalum Species in NaCl-AlCl₃ Melts at 160-300°C", *Inorg. Chem.*, 31, 1034 (1992).

L. J. Tortorelli, P. A. Flowers, B. L. Harward, G. Mamantov, and L. N. Klatt, "Spectroscopic Investigations of Catalytic Iridium Carbonyl Species in Sodium Chloroaluminate Melts", *J. Organometallic Chem.*, 429, 119 (1992).

G. Mamantov, S. D. Williams, K. D. Sienerth, C. W. Lee, and J. E. Coffield, "First Observation of Electrochemiluminescence in Molten Salt Solutions", *J. Electrochem. Soc.*, 139, L58 (1992).

G. S. Chen, I. W. Sun, K. D. Sienerth, A. G. Edwards, and G. Mamantov, "Removal of Oxide Impurities from Alkali Haloaluminate Melts Using Carbon Tetrachloride", submitted to *J. Electrochem. Soc.*

G. S. Chen and G. Mamantov, "Electrochemical Studies of Tantalum in Fluorochloroaluminate Melts at 200 - 450°C", Extended Abstract, International Symposium on Molten Salt Chemistry and Technology, Meeting of the Electrochemical Society, Honolulu, Hawaii, May 16-21, 1993.

K. D. Sienerth and G. Mamantov, "Recent Studies of the Electrochemical Behavior of Nb(V) in $\text{AlCl}_3\text{-NaCl}_{\text{sat}}$ and Related Melts", Extended Abstract, International Symposium on Molten Salt Chemistry and Technology, Meeting of the Electrochemical Society, Honolulu, Hawaii, May 16-21, 1993.

I. Introduction

This program deals with chemistry and electrochemistry in molten halides, media which are used in the production of several important elements, such as aluminum, magnesium and fluorine, in some high energy battery systems, as well as in other applications. The emphasis is placed on simple and complex chlorides and fluorides; the complex ions of particular interest are the haloaluminates such as AlCl_4^- and $\text{AlCl}_n\text{F}_{4-n}^-$ ($n \leq 4$). One can illustrate the solvent media of interest with the following examples.

Simple chlorides

e.g.

LiCl-KCl eutectic

Simple fluorides

e.g.

LiF-NaF-KF eutectic

(FLINAK)

Complex chlorides,

e.g.

NaAlCl_4 or RAlCl_4

where R is an organic cation

Complex fluorides,

e.g.

Na_3AlF_6

Mixtures of chlorides and fluorides

Pure fluorides usually have high melting points; for example, cryolite, Na_3AlF_6 , melts at 1000°C compared to NaAlCl_4 which melts at 156°C . However, the use of molten mixtures of fluorides and chlorides can result in solute chemistry which is quite different from that

observed in pure chlorides. For example, tantalum cannot be plated from alkali chloroaluminates at moderate temperatures because of high stability of cluster species. On the other hand, this metal can be plated using chlorofluoroaluminates, FLINAK, or chloride baths at high temperatures.

One complication which cannot be entirely avoided is caused by atmospheric contaminants. Even the purest alkali chloroaluminates contain millimolar quantities of complexed oxide which may result from the interaction of some melts with Pyrex glass. Therefore, studies of solute species at typical electrochemical or spectroscopic concentrations should take into account the presence of oxide species wherever possible.

II. Recent Progress

A. Studies of selected refractory and platinum group metals in molten halides

The electrochemistry and metallurgy of the transition metals of Groups IV-B, V-B, and VI-B (the refractory metals) have received much attention in the last several decades due to the increasing importance of these metals in the aerospace industry and in the construction of electrical and electronic devices. In 1965, Mellors and Senderoff [1] introduced a general method for obtaining pure, coherent deposits of each of these metals, with the exception of titanium, by electrolytic reduction from the ternary eutectic LiF-NaF-KF (46.5-11.5-45.0 mole percent), or FLINAK. Senderoff and coworkers published a series of articles describing their proposed mechanisms for the reduction of several metals [2-6], and since that time, additional research has been devoted to studies of refractory metals in

molten fluorides [7-17].

Most of our studies of refractory metals until recently have been performed in alkali chloroaluminates. By comparison with FLINAK, sodium chloroaluminate ($\text{AlCl}_3\text{-NaCl}$) melts may be considered as favorable systems in several respects. First, the liquidus temperatures for chloroaluminates lie below 200°C for melt compositions in the range from 49.8 to 100 mole percent AlCl_3 , while FLINAK has a eutectic point of 454°C , and generally temperatures in excess of 750°C are required for refractory metal deposition. The Lewis melt acidity can be varied over a broad range by changing the AlCl_3 to NaCl ratio. Finally, the highly aggressive nature of fluoride melts and the temperatures required for their use greatly limit the materials which can be used for bath construction, whereas chloroaluminate studies can be conducted using even simple Pyrex cells.

Studies of the reduction of tantalum (V) [18] (see Appendix 1), niobium (V) [19], and tungsten (VI) [20], in acidic (AlCl_3 -rich) alkali chloroaluminates show that low oxidation state cluster species, such as $\text{Ta}_6\text{Cl}_{14}$ and W_6Cl_{12} , are formed which, due to high stability and/or insolubility in the melt, prevent further reduction to the metal. Although the cluster species may not be stable in basic (usually $\text{AlCl}_3\text{-NaCl}_{\text{sat}}$) melts [21], problems can arise because of small amounts of oxide-containing species [20]. This contamination by oxides, arising either from atmospheric impurities or attack of Pyrex by the melt, can be greatly reduced by passing phosgene or carbon tetrachloride through the melt [22,23; see Appendices 2 and 3].

Fluoride-containing chloroaluminate melts are a possible compromise between the use of fluoride melts, which require somewhat severe conditions, and low-temperature

chloroaluminate melts. It was felt that the inclusion of fluoride into the chloroaluminate melts may sufficiently inhibit the formation of cluster species as to allow reduction to the metal. We have performed Raman spectroscopic studies of chloroaluminate melts containing varied amounts of fluoride [24]. These investigations indicated the existence of fluorochloroaluminate species of the form $\text{AlCl}_n\text{F}_{4-n}^-$ with n dependent on the ratio of fluoride to aluminum.

Recently we have extended our studies of selected refractory metals, specifically niobium, tantalum and tungsten, to basic AlCl_3 -NaCl which has been treated with COCl_2 or CCl_4 to remove oxide impurities. The electrochemistry of these elements is being studied as a function of temperature. Also, the electrochemistry in basic chloroaluminates is being compared with that observed in sodium fluorochloroaluminates or NAFCAL. We have determined that all three elements can be deposited from either basic NaAlCl_4 or NAFCAL at temperatures lower than those required for deposition from FLINAK (600 to 650°C compared to 750°C for FLINAK). Further studies will be needed to determine the quality of the deposit (or plate). We have also conducted plating of Ta and Nb from FLINAK; the plates appear to be comparable to those reported by Senderoff and Mellors [5] although significant electrochemical differences with those of Senderoff and Mellors were observed.

Preliminary results of the electroreduction of Ta and Nb in NAFCAL are reported in Appendix 4 [25]. As stated above, further voltammetric and spectroscopic studies of Ta, Nb and W in both basic NaAlCl_4 and NAFCAL are either in progress or are being summarized. The reduction of Ta(V) to the metal in NAFCAL appears to involve as intermediate oxidation states Ta(IV) and Ta(II) [26; see Appendix 5]. The differences in

the electrochemical behavior of Nb(V) in basic $\text{AlCl}_3\text{-NaCl}$ melts treated with CCl_4 compared to that in untreated melts are very significant [27; see Appendix 6]. The elucidation of these processes should be assisted by high temperature UV-visible spectroelectrochemical studies which have been initiated [28].

We have also examined the electrochemistry of rhenium in basic $\text{AlCl}_3\text{-NaCl}$ in order to compare the behavior of rhenium in this melt with that observed in ambient temperature organic chloroaluminate melts [29,30]. Significant differences have been noted [31; see Appendix 7]; further work is required to understand fully the chemistry involved.

We have completed spectroscopic studies of iridium carbonyls in acidic $\text{AlCl}_3\text{-NaCl}$ [32; see Appendix 8]. These studies illustrate the complexity of homogeneous Fischer-Tropsch catalysis in chloroaluminate melts and partially explain the differences observed in the studies of Muetterties and coworkers [33,34] and Collman and coworkers [35].

B. Phase diagram of the NAFCAL system

The phase diagram of the pseudo-binary system $\text{NaAlCl}_4\text{-NaF}$ has been determined using differential thermal analysis (DTA). This method results in temperatures at which endothermic and exothermic phase changes occur. The resulting phase diagram of $\text{NaAlCl}_4\text{-NaF}$ is shown below.

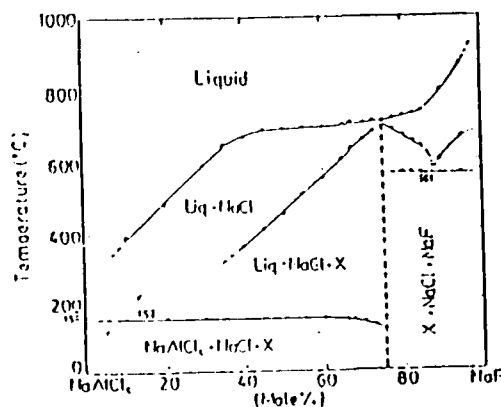


Figure 1. Phase diagram for the $\text{NaAlCl}_4\text{-NaF}$ system.

It may be seen that melts containing significant concentrations of NaF (≤ 20 mole %) have liquidus temperatures which are $\sim 500^\circ\text{C}$ or less. The results of this study are being prepared for a publication [36].

C. Application of UV-visible, Raman and electron spin resonance (ESR) spectroelectrochemistry (SE)

We have previously obtained infrared SE evidence that chloranil is reduced in two closely spaced one electron steps to the radical anion and the dianion in the acidic $\text{AlCl}_3\text{-NaCl}$ melts [37]. In basic melts no IR evidence for the formation of a radical anion was obtained. UV-visible SE of chloranil reduction in $\text{AlCl}_3\text{-NaCl}_{\text{sat}}$ melt shows a weak band at 515 nm at potentials between those at which chloranil and the dianion of chloranil exist at the electrode. This band was also observed in acidic melts. The Nernstian plot constructed from the variation of absorbance with potential results in an n-value of 1.2. Raman SE, using UV excitation (in order to minimize problems due to fluorescence) results in two weak bands at 1071 and 1350 cm^{-1} (which are only observed at potentials corresponding to the radical anion). ESR SE also shows a weak signal at intermediate potentials. Thus, application of several SE approaches [38] provides evidence for an intermediate which could not be detected by solely electrochemical measurements, such as cyclic voltammetry [37]. The experience gained in the study of this low-temperature system should be useful in studies of refractory metal species at elevated temperatures.

D. Studies of ultramicroelectrodes in molten or solid salt media

The use of ultramicroelectrodes in electrochemistry is a relatively new area that has received much attention recently [39]. With these electrodes both the charging current and

the iR drop can be greatly reduced, while a steady state of mass transfer can be established fairly readily. Our initial interest in these electrodes involved the possibility of obtaining i - E curves in frozen ionic media. Useful cyclic voltammograms for the reduction of Ag^+ in polycrystalline $NaAlCl_4$ were obtained at temperatures much lower than the melting point of $156^\circ C$ [40]. We also compared cyclic voltammetric and normal pulse voltammetric results for the reduction of $Fe(III)$ to $Fe(II)$ in molten $AlCl_3$ - $NaCl_{sat}$ at a tungsten disk ultramicroelectrode to the results obtained at a conventional tungsten disk electrode. The advantages of ultramicroelectrodes, such as reduced iR drop and rapidly established steady states of mass transfer, were observed in these studies [31; see Appendix 7].

E. Novel molten salt solvents

Characterization of ambient temperature chloroborates was extended using ^{11}B NMR and molecular orbital studies [41]. These results provide indirect evidence for the presence of $B_2Cl_7^-$ in these mixtures.

Our attempts to synthesize completely fluorinated quaternary ammonium salts were not successful [42].

Studies involving $CaCl_2$ -based melts, such as conductivity measurements and the development of a reference electrode, were transferred to a small program sponsored by the Los Alamos National Laboratory. The abstract of the M.S. thesis summarizing that work is given in Appendix 9.

F. Studies related to high energy batteries

The use of FeCl₃-containing melts, such as molten FeCl₃-NaCl, for battery applications was examined. It was found that the cell



was not stable because β' -alumina disintegrates in the presence of Fe(III).

The polarization phenomena at the β' -alumina/acidic AlCl₃-NaCl melt interface [43] are being studied by a.c. impedance spectroscopy [44]. The impedance caused by a partially blocking layer is small at short-term exposures.

G. Spectroscopic and electrochemical investigations of aromatic compounds in ambient temperature chloroaluminate melts.

In the past such studies were conducted at the Oak Ridge National Laboratory (ORNL); they were not supported by AFOSR. Approximately a year ago the program at ORNL was terminated because of the retirement of the senior scientist, G. P. Smith. Jointly with Professor R. M. Pagni, we plan to resume organic chemistry in ambient temperature chloroaluminates at the University of Tennessee; therefore, it is appropriate to summarize some accomplishments here.

Most recent studies in this area were performed by my graduate student J. E. Coffield in collaboration with Drs. G. P. Smith and S. P. Zingg at ORNL. Coffield's doctoral dissertation involved the study of the reduction of phenazine and perylene in basic AlCl₃-1-ethyl-3-methyl-1H-imidazolium chloride (EMIC) [45,46].

The redox chemistry of perylene was also studied in a neutral (1:1) AlCl₃-1,2-dimethyl-3-propyl-1H-imidazolium chloride (DMPIC). DMPIC was substituted for EMIC

in order to eliminate a possible source of protons. Two step reduction and two step oxidation of perylene was observed in this melt. In an attempt to observe an electrochemiluminescence generating reaction between the PE radical ions, the potential was first pulsed to 50 mV cathodic of the radical anion peak potential, then to 50 mV anodic of that of the radical cation. Weak light emission from the working electrode surface could be seen in a darkened room. Both glassy carbon and tungsten wire working electrodes were used. The intensity of the emission increased as the duration of the first pulse was increased from 1 to 20 seconds. The emitted light also appeared more intense when the area of the glassy carbon electrode was increased. This study, performed at the University of Tennessee, is summarized in Appendix 10 [47].

References

1. G. W. Mellors and S. Senderoff, *J. Electrochem. Soc.*, 112, 266 (1965).
2. S. Senderoff, G. W. Mellors, and W. J. Reinhart, *ibid.*, 112, 840 (1965).
3. G. W. Mellors and S. Senderoff, *ibid.*, 113, 60 (1966).
4. G. W. Mellors and S. Senderoff, *ibid.*, 113, 66 (1966).
5. S. Senderoff and G. W. Mellors, *Science*, 153, 1475 (1966).
6. S. Senderoff and G. W. Mellors, *J. Electrochem. Soc.*, 114, 586 (1967).
7. J. S. Fordyce and R. L. Baum, *J. Chem. Phys.*, 44, 1159 (1966).
8. J. S. Fordyce and R. L. Baum, *ibid.*, 44, 1166 (1966).
9. C. Decroly, A. Mukhtar, and R. Winand, *J. Electrochem. Soc.*, 115, 905 (1968).
10. D. Inman and S. H. White, *J. Appl. Electrochem.*, 8, 375 (1978).
11. I. Ahmad, W. A. Spiak, and G. J. Janz, *ibid.*, 11, 291 (1981).

12. T. Yoko and R. A. Bailey, *Proc. First Int. Symp. Molten Salt Chem. and Tech.*, 111 (1983).
13. Z. Qiao and P. Taxil, *J. Appl. Electrochem.*, 15, 259 (1985).
14. S. H. White and U. M. Twardoch, *ibid.*, 17, 225 (1987).
15. G. P. Capsimalis, E. S. Chen, R. E. Peterson, and I. Ahmad, *ibid.*, 17, 253 (1987).
16. P. Taxil and J. Mahenc, *ibid.*, 17, 261 (1987).
17. J. H. von Barner, E. Christensen, N. J. Bjerrum, and B. Gilbert, *Inorg. Chem.*, 30, 561 (1991).
18. J. H. von Barner, L. E. McCurry, C. A. Jorgensen, N. J. Bjerrum, and G. Mamantov, *Inorg. Chem.* 31, 1034 (1992).
19. G. Ting, K. W. Fung, and G. Mamantov, *J. Electrochem. Soc.*, 123, 624 (1976).
20. J.-P. Schoebrechts, P. A. Flowers, G. W. Hance, and G. Mamantov, *J. Electrochem. Soc.*, 135, 3057 (1988).
21. D. L. Brotherton, Ph.D. Dissertation, University of Tennessee, 1974.
22. I-Wen Sun, K. D. Sienerth, and G. Mamantov, *J. Electrochem. Soc.*, 138, 2850 (1991).
23. G. S. Chen, I. W. Sun, K. D. Sienerth, A. G. Edwards, and G. Mamantov, submitted to *J. Electrochem. Soc.*
24. B. Gilbert, S. D. Williams, and G. Mamantov, *Inorg. Chem.*, 27, 2359 (1988).
25. V. Taranenko, K. D. Sienerth, N. Sato, A. G. Edwards and G. Mamantov, *Materials Science Forum*, 73-75, 595 (1991).

26. G. S. Chen and G. Mamantov, Extended Abstract, International Symposium on Molten Salt Chemistry and Technology, Meeting of the Electrochemical Society, Honolulu, Hawaii, May 16-21, 1993.
27. K. D. Sienerth and G. Mamantov, Extended Abstract, International Symposium on Molten Salt Chemistry and Technology, Meeting of the Electrochemical Society, Honolulu, Hawaii, May 16-21, 1993.
28. E. M. Hondrogiannis and G. Mamantov, unpublished work.
29. S. K. D. Strubinger, I-Wen Sun, W. E. Cleland, Jr., and C. L. Hussey, *Inorg. Chem.*, 29, 993 (1990).
30. S. K. D. Strubinger, I-Wen Sun, W. E. Cleland, Jr., and C. L. Hussey, *Inorg. Chem.*, 29, 4247 (1990).
31. Chao-lan Hu, M.S. Thesis, University of Tennessee, 1991.
32. L. J. Tortorelli, P. A. Flowers, B. L. Harward, G. Mamantov, and L. N. Klatt, *J. Organometallic Chem.*, 429, 119 (1992).
33. G. C. Demitras and E. L. Muetterties, *J. Am. Chem. Soc.*, 99, 2796 (1977).
34. H.-K. Wang, H. W. Choi, and E. L. Muetterties, *Inorg. Chem.*, 20, 2661 (1981).
35. J. P. Collman, J. I. Brauman, G. Tustin, and G. S. Wann III, *J. Am. Chem. Soc.*, 105, 3913 (1983).
36. N. Sato, K. D. Sienerth, and G. Mamantov, unpublished work.
37. P. A. Flowers and G. Mamantov, *J. Electrochem. Soc.*, 136, 2944 (1989).
38. E. M. Hondrogiannis, J. E. Coffield, D. S. Trimble, and G. Mamantov, unpublished work.

39. R. M. Wightman and D. O. Wipf, in *Electroanalytical Chemistry*, Vol. 15, A. J. Bard, ed., 1989, pp. 267-344.
40. T. R. Blackburn and G. Mamantov, *J. Electrochem. Soc.*, 136, 580 (1989).
41. S. D. Williams, G. Mamantov, L. J. Tortorelli, and G. Shankle, unpublished work.
42. L. J. Tortorelli and G. Mamantov, unpublished work.
43. A. Katagiri, J. Hvistendahl, K. Shimakage, and G. Mamantov, *J. Electrochem. Soc.*, 133, 1281 (1986).
44. M. Matsunaga, A. Katagiri, J. Caja, and G. Mamantov, unpublished work.
45. J. E. Coffield, G. Mamantov, S. P. Zingg, and G. P. Smith, *J. Electrochem. Soc.*, 138, 2543 (1991).
46. J. E. Coffield, G. Mamantov, S. P. Zingg, G. P. Smith, and A. C. Buchanan, III, *J. Electrochem. Soc.*, 139, 355 (1992).
47. G. Mamantov, S. D. Williams, K. D. Sienerth, C. W. Lee, and J. E. Coffield, *J. Electrochem. Soc.*, 139, L58 (1992).

Contribution from the Institute of Mineral Industry and Molten Salts Group, Chemistry Department A, The Technical University of Denmark, DK-2800 Lyngby, Denmark, and Department of Chemistry, The University of Tennessee, Knoxville, Tennessee 37996-1600

Electrochemical and Spectroscopic Studies of Tantalum Species in NaCl-AlCl₃ Melts at 160-300 °C

J. H. von Barner,¹ L. E. McCurry,¹ C. A. Jørgensen,¹ N. J. Bjerrum,^{*,2} and G. Mamantov^{*,3}

Received December 10, 1990

The formation of complexes of Ta(V) in NaCl-AlCl₃ melts at 175 and 300 °C has been studied by potentiometric and spectrophotometric methods. The results at 175 °C could, within the pCl range 1.13 ca. 4.5 and with the Ta(V) concentration in the range 0-0.3 M, best be explained by the equilibrium TaCl₅ ↔ TaCl₃ + Cl⁻ with a pK value (based on molar concentration) of 3.89 (4) and a solubility limit for TaCl₃ of 0.087 (9) M. However, equilibria involving Ta₂Cl₁₀ could not be ruled out. UV-visible spectra of pure TaCl₃ and TaCl₅ were very difficult to obtain because of the formation of oxo chloro species. The electrochemical reduction of Ta(V) in AlCl₃ rich melts results in the formation of Ta(IV) followed by dimerization and further reduction to Ta₂Cl₁₄ and possibly other tantalum clusters. Formation of metallic tantalum was not observed in the electrolysis.

Introduction

Molten chloroaluminates have considerable interest, partly because of their ability to stabilize lower oxidation states of a number of elements, such as Hg, Cd, Bi, S, Se, and Te, and partly because of their uses in applications such as batteries. A review of chemistry in molten chloroaluminates is available.¹ The coordination and redox chemistry in these melts is a sensitive function of the chloro acidity (pCl) and the temperature. The acid-base properties in AlCl₃-NaCl melts near the 50-50 mol % composition can be described by the equilibrium²⁻⁴



In more acidic melts (i.e. melts with higher AlCl₃ content) other species such as Al₃Cl₁₀⁻ and Al₂Cl₆ have to be taken into consideration to explain Raman spectroscopic,⁵ potentiometric,^{2,3} and vapor pressure² measurements on these melts.

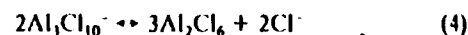
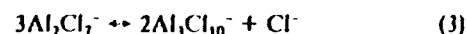
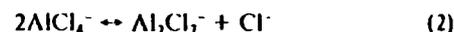
As part of our general studies of chloroaluminate melts, the present paper describes an investigation of the complex formation and redox chemistry of tantalum(V) in NaCl-AlCl₃ melts.

Molten TaCl₅ consists of molecular Ta₂Cl₁₀ at 220 °C, which gradually dissociates to TaCl₅ as the temperature is raised.⁶ TaCl₅ molecules of D_{3h} symmetry are also known to exist in the vapor phase.⁷ An examination of the binary NaCl-TaCl₅ system⁸ shows the presence of the compound NaTaCl₆, which melts incongruently at 470 °C. The fact that TaCl₅ is a Lewis acid having a strong affinity for chloride ions is also seen from the formation of octahedral TaCl₆⁻ ions in the equimolar KCl-TaCl₅⁶ and NaCl-TaCl₅⁹ melts and in basic and neutral solutions of TaCl₅ in NaCl-AlCl₃ melts⁶ as well as in basic MeFtimCl-AlCl₃ solutions (MeFtim = 1-methyl-3-ethylimidazolium).¹⁰ For acidic solutions of TaCl₅ in NaCl-AlCl₃ melts, Raman spectra indicate that molecular TaCl₅ is present at temperatures above 250 °C whereas Ta₂Cl₁₀ is the major species formed at lower temperatures.⁶ This behavior is similar to that of NbCl₅ dissolved in KCl-AlCl₃^{11,12} and in NaCl-AlCl₃ melts,¹² where NbCl₆⁻ is formed in basic solutions and NbCl₅ is found at high temperatures in acidic solutions whereas low temperatures stabilize Nb₂Cl₁₀.

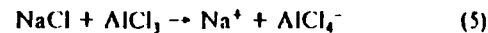
General Considerations

In the present work, the formal concentration C' of one of the added substances is defined as the initial molar amount dissolved in 1 L of the melt (unit: F). Real molar concentrations are symbolized by brackets. The volumes of the melts are calculated by assuming ideal mixing of NaCl-AlCl₃ and TaCl₅. This assumption results only in minor errors since the amounts of TaCl₅ are small compared to the amounts of AlCl₃ and NaCl. The densities of AlCl₃-NaCl and of TaCl₅ were obtained from the work of Berg et al.¹³ and of Nisel'son et al.,¹⁴ respectively. pCl is defined as the negative logarithm of the chloride ion molarity. Three

equilibria were used to describe the behavior of the NaCl-AlCl₃ molten system:



The pK values (in molar units) for reactions 2-4 used in the calculations are 7.05, 6.9, and 14 at 175 °C,² respectively. Since AlCl₃ contained small amounts of AlOCl, it was necessary to correct the melt composition. The AlOCl contents can be calculated from potentiometric measurements on the equimolar NaCl-AlCl₃ solvent. NaCl and AlCl₃ react almost quantitatively as follows:



However, in most cases an excess of NaCl relative to AlCl₃ that cannot be explained by a weighing error is observed. This is due to the presence of AlOCl in AlCl₃, since AlOCl does not react with NaCl in the pCl range investigated.¹⁵

AlOCl will further react with TaCl₅ in the melt¹⁶ according to



From potentiometric measurements on 0.3 F solutions of TaOCl₃ dissolved in NaCl-AlCl₃ melts performed at Lyngby,¹⁶ we know

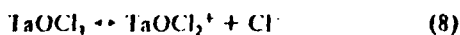
- (1) Mamantov, G.; Osteryoung, R. A. In *Characterization of Solutes in Non-Aqueous Solvent*; Mamantov, G., Ed; Plenum Press: New York, 1978; pp 223-49.
- (2) Hjuler, H. A.; Mahan, A.; von Barner, J. H.; Bjerrum, N. J. *Inorg. Chem.* 1982, 21, 402.
- (3) Fehrmann, R.; von Barner, J. H.; Bjerrum, N. J.; Nielsen, O. F. *Inorg. Chem.* 1981, 20, 1712.
- (4) Torsi, G.; Mamantov, G. *Inorg. Chem.* 1971, 10, 1900; 1972, 11, 1439.
- (5) Torsi, G.; Mamantov, G.; Begun, G. M. *Inorg. Nucl. Chem. Lett.* 1970, 6, 553.
- (6) Huglen, R.; Poulsen, F. W.; Mamantov, G.; Begun, G. M. *Inorg. Chem.* 1979, 18, 2551.
- (7) Beattie, I. R.; Orin, G. A. *J. Chem. Soc. A* 1969, 1691.
- (8) Morozov, I. S.; Korshunov, B. G.; Simonich, A. T. *Zh. Neorg. Khim.* 1956, 1, 1646.
- (9) Kipourou, G. J.; Flint, J. H.; Sadoway, D. R. *Inorg. Chem.* 1985, 24, 3881.
- (10) Barnard, P. A.; Hussey, C. L. *J. Electrochem. Soc.* 1990, 137, 913.
- (11) von Barner, J. H.; Bjerrum, N. J.; Smith, G. P. *Acta Chem. Scand.* 1978, A32, 837.
- (12) Huglen, R.; Mamantov, G.; Smith, G. P.; Begun, G. M. *J. Raman Spectrosc.* 1979, 8, 326.
- (13) Berg, R. W.; Hjuler, H. A.; Bjerrum, N. J. *J. Chem. Eng. Data* 1983, 28, 251.
- (14) Nisel'son, I. A.; Pustil'nik, A. I.; Sokolova, T. D. *Russ. J. Inorg. Chem. (Engl. Transl.)* 1964, 9, 574.
- (15) Zachariassen, K.; Berg, R. W.; Hjerrum, N. J.; von Barner, J. H. *J. Electrochem. Soc.* 1987, 134, 1153.
- (16) Jørgensen, C. A.; von Barner, J. H.; Bjerrum, N. J. Unpublished results.

¹ Institute of Mineral Industry, The Technical University of Denmark.

² The University of Tennessee.

³ Molten Salts Group, Chemistry Department A, The Technical University of Denmark.

that TaOCl_3 takes part in the equilibrium:



with the pK values 2.74 (pK_1) and 4.52 (pK_2).

Taking into consideration the above information, the experimental average coordination number of Ta(V) (in relation to pure chloride species) becomes

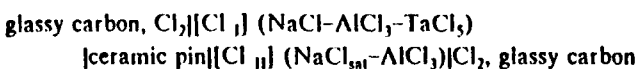
$$\bar{n}_{\text{Ta(V)}} = (C'_{\text{NaCl}} + 3C'_{\text{AlCl}_3} + 5C'_{\text{TaCl}_5} + C'_{\text{AlOCl}} - 4[\text{AlCl}_4] - 7[\text{Al}_2\text{Cl}_7] - 10[\text{Al}_3\text{Cl}_{10}] - 6[\text{Al}_2\text{Cl}_6] - 4[\text{TaOCl}_4] - 3[\text{TaOCl}_3] - 2[\text{TaOCl}_2] - [\text{Cl}]) / (C'_{\text{TaCl}_5} - C'_{\text{AlOCl}}) \quad (9)$$

In the present case where we are dealing with solute species with a limited solubility, it is, however, important to define a number that can be used when a precipitate is present and in this way utilize a larger compositional range. Such a number¹⁷ can be expressed by \bar{n}' , which in the present case is defined in eq 10, where

$$\bar{n}'_{\text{Ta(V)}} = (C'_{\text{NaCl}} + 3C'_{\text{AlCl}_3} + 5n_{\text{TaCl}_5, w} / V + C'_{\text{AlOCl}} - 4[\text{AlCl}_4] - 7[\text{Al}_2\text{Cl}_7] - 10[\text{Al}_3\text{Cl}_{10}] - 6[\text{Al}_2\text{Cl}_6] - 4[\text{TaOCl}_4] - 3[\text{TaOCl}_3] - 2[\text{TaOCl}_2] - \text{Cl}) / (n_{\text{TaCl}_5, w} - n_{\text{AlOCl}, w}) \quad (10)$$

$n_{\text{TaCl}_5, w}$ is the total number of moles of TaCl_5 that was weighed (but not necessarily the number of moles in solution). (In this way we obtain an average coordination number including both precipitate and solution.) $n_{\text{AlOCl}, w}$ is a similar number for the AlOCl impurity in the AlCl_3 used. This impurity amounts to about 0.2 mol % of the used AlCl_3 or 0.016 F in a melt (without Ta(V)). This value has been determined potentiometrically as described earlier.¹⁸ V is the volume of the melt.

The electrochemical cell used for the potentiometric measurements was a chlorine-chlorine concentration cell:¹⁹



I and II refer to measuring and reference compartments, respectively. It has been shown previously^{20,21} that, in KCl-AlCl₃ melts near the 1:1 composition, cell potential, within experimental uncertainties, is given by

$$E = \frac{-RT}{F} \ln \frac{[\text{Cl}]_{II}}{[\text{Cl}]_I} \quad (11)$$

Similar calculations on the NaCl-AlCl₃ system² show that eq 11 is valid also in the compositional range $0.51 > X_{\text{NaCl}} > 0.49$ investigated in this work. The $p\text{Cl}$ of the melt in the measuring compartment can then be expressed as

$$p\text{Cl}_I = -(F/(RT \ln 10))\Delta E + p\text{Cl}_{II} \quad (12)$$

where $p\text{Cl}_{II}$ is the $p\text{Cl}$ of a NaAlCl_4 melt saturated with NaCl used as the reference electrode. The $p\text{Cl}_{II}$ value is 1.128 at 175 °C.^{2,3}

In the spectrophotometric work, the Bouguer-Beer law and the law of additive absorbances were assumed to be valid. The formal absorptivity of TaCl_5 is the absorbance divided by the product of the path length and the formality of TaCl_5 . The absorbances for the liquid-phase spectra were corrected for the absorbance of the solvent and the amount of the Ta(V) oxo chloro species present in the melt as well as the TaCl_5 in gas phase above the melt (see later).

Table I. Cell Potentials and Compositions of 0.23-0.30 F Solutions of TaCl_5 in Molten NaCl-AlCl₃ at 175 °C

$-\Delta E, \text{V}$	mole fractions ^a		
	NaCl	AlCl ₃	TaCl ₅
292.0 ^b	0.4878 ₀	0.4950 ₁	0.0171 ₉
254.8 ^b	0.4919 ₂	0.4907 ₄	0.0173 ₀
235.39 ^b	0.4933 ₄	0.4891 ₄	0.0161 ₄
217.82	0.4950 ₄	0.4879 ₃	0.0129 ₄
217.56 ^b	0.4957 ₁	0.4873 ₀	0.0163 ₁
212.21	0.4966 ₄	0.4863 ₃	0.0154 ₁
195.90	0.4963 ₃	0.4865 ₀	0.0130 ₁
179.20	0.4980 ₇	0.4846 ₁	0.0160 ₁
148.94	0.4991 ₀	0.4838 ₂	0.0154 ₄
125.42	0.4992 ₂	0.4835 ₀	0.0159 ₁
61.62	0.5005 ₃	0.4822 ₇	0.0165 ₄
43.54	0.5001 ₇	0.4825 ₉	0.0159 ₃
35.45	0.5011 ₁	0.4822 ₁	0.0166 ₄
10.40	0.5017 ₉	0.4815 ₃	0.0166 ₄

^aCorrected for the presence of AlOCl in the solvent, assuming quantitative reaction between AlOCl and TaCl_5 producing AlCl_3 and TaOCl_3 . ^bPrecipitate present (visual inspection).

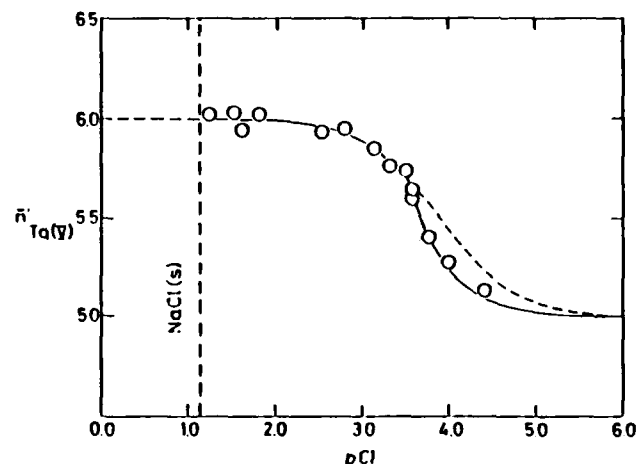


Figure 1. Average experimental coordination number (with precipitate included) ($\bar{n}'_{\text{Ta(V)}}$) for Ta(V) in NaCl-AlCl₃ at 175 °C as a function of $p\text{Cl}$. The formal concentrations (in the $p\text{Cl}$ range where no precipitate was present) were 0.23-0.30 F. Calculated values of \bar{n}' (for the reaction $\text{TaCl}_5 \leftrightarrow \text{TaCl}_3 + \text{Cl}$) are indicated by a full curve. The dashed curve shows for a hypothetical extrapolation what would happen if no precipitation occurred. The vertical dashed line shows the limiting $p\text{Cl}$, due to saturation with NaCl.

Experimental Section

AlCl_3 and NaCl were prepared as described previously.^{2,21} The solvent melts were formed by weighing the proper amounts of AlCl_3 and NaCl in nitrogen-filled dryboxes with measured water contents of approximately 5 ppm or less.

TaCl_5 (99.9% from Fluka) was purified by sublimation at 200 °C. Two different batches of TaCl_5 were made for the spectrophotometric measurements. The first had a chlorine content of $49.21 \pm 0.21\%$, and the second, a content of $47.46 \pm 0.23\%$. Both values were obtained as an average of four measurements and should be compared with the theoretical value of 49.49%. Thus, it can be seen that the first batch consists of almost pure TaCl_5 , whereas the second batch must contain a certain amount of oxide chloride. In the experiments where the latter batch was used, a correction was made for the oxide chloride content (see below).

The chlorine/chloride electrode cell¹⁹ used for the potentiometric measurements, as well as the furnace used, has been described previously.^{22,23} The connecting tube between the two compartments of this cell was sealed after the addition of TaCl_5 in order to prevent distillation from one chamber to the other. The optical cells used for the spectrophotometric measurements were of fused quartz (Ultrasil from Hellma). Due to the large molar absorptivity of Ta(V), it was necessary to use cells

(22) Laursen, M. M.; von Barner, J. H. *J. Inorg. Nucl. Chem.* 1979, 41, 185.

(23) Andreasen, H. A.; Bjerrum, N. J.; Foverskov, C. E. *Rev. Sci. Instrum.* 1977, 48, 1340.

(17) von Barner, J. H.; Brekke, P. B.; Bjerrum, N. J. *Inorg. Chem.* 1985, 24, 2162.

(18) Zachariassen, K.; Berg, R. W.; Bjerrum, N. J.; von Barner, J. H. *J. Electrochem. Soc.* 1987, 134, 1151.

(19) von Barner, J. H.; Bjerrum, N. J. *Inorg. Chem.* 1973, 12, 1891.

(20) von Barner, J. H.; Bjerrum, N. J.; Kiens, K. *Inorg. Chem.* 1974, 13, 1708.

(21) Marassi, R.; Chambers, J. Q.; Mamantov, G. *J. Electroanal. Chem. Interfacial Electrochem.* 1976, 69, 345.

Table II. pK Values, Solubilities, and Variances for Different Models of Chloro Complex Formation of Ta(V) in NaCl-AlCl₃ Melts at 175 °C^a

equilibria	pK_1	pK_2	solubility [TaCl ₅] _{max} M	var × 10 ⁴
TaCl ₅ ↔ TaCl ₄ ⁻ + Cl	3.89 (4)		0.087 (9)	10.8*
TaCl ₅ ↔ TaCl ₄ (s)				
2TaCl ₅ ↔ Ta ₂ Cl ₁₀ + 2Cl	7.27 (8)		0.03 (3)	100.0
Ta ₂ Cl ₁₀ ↔ 2TaCl ₅ (s)				
TaCl ₅ ↔ TaCl ₄ ⁻ + Cl	3.95 (6)	-0.33 (19)	0.019 (7)	24.0*
2TaCl ₅ ↔ Ta ₂ Cl ₁₀				
Ta ₂ Cl ₁₀ ↔ 2TaCl ₅ (s)				
TaCl ₅ ↔ TaCl ₄ ⁻ + Cl	3.91 (13)	0.5 (31)	0.08 (3)	12.6*
2TaCl ₅ ↔ Ta ₂ Cl ₁₀				
TaCl ₅ ↔ TaCl ₄ (s)				

^aNumber of measurements 10 (number of different cells 5). Asterisks: based on $F_{0.10}(9.3) = 5.24$ and $F_{0.10}(8.3) = 5.25$.

with path lengths of less than 5×10^{-1} cm. These path lengths were obtained by placing fused-silica inserts into 0.5-cm cells. Before each experiment, the cells were calibrated with alkaline chromate solutions. The absorption spectra were recorded on a Cary 14R spectrophotometer equipped with an aluminum core furnace.²⁴ The temperatures in the furnace were measured with chromel-alumel thermocouples (from Pyrotentax) calibrated at the freezing points of pure tin and lead. The methodology used for voltammetric measurements has been described previously.²¹

Results and Discussion

Potentiometric Measurements on NaCl-AlCl₃-TaCl₅ Melts. The values of the measured cell potential for different melt compositions (all containing 0.3 F TaCl₅) at 175 °C are given in Table I. From the $-\Delta E$ values in this table, the experimental average coordination number \bar{n}' (corrected for precipitation and the presence of oxo chloro complexes) could be calculated as a function of pCl. The results of these calculations are shown in Figure 1. It can be seen that at low pCl the average coordination number is close to 6. An average value of 6.00 (4) was obtained from the last four measurements in Table I. This result, when combined with the previously reported Raman spectra,⁶ clearly indicates that Ta(V) is present as the complex ion TaCl₆⁻ in melts of low pCl. When the pCl is increased, \bar{n}' drops below 6.0, which indicates the formation of Ta(V)-chloride species other than TaCl₆⁻. At even higher pCl values (greater than ca. 3.6), a white precipitate was observed in the melt. On the basis of the previously reported Raman spectra,⁶ it is most likely that the Ta(V) species formed at higher pCl is either TaCl₅ or Ta₂Cl₁₀ or a combination of these two. Consequently, hypotheses involving equilibria between TaCl₆⁻ and TaCl₅ and Ta₂Cl₁₀ and precipitates of solid TaCl₅ were tested using a computer program. This program was based on a non-linear least-squares regression analysis which calculated the average coordination numbers using the pK values for the equilibria between the different tantalum species as independent variables. In this way a minimum variance between measured and calculated \bar{n}' values was obtained for each model. In these calculations only the data given in Table I with $-\Delta E$ values higher than 125 mV were used. The data with $-\Delta E$ values of less than 125 mV are not useful for a discrimination between models because all models will have similar variances in this range.

The results of the computations are shown in Table II. The experimental variance can be calculated from the measurements where \bar{n}' theoretically should be equal to 6.00. Here a value of 17.3×10^{-4} was found. By the use of an F test¹¹ it is possible to distinguish between models which have a probability of either greater or less than 90%. Only models with a probability of greater than 90% were considered as being able to explain the potentiometric measurements; these models are marked with asterisks.

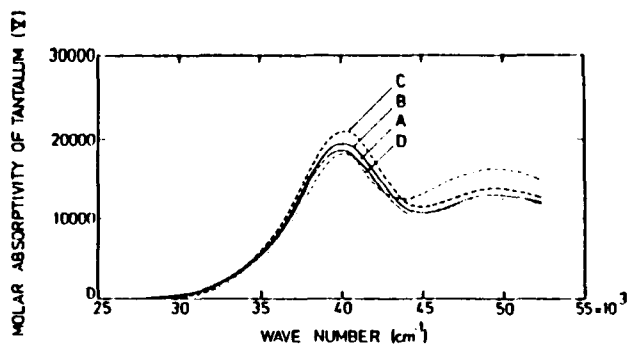


Figure 2. Ultraviolet-visible spectra of tantalum(V) in acidic melts. Spectra A and B are of measured solutions with the following mole fractions of NaCl and AlCl₃, formal concentration of TaCl₅, pCl, and \bar{n}' , respectively: (A) 0.4943, 0.5048, 0.0144, 4.46, 5.17; (B) 0.4941, 0.5046, 0.0219, 4.46, 5.19. In spectrum C the influence of oxide impurities has been eliminated by subtracting spectrum A from spectrum B. In spectrum D a further subtraction has removed the spectrum of TaCl₆⁻, giving the calculated spectrum of TaCl₅.

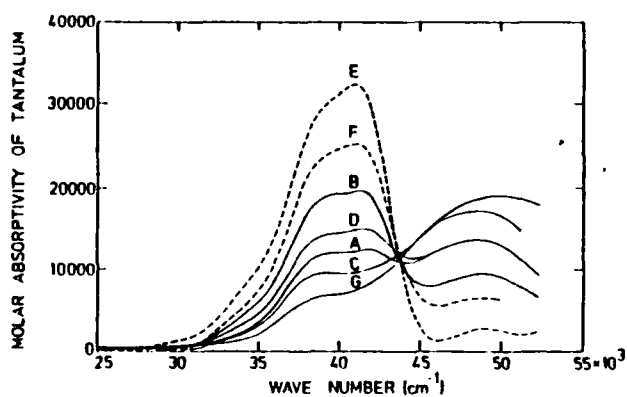


Figure 3. Ultraviolet-visible spectra of tantalum(V) in basic melts. Spectra A-D and G are of measured solutions with the following mole fractions of NaCl and AlCl₃, formal concentration of TaCl₅, pCl, and $\bar{n}'_{Ta(V)}$, respectively: (A) 0.5029, 0.4962, 0.0141, 1.12, 5.99; (B) 0.5029, 0.4957, 0.0229, 1.12, 5.99; (C) 0.5031, 0.4960, 0.0144, 1.12, 5.99; (D) 0.5031, 0.4955, 0.0244, 1.12, 5.99; (G) 0.5014, 0.4938, 0.0243, 1.12, 3.99. The solution which gives rise to spectrum G has, besides NaCl, AlCl₃, and TaCl₅, an addition of Na₂O (mole fraction 0.0033, or formality 0.0598). The average experimental coordination number for chloride ions is in this case close to 4 due to the formation of TaOCl₄⁻.

As may be seen from Table II, the only model that is not able to explain the measurements is the one where only Ta₂Cl₁₀ is formed together with TaCl₆⁻.

Spectrophotometric Measurements on NaCl-AlCl₃-TaCl₅ Melts. The spectra of tantalum(V) in slightly acidic melts at 175 °C are shown in Figure 2 (spectra A and B). In both spectra a small correction has been made for the amount of TaCl₅ present in the gas phase above the melt (see Appendix). The melt compositions correspond to pCl values of 4.46, and 4.46, respectively. It should be noted that spectra A and B resemble each other closely. Since the concentrations of tantalum(V) differ in the two melts, it is reasonable to expect that the spectra are not much affected by oxide impurities present in the melts, because a constant oxide impurity will affect a low tantalum concentration more than a high tantalum concentration.

The influence of the oxide impurities can be further eliminated by subtracting the two spectra from each other and calculating the formal absorptivity of the difference as shown in spectrum C. Since the \bar{n}' value for tantalum(V) in solution is not 5 but 5.17-5.19, (i.e. TaCl₆⁻ is also present), a further correction is necessary in order to obtain the spectrum of pure TaCl₅. To perform this correction, the spectrum of pure TaCl₆⁻ is needed. The spectrum of this complex is taken from Figure 3E and will be discussed below. Spectrum D (in Figure 2) is the result of this correction and should be the spectrum of pure TaCl₅. It can be

(24) Fehrmann, R.; Bjerrum, N. J.; Poulsen, F. W. *Inorg. Chem.* 1978, 17, 1195.

Table III. Band Maxima for TaCl₆⁻, NbCl₆⁻, and WCl₆ in UV-Visible Spectra [ν_{max} , 10³ cm⁻¹ (ϵ_{max} , 10³ M⁻¹ cm⁻¹)]

complex	NaCl-AlCl ₃		KCl-AlCl ₃ 300 °C	gas phase 175 °C	MeEtimCl-AlCl ₃	
	E = spectrum E F = spectrum F 175 °C				$\alpha = 51.0/49.0$ mol % $\beta = 55.6/44.4$ mol % room temp	acetonitrile room temp
TaCl ₆ ⁻	E: 34.0 (sh), ^a 38.9 (sh), 41.1 (32.4), 49.0 (2.9) ^b F: 34.0 (sh), 38.9 (sh), 41.1 (25.2), 49.0 (6.5) ^b		31.8 (sh), 34.4 (26.3), 41.3 (6.7) ^f	27 (sh), 30.8 (23.7), 39.2 (7.4) ^h	α : 33.9 (6.3), 37.6 (23), 34.8 (5.8), 38.0 (23.8), 41.0 (31) ^e β : 34.2 (7.5), 37.9 (24), 41.2 (31) ^e	34.8 (5.8), 38.0 (23.8), 41.5 (38.0), 49.5 (11.0) ^d
NbCl ₆ ⁻						28.9 (sh <2.0), 31.8 (sh 11.4), 34.5 (28.9), 41.4 (6.4) ^d
WCl ₆						

^ash = shoulder. ^bThis work. ^cReference 10. ^dReference 25. ^eNot known. ^fReference 11. ^gReference 26. ^hReference 27.

seen that TaCl₆⁻ has two band maxima located at ca. 40.2×10^3 and 49.6×10^3 cm⁻¹.

A comparison between the spectrum of TaCl₆⁻ obtained in this work and the spectrum of NbCl₆⁻ in KCl-AlCl₃ from previous work¹¹ shows that the bands of TaCl₆⁻ are found at somewhat higher frequencies than the corresponding bands for NbCl₆⁻ (which are located at 33.7×10^3 and 43.8×10^3 cm⁻¹, respectively). The molar absorptivities of the TaCl₆⁻ bands are also higher than the molar absorptivities of the corresponding NbCl₆⁻ bands.

The spectra of tantalum(V) in a basic melt saturated with NaCl at 175 °C are shown in Figure 3 (spectra A-D). Under the given circumstances, we know from the potentiometric measurements that the average experimental coordination number for chloride is close to 6. Spectrum G (Figure 3) is also obtained from a saturated melt, but in this case an excess of Na₂O has been added, converting TaCl₆⁻ completely to TaOCl₄ (TaOCl₄ is distinguished from for example TaOCl₅²⁻ by model discrimination¹⁶).

The chloride activity is the same for all spectra in Figure 3; therefore, the differences in the spectra must be due to different degrees of conversion to oxo chloro complexes. Furthermore, the spectra seem to form a (not very well defined) isosbestic point around 43.8×10^3 cm⁻¹. This indicates, as expected,¹⁶ the formation of only one oxide species together with TaCl₆⁻. The rather low quality of the isosbestic point is probably due to difficulties in obtaining a correct value for the path length of the melt and to a smaller extent due to the uncertainty in the concentration of the added tantalum(V). A further error results from the uncertainty in the amount of oxide impurity found in the TaCl₆⁻ added. Spectra A and B have not been corrected for this oxide impurity (because an analysis showed it to be very small). However, in the case of spectra C, D, and G, such a correction has been performed. (It should be noted that the value for the oxide content used in this correction is determined indirectly from a chlorine analysis of TaCl₆⁻). In order to make a correction in spectra C and D, it is furthermore necessary to know the spectrum of the pure oxo species formed in NaCl-saturated solutions. Spectrum G represents such a spectrum, obtained when an excess of oxide is present.

Since spectra A and B are obtained from melts made from the same batch of chemicals, a subtraction of spectrum A from spectrum B should to a large extent remove the influence of the oxo chloro compound due to impurities in the melt (i.e. from AlOCl). The result of this subtraction (multiplied by the proper constant) is given as spectrum E, which should then be the spectrum of pure TaCl₆⁻. However, spectra C and D are also made with chemicals from the same batch and a similar subtraction procedure will in this case give spectrum F. It can be seen that there is a significant difference in molar absorptivities between spectra E and F. One explanation could be that our assumption about an equal concentration of oxide in each of the two sets of melts used to obtain spectra A and B and spectra C and D, respectively, is not correct.

It should be noted that even if there is a fairly large difference in the molar absorptivity between spectra E and F, the shapes of two spectra are similar (and the bands are at the same frequencies). Furthermore, since we are dealing with a two-species system, the possible maximum molar absorptivity of the main band located

around 41.1×10^3 cm⁻¹ cannot be much higher than found in spectrum E. A further increase in the absorptivity of this band (obtained for example by assuming higher amounts of oxide in the melt giving rise to spectrum B than in the melt giving rise to spectrum A) will result in negative values of the molar absorptivity in the wavenumber range above 46×10^3 cm⁻¹. We can therefore conclude that spectrum E represents the upper limit for the absorptivity of the spectrum of TaCl₆⁻. It is not clear whether spectrum F represents the lower limit, but at least the molar absorptivity of the 41.1×10^3 cm⁻¹ band has to be higher than what is found in the case of spectrum B.

An inspection of spectrum E indicates that the two main bands of TaCl₆⁻ are located at ca. 41.1×10^3 and ca. 49.0×10^3 cm⁻¹ with molar absorptivities of 32.4×10^3 and 2.9×10^3 M⁻¹ cm⁻¹, respectively. These band positions should be compared with the band positions found for TaCl₆⁻ in basic MeEtimCl-AlCl₃²⁴ and in acetonitrile.²⁵ The band positions in these three media agree rather well with each other, as can be seen in Table III. In Table III is also shown a comparison with NbCl₆⁻ in KCl-AlCl₃¹¹ and acetonitrile.²⁵ It can be seen that, in this case as well, there is a shift to higher band frequencies from niobium(V) to tantalum(V) whereas the molar absorptivities are rather similar. It should be noted further that a well-defined shoulder can be found in the spectrum of TaCl₆⁻ around 38.9×10^3 cm⁻¹. In the case of NbCl₆⁻ in KCl-AlCl₃¹¹ this shoulder, which is not very pronounced, is found around 31.8×10^3 cm⁻¹. It is also interesting to compare the spectrum of TaCl₆⁻ with the spectrum of the isoelectronic complex WCl₆. Because of oxo chloro formation, the spectrum of WCl₆ is not known with high accuracy in NaCl-AlCl₃ solutions.²⁶ It is however clear that the strongest band is located at 30.0×10^3 cm⁻¹ and a shoulder seems to be present around 27×10^3 cm⁻¹ whereas it is difficult to predict where the other main band is located. Contrary to this, the spectrum of WCl₆ is known fairly accurately in the gas phase.^{26,27} The strongest band in this case is located at 30.8×10^3 cm⁻¹, which is not far from the position in the NaCl-AlCl₃ melt. Therefore, there are reasons to believe that the other main band located at 39.2×10^3 cm⁻¹ in the gas phase has approximately the same position in NaCl-AlCl₃ melts.

It can be seen that these band positions are far removed from the band positions in the spectrum of TaCl₆⁻ in NaCl-AlCl₃. This difference is probably due to the negative charge on the TaCl₆⁻ complex. From Table III it can be seen that the molar absorptivity for the 30.0×10^3 cm⁻¹ band of WCl₆ in NaCl-AlCl₃ is somewhat lower than the molar absorptivity of the similar band for TaCl₆⁻ in NaCl-AlCl₃ (whereas the molar absorptivities for WCl₆ in the gas phase are rather similar to the molar absorptivities of TaCl₆⁻ in NaCl-AlCl₃).

Voltammetric Measurements of the Reduction of Ta(V) in NaCl-AlCl₃ Melts. The redox chemistry of Ta(V) in several compositions of NaCl-AlCl₃ was studied using electrochemical methods. Studies in melts saturated with NaCl (pCl = 1.1) have

(25) Vallotton, M.; Merbach, A. E. *Helv. Chim. Acta* 1974, 57, 2345.

(26) Schochrechts, J.-P.; Flowers, P. A.; Hance, G. W.; Mamantov, G. J. *Electrochem. Soc.* 1988, 135, 3057.

(27) Takuma, T.; Kawakubo, S. *Nippon Kagaku Kaishi* 1972, 3, 865.

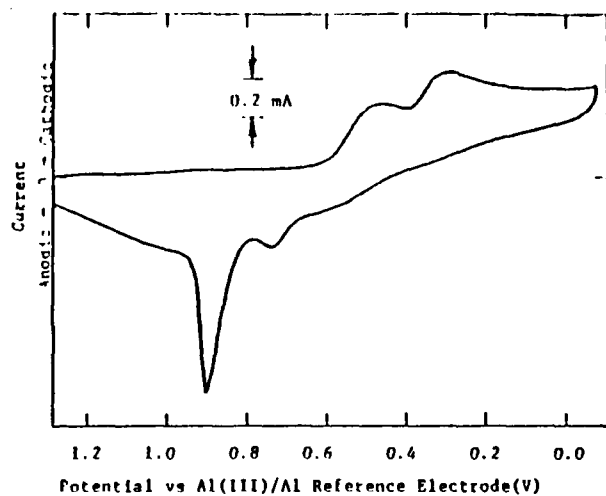


Figure 4. Cyclic voltammogram for the reduction of Ta(V) at a platinum electrode at 175 °C in NaCl-AlCl₃ (49-51 mol %): electrode area 0.09 cm²; Ta(V) concentration 3.05 × 10⁻² M; scan rate 0.1 V/s.

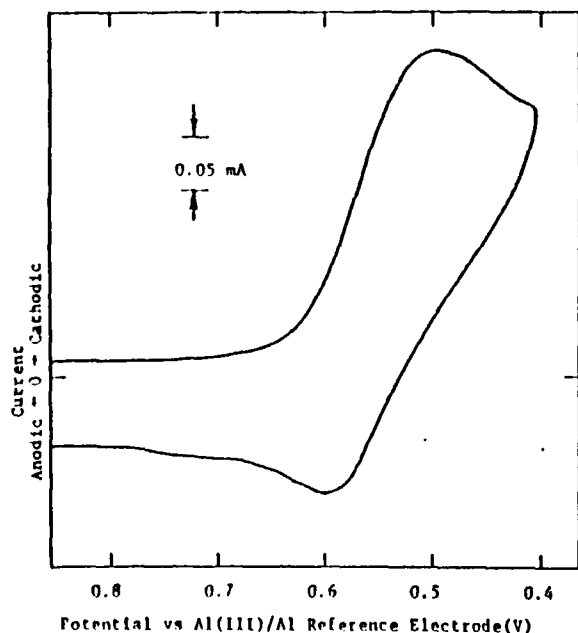


Figure 5. Cyclic voltammogram for the first reduction wave of Ta(V) at a platinum electrode at 160 °C in NaCl-AlCl₃ (49-51 mol %): electrode area 0.09 cm²; Ta(V) concentration 3.05 × 10⁻² M; scan rate 0.1 V/s.

dealt primarily with the differences in the electrochemical behaviors of TaCl₆⁻ and TaOCl₄⁻. These studies have resulted in an electroanalytical method for the determination of dissolved oxide in these melts; this work has been reported previously.²⁸ The most conclusive results were obtained using the NaCl-AlCl₃ (49-51 mol % = 49/51) melt. Cyclic voltammetric studies were carried out in the 49/51 melt (pCl = 4.5) to examine the effect of scan rate, temperature, and Ta(V) concentration. A typical cyclic voltammogram (CV) for the overall reduction of Ta(V) at a Pt electrode at 175 °C and a scan rate of 0.1 V/s is shown in Figure 4. It may be seen that two reduction steps are involved. The CV for the first reduction step at 160 °C is relatively simple (Figure 5). The peak current for this reduction is proportional to the Ta(V) concentration, the current function ($i_p/v^{1/2}$) is constant up to 1-2 V/s, and the peak current ratio (i_p^2/i_p^c) approaches unity at faster scan rates (1-2 V/s). On the other hand, the peak potential E_p for the first reduction wave shifts anodically with increasing Ta(V) concentration. Such a shift provides ev-

Table IV. Comparison between X-ray Powder Patterns for Ta₆Cl₁₄

$d, \text{\AA}$		$d, \text{\AA}$		$d, \text{\AA}$	
this work	ref 31	this work	ref 31	this work	ref 31
8.59 s	8.58 s	2.72 m	2.70 m	2.03 w	
7.76 s	7.76 s	2.55 w		1.97 m	1.96 m
5.68 s	5.66 s	2.47 s	2.48 s	1.77 m	1.78 m
4.01 w		2.28 w		1.73 m	1.71 m
3.01 w	2.98 vw	2.22 w		1.56 w	
2.92 w		2.14 w	2.16 vw	1.52 w	
2.85 w		2.09 m	2.08 m		

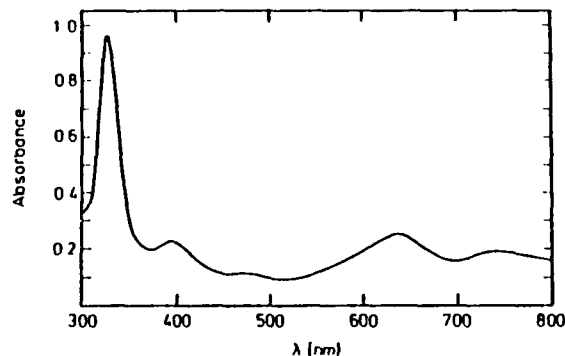
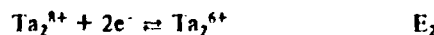


Figure 6. Adsorption spectrum of the Ta(V) reduction product in NaCl-AlCl₃ (49-51 mol %) dissolved in deoxygenated water (path length 1 cm).

idence for dimerization occurring after the reversible charge transfer.²⁹ As expected,²⁹ the plot of E_p vs log $C_{\text{Ta(V)}}$ is linear. The theoretical slope of this plot of $2.303RT/2nF$; an n value of 1.02 has been obtained from this plot. The second reduction step in Figure 4 is quite irreversible even at scan rates of 2 V/s. The sharp reoxidation peak at 0.9 V, observed only if the reduction is extended to the second step, is characteristic of the reoxidation of a deposit on the electrode. To learn more about the product of the second reduction step, a controlled-potential coulometric experiment was performed. The potential of the glassy-carbon cathode was controlled at 0.13 V (vs the Al(III) in the 37/63 melt/Al reference electrode). A dark green deposit was formed on the electrode surface. This deposit was removed from the electrode surface, filtered, and treated with molten AlCl₃ to remove any residual melt.³⁰ The X-ray powder pattern of the dark green powder was essentially identical to that of Ta₆Cl₁₄³¹ (see Table IV). The nonlinear log i vs time plot for the electrolysis points in the direction of a catalytic or an ECE mechanism.³² Although the n value obtained from electrolysis was 2.07, it is probably too low, since the current did not decay to background. The UV-visible spectrum of the pale green solidified melt used in the electrolysis and dissolved in deoxygenated water (see Figure 6) is identical to the spectrum of Ta₆Cl₁₂^{24,33}. The results summarized above point to the following reaction sequence for the reduction of Ta(V) in the 49/51 NaCl-AlCl₃ melt:



Although formation of metallic tantalum was not observed in the electrolysis, addition of aluminum to the green melt containing the tantalum cluster resulted, after 5 weeks at 175 °C, in bright

(29) Saveant, J. M.; Vianello, E. *Electrochim. Acta* 1967, 12, 1545.

(30) McCurry, L. F. Ph.D. Dissertation, University of Tennessee, 1978.

(31) Meyer, J. L.; McCarley, R. E. Private communication.

(32) Meites, L. In *Techniques of Chemistry, Volume 1*; Weissberger, A., Rossiter, B. W., Eds.; Wiley-Interscience: New York, 1971; Part IIA, pp 645-712.

(33) Kuhn, P. J.; McCarley, R. E. *Inorg. Chem.* 1965, 4, 1482.

(28) Laher, T. M.; McCurry, L. E.; Mamantov, G. *Anal. Chem.* 1985, 57, 500.

metallic particles which had an X-ray powder pattern identical to that of tantalum metal. The reduction of Ta₆Cl₁₄ to tantalum in the 49/51 melt at 175 °C may be slow because of the low solubility of Ta₆Cl₁₄ in the melt. It is not unlikely that the Ta₆Cl₁₄ layer on the electrode surface blocks further reduction of tantalum in this melt.

Conclusions

It has been shown that tantalum(V) forms two complexes, TaCl₆⁻ and TaCl₅, in basic and moderately acidic NaCl-AlCl₃ melts at 175 °C, respectively. These complexes have been characterized by their visible and ultraviolet spectra and by the pK value for the acid/base equilibrium between them at 175 °C. The existence of other complexes such as Ta₂Cl₁₀ is not very likely but cannot be completely ruled out.

Solvation has not been examined in the present investigation, but it is possible that TaCl₅ reacts with AlCl₃ (or TaCl₅⁺ with AlCl₄⁻), forming TaAlCl₇ in very acidic melts, similar to what has been found for NbCl₅.¹⁴ However, the experimental methods used are not suited for such an investigation. In the course of the present work, it was found to be very difficult to obtain spectra of the pure chloro complexes due to the high affinity of these complexes for oxide ions. TaCl₅ was extremely reactive in the gaseous phase (it reacted with the silica wall); therefore, it was not—in contrast to the case for NbCl₅—possible to obtain the gas-phase spectrum of this compound. The electrochemical reduction of tantalum(V) in acidic alkali-metal chloroaluminate melts results in cluster formation. No tantalum metal was observed in the electrolysis.

Acknowledgment. The molten salt research at The University of Tennessee was supported by the Air Force Office of Scientific Research. The research at The Technical University of Denmark was supported by the Danish Council for Technical Research. G.M. and N.J.B. acknowledge a NATO Travel Grant which made possible cooperation between the two research groups.

Appendix

In order to examine the influence of TaCl₅ in the gas phase above the melt, two different considerations were made. One involved vapor pressure measurements from the literature; the other measurements involved the distribution coefficient between the gas phase and the liquid phase for TaCl₅.

The vapor pressure of pure solid TaCl₅, P_{TaCl_5} , has been measured by Sadoway and Flengas,¹⁵ who found the following empirical equation:

$$\ln (P_{TaCl_5}/\text{atm}) = 42.180 - 111237 T^{-1} - 3.2207 \ln T - 1.761 \times 10^4 T^{-2}$$

(34) Krebs, B.; Janssen, H.; Bierum, N. J.; Berg, R. W.; Papatheodorou, G. N. *Inorg. Chem.* 1984, 23, 164.

(35) Sadoway, D. R.; Flengas, S. N. *Can. J. Chem.* 1976, 54, 1692.

which at a temperature of 175 °C gives

$$P_{TaCl_5(g)} = 0.0916 \text{ atm}$$

The highest concentration of TaCl₅ in the gas phase must be obtained when the melt is saturated with TaCl₅. If we assume that no vapor complexes are formed, the pressure of TaCl₅ above the melt should be equal to the pressure above solid TaCl₅ at 175 °C.

The volume above the melt in the potentiometric cell is not more than 10 cm³. The ideal gas equation indicates in this case that 8.84 × 10⁻³ g of TaCl₅ should be present in the gas phase. Since ca. 0.650 g of TaCl₅ was added to the potentiometric cell, this corresponds to only 1.4% of the total added TaCl₅.

Another way to check the amount of TaCl₅ in the gas phase while allowing also for the formation of vapor complexes with Al₂Cl₆ (from the solvent) is to use the distribution coefficient between the gas phase and the liquid phase. A few unfortunately not very accurate measurements have been made to obtain this value. An average of four measurements gave a value of 0.045 ± 0.013 for TaCl₅ in NaAlCl₄ (pCl range 4.13–4.57) at 175 °C.¹⁶ This should be compared with a value of 0.133 ± 0.011 found for NbCl₅ in KAlCl₄ (pCl range 4.24–5.39) at 300 °C.¹¹ The main reason for the higher value in this latter case is probably the temperature. (The distribution coefficient (but not the vapor pressure) was found to be independent of pCl in the range studied.) The vapor pressure above the solid or liquid phase is higher for TaCl₅ than for NbCl₅ at the measured temperatures.¹⁵ An average of three measurements gave a higher value (i.e. 0.99 ± 0.34) for the distribution coefficient for TaCl₅ at 300 °C²⁸ than for NbCl₅ at 300 °C.¹¹

Since we know from the potentiometric measurements that the concentration of TaCl₅ in the TaCl₅-saturated solution at 175 °C is close to 0.807 ± 0.09 M, we can calculate the amount in the gas phase above the melt in the potentiometric cell to be 10 × 10⁻³ × 0.087 × 0.045 × M_{TaCl_5} = 14.0 × 10⁻³ g, which corresponds to 2.2% of the total amount of Ta(V). It can be seen that this value is not (the uncertainty taken into consideration) very different from the value calculated from the vapor pressure measurements. This does not, however, exclude the formation of vapor-phase complexes, especially at higher temperatures, where the vapor pressure of Al₂Cl₆ above the melt is higher. Such vapor complexes have been found in connection with NbCl₅.¹⁴

Because of the above consideration, no correction was made for the amount of TaCl₅ present above the melt in the potentiometric measurements. However, in the spectrophotometric cells, a correction is necessary because of the much smaller melt volume (ca. 3.2 cm³). It can be calculated that in the slightly acidic melts (spectra A and B) ca. 11.5% of all Ta(V) was found in the gas phase.

Registry No. Ta, 7440-25-7; NaCl, 7647-14-5; AlCl₃, 7446-70-0; TaCl₅, 21640-07-3; TaCl₆, 7721-01-9.



Reprinted from JOURNAL OF THE ELECTROCHEMICAL SOCIETY
 Vol. 138, No. 10, October 1991
 Printed in U.S.A.
 Copyright 1991

The Use of Phosgene for the Removal of Oxide Impurities from a Sodium Chloroaluminate Melt Saturated with Sodium Chloride

I.-Wen Sun,* Karl D. Sienerth,* and Gleb Mamantov**

Department of Chemistry, The University of Tennessee, Knoxville, Tennessee 37996

ABSTRACT

A method based on the use of phosgene to remove oxide impurities from sodium chloroaluminate melts saturated with sodium chloride was investigated using infrared spectroscopy as a probe for melt oxide species. The efficiency of phosgene to remove oxide impurities was found to be affected by temperature. The practical value of this method for oxide removal was demonstrated by the preparation of a solution of pure transition metal chloride complex in a phosgene-purified melt.

Molten chloroaluminates are of considerable interest because of their composition-dependent Lewis acidities and because they have been found to be effective media for unusual redox and coordination chemistry of many elements (1). However, oxide impurities in these molten salts are extremely difficult to avoid and may have pronounced effects on the behavior of other solute species of interest (2-4). Several methods for the determination of the oxide content of chloroaluminate melts via electrochemical and spectroscopic techniques have been reported (5-7), but in most of these methods the oxide level is determined indirectly. Recently, Mamantov *et al.* (8) showed that the intensities of two infrared bands in the region 680-800 cm^{-1} were linearly related to oxide concentration in both basic and acidic sodium chloroaluminate melts. Based on this relationship, Flowers and Mamantov (9) developed a method for direct spectroscopic determination of oxide

concentration in these melts. Using this method, sodium chloroaluminate melts saturated with sodium chloride ($\text{AlCl}_3\text{-NaCl}_{\text{sat}}$) which are prepared in our laboratory were found to contain from 2 to 12 mM oxide impurities, which is often on the order of the concentration of solute species under study. It is, therefore, of interest to develop a method for eliminating oxide from alkali chloroaluminate melts.

Many chlorinating reagents have been used for converting metal oxides into their respective metal chlorides. Among these reagents, carbonyl chloride (COCl_2) is one of the most effective (10). Abdul-Sada and co-workers (11) have shown recently that by using COCl_2 , oxide impurities could be removed from basic aluminum chloride-1-methyl-3-ethylimidazolium chloride ($\text{AlCl}_3\text{-MEIC}$) melts (1b). Carbonyl chloride can be used to affect the *in situ* conversion of some transition metal oxychloride complexes to the respective chloride complexes in basic $\text{AlCl}_3\text{-MEIC}$ melts, as indicated by the studies of Sun *et al.* on the titanium(IV) (12), niobium(V), niobium(IV) (13), and tan-

* Electrochemical Society Student Member
 ** Electrochemical Society Active Member

talium(V) (14) systems. Although a method based on the use of HCl to minimize the level of oxide impurities in $\text{AlCl}_3\text{-NaCl}_{\text{sat}}$ melts has been reported (8), the efficiency of this method was found to be limited. The studies by Hussey and co-workers (12-14) indicated that essentially complete removal of oxide from $\text{AlCl}_3\text{-MEIC}$ melts is possible with the use of COCl_2 . To date, no report concerning the use of COCl_2 to remove oxide impurities from alkali chloroaluminates has appeared. We describe in this paper studies of the use of carbonyl chloride to eliminate oxide impurities from sodium chloroaluminate melts.

Experimental

Procedures for the purification of starting materials (AlCl_3 and NaCl) and the preparation of melts have been described elsewhere (15). Phosgene was obtained from Matheson Gas Products and used as received. The oxide levels of the $\text{AlCl}_3\text{-NaCl}_{\text{sat}}$ melts were monitored by the infrared spectroscopic method described by Flowers and Mamantov (9), except that a transmittance optical cell (16) utilizing silicon windows (Wilmad Glass Company, Inc.) was used in the present work. The optical cell was loaded with $\text{AlCl}_3\text{-NaCl}_{\text{sat}}$ melt inside an inert atmosphere dry box and then connected to the phosgene introduction setup (12). The cell was then heated until the contents were molten using a furnace constructed in-house for use in optical spectroscopy. [NOTE: Because COCl_2 is a highly poisonous gas, the system was operated in a well-ventilated fume hood.] The entire system, including the cell, was evacuated to a pressure lower than 0.025 torr, and then COCl_2 was slowly introduced into the cell from the tank and allowed to react with oxide in the solution. The pressure of the system during this period was monitored with a Hg manometer and was kept as close as possible to atmospheric pressure. After the reaction had proceeded for a set period of time, the unreacted COCl_2 was evacuated from the cell and condensed in a liquid nitrogen trap for later disposal by reaction with a 10% (V/V) NaOH solution. The optical cell was then disconnected from the setup and transferred with the furnace to a Bio-Rad Model FTS-7 Fourier transform infrared spectrophotometer.

Electrochemical experiments were conducted using either a glassy carbon disk or a platinum wire working electrode, a platinum wire counterelectrode, and an Al(III) ($\text{AlCl}_3\text{-NaCl}$, 66.7-33.3 mole percent [m/o])/Al reference electrode. A Princeton Applied Research Model 174 polarographic analyzer coupled with a PAR Model 175 universal programmer and a Houston Instruments Model 2000 X-Y recorder was used to obtain cyclic voltammograms.

Results and Discussion

An infrared absorption spectrum showing the region from 850 to 650 cm^{-1} for a $\text{AlCl}_3\text{-NaCl}_{\text{sat}}$ melt of medium oxide concentration ($\sim 15 \text{ mM}$) is shown in Fig. 1a. The two

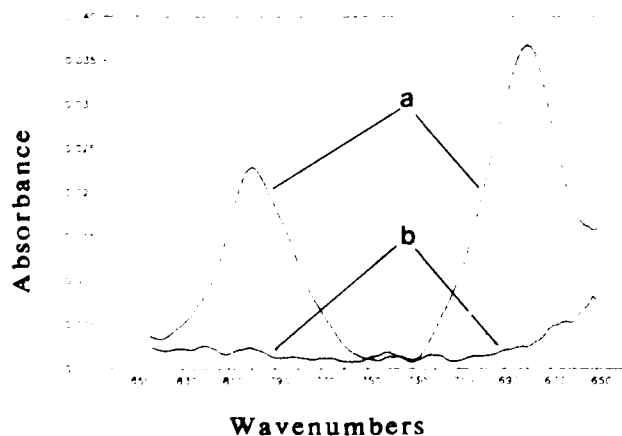


Fig. 1. Infrared absorption spectra of $\text{AlCl}_3\text{-NaCl}_{\text{sat}}$ melt at 200°C: (a) $[\text{O}^{2-}] = 15 \text{ mM}$; (b) same melt after treatment with COCl_2 for 4 h and evacuation for 1 h.

Table I. Variation of infrared absorbances at 801 cm^{-1} with reaction time.

Time (h)	Absorbance	Oxide concentration (mM)
0	0.108	34.0
4	0.054	17.0
6	0.027	8.5
8	— ^a	0.0

^a The absorbance was below the noise level.

absorption bands at 680 and 801 cm^{-1} in this figure are typical of those observed for a $\text{AlCl}_3\text{-NaCl}_{\text{sat}}$ melt containing oxide, as described by Flowers and Mamantov (9). When COCl_2 was allowed to react with this melt at a temperature of 200°C and a pressure of 1 atm for 4 h, both of the absorption bands due to oxide-containing species disappeared. The introduction of COCl_2 also resulted in the appearance of a new sharp absorption peak at ca. 1802 cm^{-1} and a broad band at ca. 886 cm^{-1} , both of which are attributed to the presence of excess COCl_2 in the melt. These bands are shifted with respect to those observed for gaseous COCl_2 , which have been given by Overend and Evans as 1827 cm^{-1} (attributed to the C=O stretch) and 849 cm^{-1} (corresponding to the C—Cl stretch), respectively (17). The carbonyl chloride peaks seen in the melt spectra diminished in height when the melt was further evacuated at 200°C, indicating that COCl_2 could be removed easily from the melt. This is important because COCl_2 is reduced irreversibly in this melt ($E_p \approx -0.35 \text{ V}$ vs. the $\text{Al}^{\text{III}}/\text{Al}$) and could therefore interfere with electrochemical studies of other solutes. The spectrum obtained for this melt after evacuation for 1 h is shown in Fig. 1b. It is apparent that the oxide impurities and COCl_2 were essentially absent. As a further test, a $\text{AlCl}_3\text{-NaCl}_{\text{sat}}$ melt of higher oxide concentration, 34 mM, was prepared and COCl_2 was introduced into the melt at 200°C. The absorbances for the oxide-containing species band at 801 cm^{-1} were recorded after COCl_2 was allowed to react with the oxide-containing species for different periods of time. The results, summarized in Table I, show that during the first four-hour period of reaction, only 14 mM of the oxide impurities had reacted; a period of reaction as long as 8 h was needed in order to remove all of the oxide impurities from this melt. It is not unlikely that poor mixing contributed to the slow rate of the reaction; the time needed for complete removal of oxide impurities might be reduced by rapid stirring of the solution or by bubbling the COCl_2 through the melt.

Experiments similar to those reported above were also conducted at a temperature of 165°C. However, the results obtained were less satisfactory than those obtained at 200°C, possibly indicating that oxide impurities are more stable in the $\text{AlCl}_3\text{-NaCl}_{\text{sat}}$ melt than in the $\text{AlCl}_3\text{-MEIC}$ melts, in which oxides easily react with COCl_2 under much milder conditions (12).

The utility of this method for the purification of melts for use in oxide-sensitive studies can be demonstrated by the preparation of a solution of a pure transition metal chloride complex. An example is given for the tantalum(V) chloride and oxide chloride systems. Figure 2 shows the cyclic voltammograms of Ta(V) species in the $\text{AlCl}_3\text{-NaCl}_{\text{sat}}$ melt obtained using a glassy carbon working electrode; identical behavior was observed when a platinum working electrode was used. Figure 2a shows the cyclic voltammogram of a solution of TaCl_5 in a $\text{AlCl}_3\text{-NaCl}_{\text{sat}}$ melt which contained an excess of oxide, introduced as Li_2CO_3 or Na_2CO_3 . Two reduction waves are observed at potentials of -0.16 and -0.51 V (vs. $\text{Al}^{\text{III}}/\text{Al}$) in this figure; these voltammetric reduction waves are typical for a melt containing only Ta(V) oxide chloride (3). Figure 2b shows a typical voltammogram for a solution containing both Ta(V) oxide chloride and Ta(V) chloride. It is observed that, in addition to the two reduction waves due to Ta(V) oxide chloride, a wave attributed to Ta(V) chloride reduction is located at a potential of ca. 0.06 V. Figure 2c shows the voltammogram

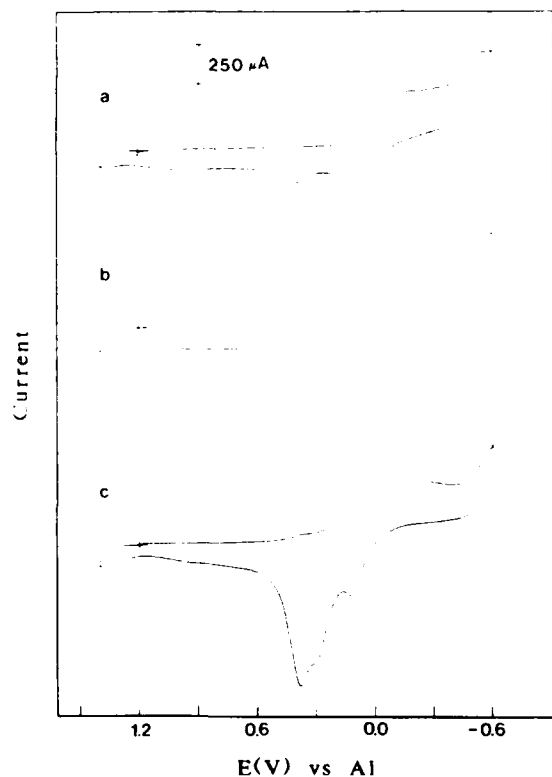


Fig. 2. Cyclic voltammograms of Ta(V) chloride in the $\text{AlCl}_3\text{-NaCl}_{\text{sat}}$ melt at 175°C at a glassy carbon disk electrode: (a) melt containing 21.4 mM of Ta(V) and an excess of oxide relative to the Ta(V); (b) melt containing 22.7 mM of Ta(V) and ca. 7.8 mM oxide; and (c) 23.4 mM Ta(V) chloride in a melt that had been treated with COCl_2 . The potentials are reported vs. an Al(III) ($\text{AlCl}_3\text{-NaCl}$, 66.7-33.3 m/o)/Al reference electrode. The sweep rate is 100 mV s^{-1} .

of a Ta(V) chloride solution prepared using a COCl_2 -treated $\text{AlCl}_3\text{-NaCl}_{\text{sat}}$ melt. The two waves due to the reduction of Ta(V) oxide chloride species are not seen, indicating that the melt was free of oxide. It is interesting to note that in addition to the reduction wave located at 0.06 V, a new reduction wave at -0.05 V also appears in this voltammogram. Initially, it was thought that this peak may be due to the residual oxide because its peak potential is similar to that of one of the Ta(V) oxide chloride waves. However, the peak current of this reduction wave increased as the concentration of Ta(V) chloride was increased and decreased when oxide was introduced, indicating that this wave was indeed related to the Ta(V) chloride species. Further investigation of the redox behavior of Ta(V) species in the $\text{AlCl}_3\text{-NaCl}_{\text{sat}}$ melt is now in progress in our laboratory and will be discussed later in greater detail (18).

It is of interest that the electrochemistry of Ta(V) chloride and oxide chloride species in the $\text{AlCl}_3\text{-NaCl}_{\text{sat}}$ melt is very different from that observed in basic $\text{AlCl}_3\text{-MEIC}$ (14).

The above results show that oxide impurities can be removed from an $\text{AlCl}_3\text{-NaCl}_{\text{sat}}$ molten salt when the melt is

exposed to COCl_2 at a temperature of 200°C . Advantages to using COCl_2 over other chlorinating reagents include its relative efficiency in eliminating oxide and the fact that the only byproducts of the reaction are CO_2 , which is easily removed from the melt by evacuation, and Cl^- ion, which is simply a component of the melt.

Acknowledgment

This work was supported by the Air Force Office of Scientific Research, Grant No. 88-0307.

Manuscript submitted March 4, 1991; revised manuscript received May 7, 1991.

The University of Tennessee assisted in meeting the publication costs of this article.

REFERENCES

- (a) G. Mamantov and R. A. Osteryoung, in "Characterization of Solutes in Nonaqueous Solvents," G. Mamantov, Editor, pp. 223-249, Plenum, New York (1978); (b) C. L. Hussey, in "Advances in Molten Salt Chemistry," Vol. 5, G. Mamantov, Editor, pp. 185-230, Elsevier Science Publishing Co., Amsterdam (1983); and (c) C. L. Hussey, *Pure Appl. Chem.*, **60**, 1763 (1988).
- G. Ting, Ph.D. Dissertation, University of Tennessee, Knoxville, TN (1973).
- L. E. McCurry, Ph.D. Dissertation, University of Tennessee, Knoxville, TN (1978).
- J. B. Scheffler, C. L. Hussey, K. R. Seddon, C. M. Kear, and P. D. Armitage, *Inorg. Chem.*, **22**, 2089 (1983).
- Z. Stojek, H. Linga, and R. A. Osteryoung, *J. Electroanal. Chem. Interfacial Electrochem.*, **119**, 365 (1981).
- T. M. Laher, L. E. McCurry, and G. Mamantov, *Anal. Chem.*, **57**, 500 (1985).
- J.-P. Schoebrechts, P. A. Flowers, G. W. Hance, and G. Mamantov, *This Journal*, **135**, 3057 (1988).
- C. B. Mamantov, T. M. Laher, R. P. Walton, and G. Mamantov, in "Light Metals 1985," H. O. Bohner, Editor, pp. 519-528, The Metallurgical Society of AIME (1985).
- P. A. Flowers and G. Mamantov, *Anal. Chem.*, **59**, 1062 (1987).
- B. L. Tremillon and G. S. Picard, in "Molten Salt Chemistry: An Introduction and Selected Applications," G. Mamantov and R. Marassi, Editors, p. 305, NATO ASI Series, D. Reidel Publishing, Dordrecht, Holland (1987).
- A. K. Abdul-Sada, A. G. Avent, M. J. Parkington, T. A. Ryan, K. R. Seddon, and T. Welton, *J. Chem. Soc. Chem. Commun.*, 1643 (1987).
- I.-W. Sun, E. H. Ward, and C. L. Hussey, *Inorg. Chem.*, **26**, 4309 (1987).
- I.-W. Sun and C. L. Hussey, *ibid.*, **28**, 2731 (1989).
- P. A. Barnard and C. L. Hussey, *This Journal*, **137**, 913 (1990).
- R. Marassi, J. Q. Chambers, and G. Mamantov, *J. Electroanal. Chem. Interfacial Electrochem.*, **69**, 345 (1976).
- P. A. Flowers and G. Mamantov, *Anal. Chem.*, **61**, 190 (1989).
- J. Overend and J. C. Evans, *Trans. Faraday Soc.*, **55**, 1817 (1959).
- V. Taranenkov, Guang-Sen Chen, and G. Mamantov, Unpublished work.

*Submitted to
J. Electrochem. Soc.*

REMOVAL OF OXIDE IMPURITIES FROM ALKALI HALOALUMINATE MELTS USING
CARBON TETRACHLORIDE

Guang-Sen Chen, I-Wen Sun, Karl D. Sienerth,
Anna G. Edwards and Gleb Mamantov
Department of Chemistry, The University of Tennessee,
Knoxville, TN 37996-1600

ABSTRACT

Small amounts of oxide impurities in alkali chloroaluminate and fluorochloroaluminate melts can markedly complicate the electrochemical and spectroscopic behavior of other solute species in these melts. A simple method for the removal of oxides from these melts has been developed in our laboratory. This method is based on the reaction of carbon tetrachloride with oxides to convert them to chlorides. Spectroscopic techniques (UV-visible and IR spectroscopy) have shown that addition of carbon tetrachloride results in the complete conversion of oxides to chlorides.

INTRODUCTION

Oxide impurities in molten chloroaluminates (1) may have pronounced effects on the behavior of other solute species in these media (2-4); these impurities are very difficult to avoid. We have recently reported on the removal of oxide impurities by means of phosgene(COCl_2) from a sodium

chloroaluminate melt saturated with NaCl (5). Prior studies on the determination and removal of oxide species from chloroaluminate melts are summarized briefly in that paper (5).

Phosgene is a very poisonous gas and has to be handled with extreme caution. In addition, we have found that the removal of oxide impurities from acidic sodium chloroaluminate melts ($\text{AlCl}_3/\text{NaCl}$ mole ratio > 1) using COCl_2 is not complete (6).

In this paper, we report a simple method for the removal of oxides from both acidic and basic alkali chloroaluminate melts, as well as fluoroaluminate melts. This method is based on the reaction of carbon tetrachloride with oxide species to convert these species to the corresponding chloride complexes. Using CCl_4 as a chlorinating reagent is advantageous compared to the COCl_2 -treatment in that CCl_4 is much easier to handle.

EXPERIMENTAL

Aluminum chloride (Fluka, $>99.0\%$) was purified by subliming it twice under vacuum in a sealed Pyrex tube. Sodium chloride (Mallinckrodt, reagent grade) was dried under vacuum (<50 mTorr) at 450°C for at least 48hrs. High purity sodium fluoride (ASAR, puratronic, 99.995%), niobium pentachloride (ASAR, puratronic, 99.99%), and tungsten oxychloride (WOCl_4 , Aldrich) were used without further purification. Carbon tetrachloride (water 0.001%) was purchased from Baxter Diagnostics, Inc.

AlCl_3 -NaCl melts were prepared from purified aluminum chloride and vacuum dried sodium chloride. Any remaining base metal impurities in the melts were removed by adding aluminum metal (AESAR, 99.999%) in the process of preparing the melts.

Sodium fluorochloroaluminate melts(7) were prepared by mixing $\text{AlCl}_3\text{-NaCl}_{\text{sat}}$ salts with high purity sodium fluoride in a suitable ratio, followed by premelting this mixture in a quartz tube. All handling of melts and solutes was performed in a nitrogen filled drybox (moisture level <2 ppm). Cells and ampoules were torch-sealed under vacuum (<50 mTorr).

Ultraviolet-visible absorption spectra were obtained using 2 mm path length quartz cells and a Hewlett Packard 8452A diode array spectrophotometer with a water-cooled furnace. Infrared spectra were recorded with a Bio-Rad FTS-7 Fourier transform infrared (FTIR) spectrophotometer which was controlled by a microcomputer system.

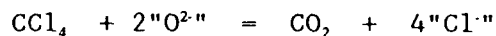
The *in situ* infrared spectra of the molten salts were obtained using a cell similar to that described by Flowers and Mamantov (8,9). The cell utilized silicon windows which were torch-sealed to the Pyrex body of the cell. AceThred adapters on the top of the cell provided access for loading and sample addition, and produced an airtight seal when closed. One AceThred adapter on the cell was covered with a septum. An appropriate amount of CCl_4 was added by injecting it through the septum using an airtight microsyringe (Baxter Diagnostics, Inc.). A furnace with diametrically opposed holes, which was constructed in-house, allowed heating of the melt inside the sample chamber of the FTIR instrument.

RESULTS AND DISCUSSION

$\text{AlCl}_3\text{-NaCl}_{\text{sat}}$ Melt at 200°C. Fig.1 shows typical infrared absorption spectra in the region from 640cm^{-1} to 840cm^{-1} for the $\text{AlCl}_3\text{-NaCl}_{\text{sat}}$ melt containing 20.3 mM Na_2CO_3 . The amount of Na_2CO_3 in this cell was 0.568×10^{-3} moles, which corresponds to $138\mu\text{L}$ CCl_4 (at 25°C) assuming a 1:1 molar reaction. Two absorption bands for aluminum oxychloride were observed at 680cm^{-1} and 800cm^{-1} , which is in very good agreement with the previous results reported by Flowers and Mamantov(10). Thirty minutes after an addition of $150\mu\text{L}$ CCl_4 , which was approximately equal to the molar amount of oxide

in the melt, was made, the intensity of the absorption band at 800cm^{-1} was decreased to ca. 80% of the initial absorption intensity; the signal further decreased to 75% after 60 minutes and remained unchanged for 2 hrs. Subsequently, an excess of CCl_4 , $450\mu\text{L}$ in total, was added to the same cell. After 70 minutes, 70% of the oxide was converted to the corresponding chloride species. After 120 minutes, no infrared absorption bands for the aluminum oxychloride species were detected in the melt. It was apparent that all of the oxide impurities were eliminated in 2hrs. The reaction of the oxide with CCl_4 was much faster than that with phosgene since four and eight hours were needed to remove 14 mM and 34 mM of the oxide, respectively, using COCl_2 (5).

It was also noticed that a doublet occurring at 2342 cm^{-1} and 2357 cm^{-1} , which is typical of the infrared spectrum of CO_2 (11-13), increased significantly with the introduction of CCl_4 into the melt (Fig.2). The doublet bands were observed even in the absence of the sample cell; however, the band intensities were much weaker than those after the addition of CCl_4 . Prior to CCl_4 addition, these weak bands probably resulted from the trace amounts of CO_2 in the sample chamber of the FTIR instrument. From the results depicted in Fig.2, we can reasonably conclude that the reaction of CCl_4 with " O^{2-} " formed CO_2 and " Cl^- " as follows:



where " O^{2-} " and " Cl^- " represent the oxide species and free chloride ions or the chloride species, respectively.

The spectrum obtained for this melt after evacuation for one hour is also shown in Fig.2. It is evident that the CO_2 absorption bands were markedly reduced. After one more hour of evacuation, these bands were further decreased to the level observed before the introduction of CCl_4 . These results indicate that the by-product (CO_2) formed by the reaction of CCl_4 with the oxide impurities was easily removed by evacuation.

An alternative way to measure oxide impurities is to examine the UV-visible spectra of Nb(V) in the melts. This approach may be more sensitive for detecting a very low concentration of oxide species in the melts than the infrared spectral approach. A UV-visible absorption spectrum using niobium(V) species as a probe is shown in Fig.3. The concentration of the initial niobium oxychloride, which was added as NbOCl_3 , was 0.17mM. The results are summarized in Table 1 along with the literature data. The spectrum obtained before the introduction of CCl_4 (Fig.3a) showed two main bands at 220nm and 270nm, which were similar to those for NbOCl_3 in HCl and in basic room temperature melts(19) (see Table 1). We also observed results similar to the literature data for niobium oxychloride in NaAlCl_4 -NaF(90-10mol%) at 480°C at a higher concentration of 1mM.

With the addition of CCl_4 to this cell, a significant change in the UV-visible spectrum was observed (Fig. 3b). After 45 minutes, the spectrum exhibited a much higher absorbance in the 250 - 350nm region than that observed for the oxychloride species. Several absorbance maxima were observed at 242, 290, 316(sh) and 350nm(sh), which are in excellent agreement with those for NbCl_5 in other solvents (Table 1). These results indicated clearly that using CCl_4 can reduce the oxide impurities to an extremely low level.

AlCl_3 -NaCl (63-37mol%) Melt. The oxide contamination in acidic chloroaluminates also complicates the electrochemical and spectroscopic behavior of some solutes of interest in these melts(14). However, removal of oxide impurities from acidic chloroaluminate melts has not been reported previously. As mentioned above, phosgene cannot eliminate the oxide completely from these melts(6). Therefore, we attempted to remove the oxide impurities from an acidic melt, AlCl_3 -NaCl (63-37mol%), using CCl_4 . The efficiency was monitored by measuring the UV-visible spectra of melts containing a W(VI) species, which was employed as the probe.

Fig.4 shows the change in the UV-visible spectrum of tungsten(VI) species in the acidic melts with the addition of CCl_4 . The features of these spectra are

summarized in Table 2 together with the literature data. From these results it may be concluded that the tungsten(VI) species in the initial melt was $WOCl_4$. A significant change in the spectrum was observed ca. 2 hrs after the introduction of CCl_4 . The new spectrum was characteristic of WCl_6 (see Table 2). It is clear that the use of CCl_4 can remove all of the oxide impurities in these melts. It was also noted that the reaction in the acidic melts was slower than that in $AlCl_3$ - $NaCl_{mol}$ melts.

NaAlCl₄-NaF (90-10mol%) Melt. Sodium fluorochloroaluminate melts are interesting solvents because the electrochemistry and spectroscopy of solutes can be investigated over a large temperature region, ca. 200°C -800°C or higher(15). There exists a large quantity of liquid phase for the $NaAlCl_4$ - NaF (90-10mol%) at temperatures $\geq 200^\circ C$, although the liquidus temperature at which the melt is completely molten, is 395°C.

We first attempted to remove the oxide impurities at a relatively low temperature (200-250°C) using CCl_4 . However, it was observed that CCl_4 only partially converted the oxides to the chlorides. This was probably due to the presence of the solid precipitate which prevented the complete conversion.

As the temperature was increased to the liquidus temperature, 395°C or higher, the complete conversion of the oxides to chlorides by CCl_4 was obtained in less than five minutes as indicated by the UV-visible spectral changes of Nb(V) species contained in the melt (Table 2). We also noticed that the chloride species transformed again to the oxide species ca. 45 minutes after the introduction of 10 μ L CCl_4 to 2.38g of the fluorochloroaluminate melt with 1 mM Nb(V) species in a quartz UV cell (2mm in path length). This may be caused by the slight reaction of the melt with the quartz cell.

In summary, an oxide-free fluorochloroaluminate melt can be obtained by the following procedure: 1) increase the temperature to 400°C or higher for $NaAlCl_4$ - NaF (90-10mol%); 2) add an excess of CCl_4 to the cell after the melt becomes molten; 3) keep the cell at the high temperature for ca. 30 minutes; 4) cool the cell to

300°C or lower; 5) evacuate the excess CCl_4 and CO_2 at this temperature for ca. 2 hours; and 6) cool the melt to room temperature.

CONCLUSIONS

Spectroscopic techniques (IR and UV-visible spectroscopies) indicate that the addition of carbon tetrachloride removes all traces of oxide impurities from both basic and acidic sodium chloroaluminate melts, as well as from fluorochloroaluminate melts. This method has an obvious advantage over other using chlorinating reagents, such as COCl_2 and HCl , since CCl_4 is much easier to handle. This method may also be suitable for the removal of oxide impurities from other alkali chloride melts such as LiCl-KCl and KCl-NaCl .

ACKNOWLEDGMENT

This work was supported by the Air Force Office of Scientific Research, Grant No. 88-0307.

REFERENCES

- 1) T.M. Laher, L.E. McCurry, and G. Mamantov, *Anal. Chem.*, **57**, 500(1985).
- 2) B. Gilbert and R.A. Osteryoung, *J. Am. Chem. Soc.*, **100**, 2725(1978).
- 3) K. Zachariassen, R.W. Berg and N.S. Bjerrum, *J. Electrochem. Soc.*, **134**, 1153(1987).
- 4) I-W. Sun, E.H. Ward, and C.L. Hussey, *Inorg. Chem.*, **26**, 4309(1987).
- 5) I-W. Sun, K.D. Sienerth, and G. Mamantov, *J. Electrochem. Soc.*, **138**, 2850(1991).
- 6) I-W. Sun, K.D. Sienerth, and G. Mamantov, unpublished results.
- 7) B. Gilbert, S.D. Williams, and G. Mamantov, *Inorg. Chem.*, **27**, 2359(1988).

- 8) P.A. Flowers and G. Mamantov, J. Electrochem. Soc., 136, 2944(1989).
- 9) P.A. Flowers and G. Mamantov, Anal. Chem., 61, 190(1989).
- 10) P.A. Flowers and G. Mamantov, ibid., 59, 1062(1987).
- 11) J.H. Taylor, W.S. Benedict, and J. Strong, J. Chem.Phys., 20, 1884(1952).
- 12) A.H. Nielsen and R.J. Lageman, ibid., 22, 36(1954).
- 13) N.B. Colthup, L. H. Daly, and S.E. Wiberley, "Introduction to Infrared and Raman Spectroscopy", Academic Press, New York, (1975) pp.43-45.
- 14) J.-P. Schoebrechts, P.A. Flowers, G.W. Hance, and G. Mamantov, J. Electrochem. Soc., 135, 3057(1988).
- 15) G.-S. Chen, A.G. Edwards, and G. Mamantov, in preparation.
- 16) R.F.W. Bader and A.D. Westland, Can. J. Chem, 39, 2306(1961).
- 17) B.J. Brisdon, G.W.A. Fowles, D.J. Tidmarsh, and R.A. Walton, Spectrochim. Acta, 25A, 999(1969).
- 18) M. Volloton and A.E. Merbach, Helv. Chim. Acta, 57, 2345(1974).
- 19) I-W. Sun and C.L. Hussey, Inorg, Chem., 28, 2731(1989).
- 20) E. Hondrogiannis and G. Mamantov, unpublished results.
- 21) C.K. Jorgesen, Mol. Phys., 2, 309(1959).
- 22) E. Thorn-Csanyi and H. Timm, J. Mol. Cat., 28, 37(1985).

Table 1 UV-visible Spectroscopic Data for Niobium(V) Species

Species	Solvent	λ/nm ($\epsilon/\text{M}^{-1}\text{cm}^{-1}$)	Ref
NbCl_5	gas at 100°C,	240(1.0×10^4), 285(1.0×10^4)	16
NbCl_6^-	CH_3CN	242(8.1×10^3), 294(3.4×10^4), 318(1.4×10^4), 355(sh, 2.5×10^3)	17
$\text{Et}_4\text{NNbCl}_6$	CH_3CN	242(6.4×10^3), 290(2.9×10^4), 315(sh, 1.1×10^4), 355(sh, 2.0×10^3)	18
NbCl_6^-	AlCl_3 -MEIC (44.4/44.6mol%)	291(3.2×10^4), 316(1.7×10^4) 360(sh, 4.1×10^3)	19
NbCl_5	AlCl_3 - NaCl_{sat}	240(1.1×10^4), 288(1.3×10^4)	20
NbCl_6^-	AlCl_3 - NaCl_{sat} (CCl_4 -treated, at 200°C)	242(5.3×10^3), 290(1.4×10^4), 316(sh, 9.1×10^3), 350(sh, 3.4×10^3)	this work
NbOCl_5^{2-}	12M HCl	228(3.6×10^3), 280(1.1×10^4) 320(sh, 1.3×10^3)	19
NbOCl_5^{2-}	AlCl_3 -MEIC	278(1.3×10^4), 317(sh, 1.2×10^3)	19
$\text{NbOCl}_y^{(y-3)-}$	AlCl_3 - NaCl_{sat} at 200°C	220(6.9×10^3), 270(4.7×10^3)	this work
NbOCl_5^{2-}	NaAlCl_4 -NaF (90-10mol%) at 480°C.	278(S)	this work

Table 2 UV-visible Spectroscopic Data for Tungsten(VI) Species

Species	Solvent	λ/nm ($\epsilon/\text{M}^{-1}\text{cm}^{-1}$)	Ref
WCl ₆	CCl ₄	334(8.0x10 ³), 379(3.0x10 ³) 447(8.0x10 ²), 514(? , 1.7x10 ²) 585(? , 60), 720(?)	21
WCl ₆	vapor	220(s), 275(sh), 330(s), 375(sh) 430(w)	14
WOCl ₄	toluene	355(s)	22
WOCl ₄	vapor	220(s), 250(sh), 270(sh), 355(s) 460(w)	14
WCl ₆	AlCl ₃ -NaCl (63-37mol%) at 200°C	228(4.3x10 ³), 266(sh, 2.1x10 ³), 284(sh, 1.4x10 ³), 360(3.8x10 ³)	this work
WCl ₆	AlCl ₃ -NaCl (63-37mol%) (after CCl ₄ - treatment at 200°C	332(9.7x10 ³), 378(sh, 4.6x10 ³), 434(sh, 1.9x10 ³), 484(8.4x10 ²)	this work

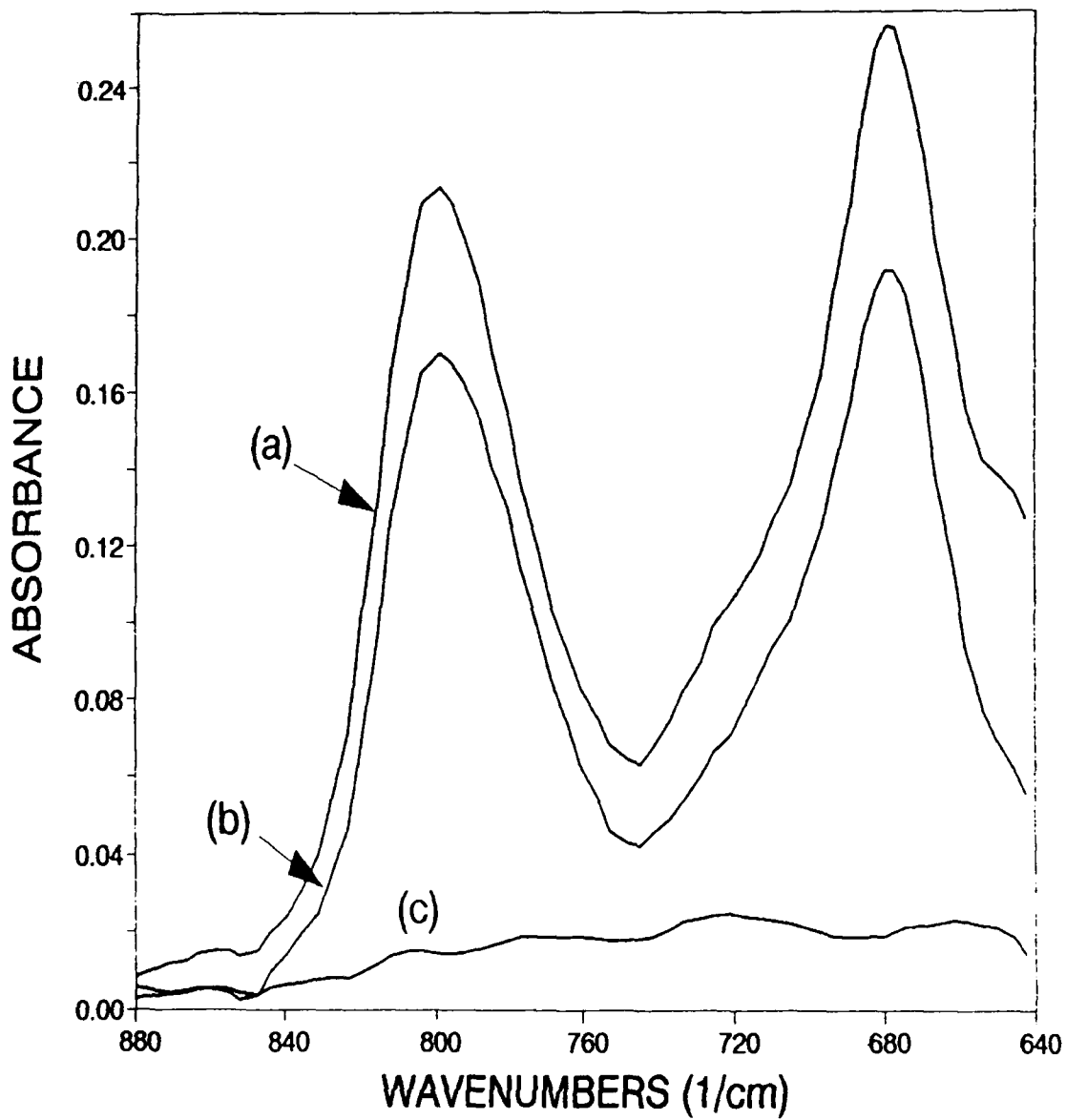
Figure Captions

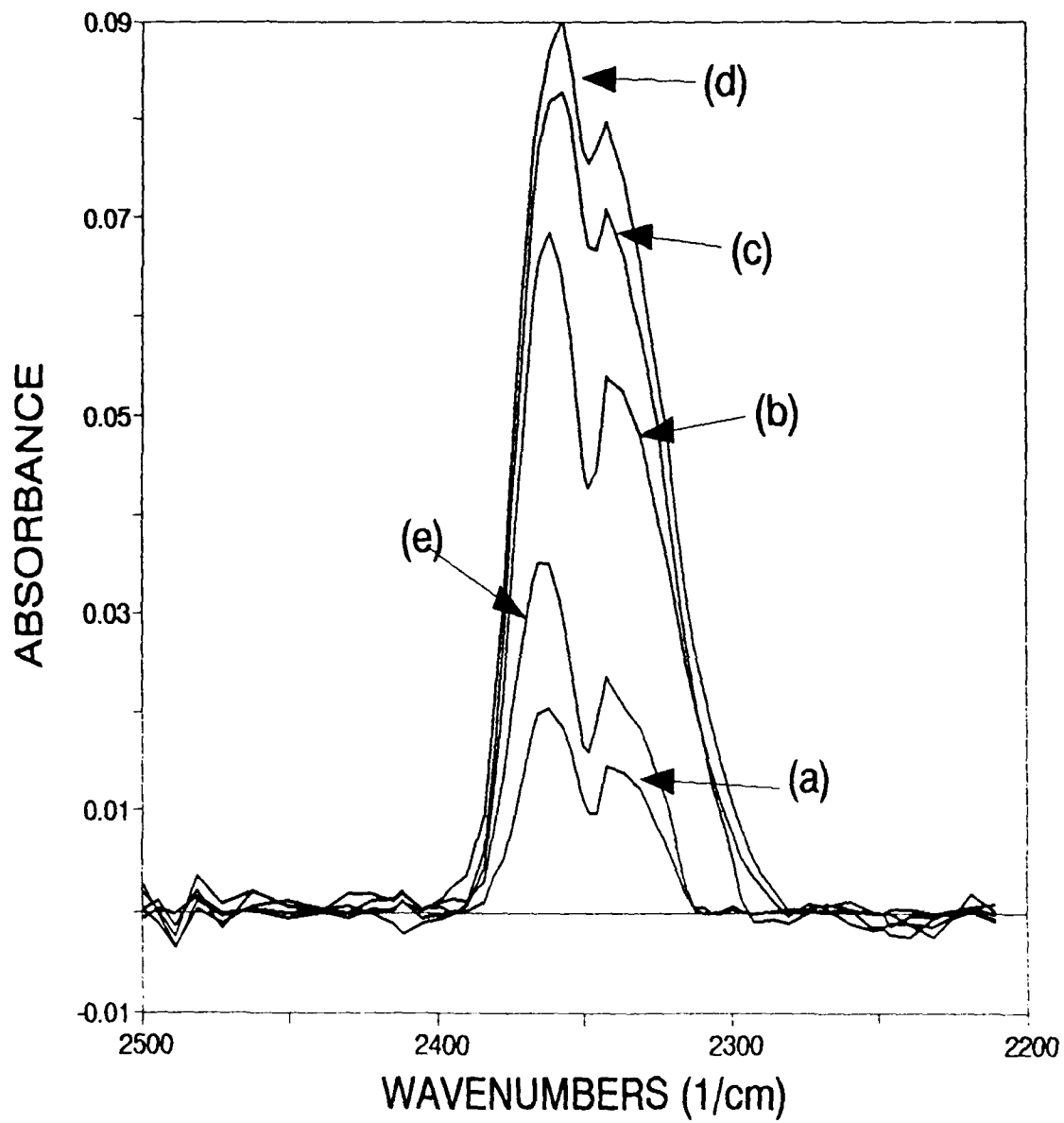
Fig.1 Infrared absorption spectra of the aluminum oxychloride species in a $\text{AlCl}_3\text{-NaCl}_{\text{sat}}$ melt containing 20.3 mM Na_2CO_3 at 200°C. (a) the initial melt; (b) 30 minutes after the introduction of 150 μL CCl_4 ; (c) 120 minutes after the introduction of 450 μL CCl_4 total.

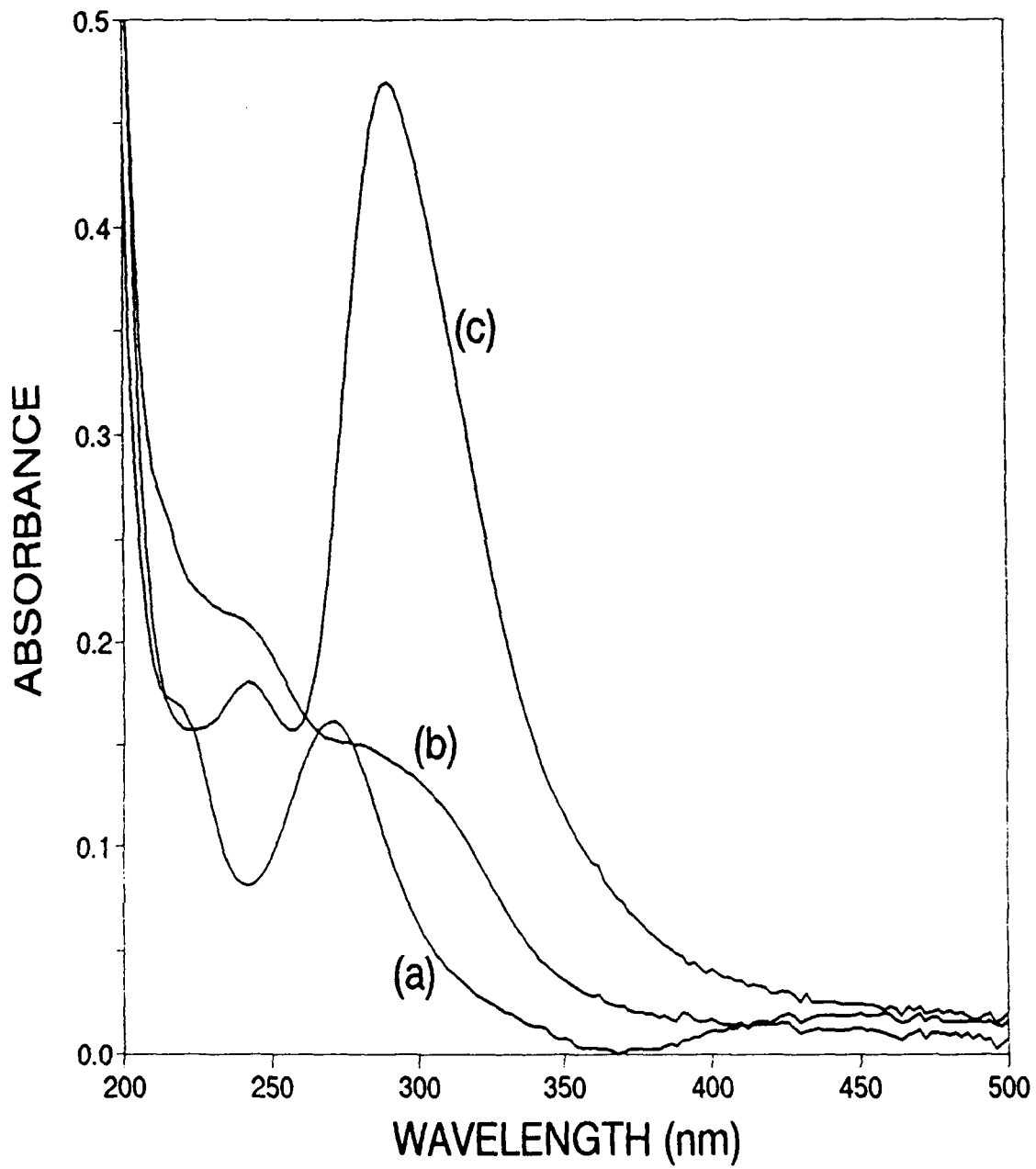
Fig.2 Infrared absorption spectra of CO_2 in the $\text{AlCl}_3\text{-NaCl}_{\text{sat}}$ melt containing 20.3mM Na_2CO_3 at 200°C. (a) the initial melt; (b) 25 minutes after the addition of 50 μL CCl_4 ; (c) 30 minutes, 150 μL CCl_4 ; (d) 135 minutes, 450 μL CCl_4 ; (e) after one hour of evacuation.

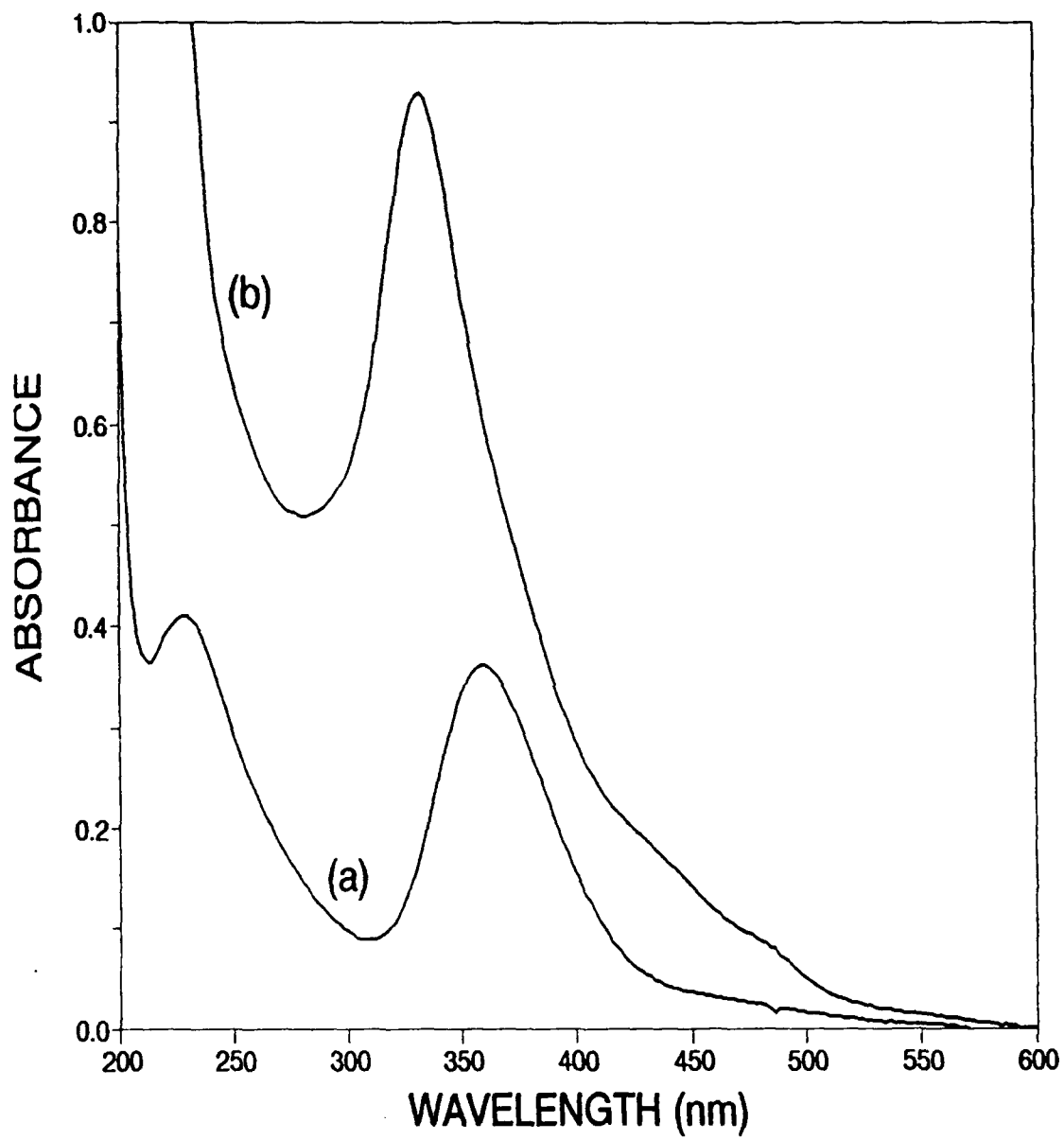
Fig.3 UV-visible absorption spectra of niobium (V) species in a basic melt, $\text{AlCl}_3\text{-NaCl}_{\text{sat}}$ (2.317g), at 200°C. (a) the initial melt containing 0.17 mM NbOCl_3 ; (b) 16 minutes, and (c) 45 minutes after the introduction of 10 μL CCl_4 . The quartz cell path length was 2 mm.

Fig.4 UV-visible absorption spectra of tungsten (VI) species in an acidic melt, $\text{AlCl}_3\text{-NaCl}$ (63-37mol%, 2.781g), at 200°C. (a) the initial melt containing 0.478 mM WOCl_4 ; (b) 120 minutes after the introduction of 20 μL CCl_4 . The quartz cell path length was 2 mm.









STUDIES OF THE ELECTROREDUCTION OF TANTALUM AND NIOBIUM IN FLUROCHLOROALUMINATE MELTS

V. Taranenکو, K.D. Sienerth, N. Sato, A.G. Edwards and G. Mamantov

Department of Chemistry, University of Tennessee
Knoxville, TN 37996-1600, USA

ABSTRACT

The electrochemistry of Ta(V) and Nb(V) in sodium fluorochloroaluminate melts has been examined. The electrolysis of Ta(V) in these melts has been studied, and deposits of tantalum metal have been obtained. The quality of the deposit has been found to depend on the amount of fluoride in the melt, the Ta(V) concentration, the current density, and the temperature. The Raman spectroscopy of Ta(V) species in fluorochloroaluminate melts has been investigated.

Introduction

The electrochemistry and metallurgy of the transition metals of Groups IV-B, V-B, and VI-B (the refractory metals) have received much attention in the last several decades due to the increasing importance of these metals in the aerospace industry and in the construction of electrical and electronic devices. In 1965, Mellors and Senderoff[1] introduced a general method for obtaining pure, coherent deposits of each of these metals, with the exception of titanium, by electrolytic reduction from the ternary eutectic LiF:NaF:KF (46.5:11.5:42.0 mole percent), or FLINAK. Senderoff and coworkers published a series of articles describing their proposed mechanisms for the reduction of several metals[2-6], and since that time, additional research has been devoted to studies of refractory metals in molten fluorides.[7-17]

Studies of niobium and tantalum in other media have also been conducted; of particular interest is the use of alkali chloroaluminate melts. By comparison with FLINAK, sodium chloroaluminate ($\text{AlCl}_3\text{-NaCl}$) melts may be considered as favorable systems in several respects. First, the liquidus temperatures for chloroaluminates lie below 200 °C for melt compositions in the range from 49.8 to 100 mole percent AlCl_3 , while FLINAK has a eutectic point of 454 °C, and generally temperatures in excess of 750 °C are required

for refractory metal deposition. The Lewis melt acidity can be varied over a broad range by changing the AlCl_3 to NaCl ratio. Finally, the highly aggressive nature of fluoride melts and the temperatures required for their use greatly limit the materials which can be used for bath construction, whereas chloroaluminate studies can be conducted using even simple Pyrex cells.

Investigations of the reduction of tantalum in chloroaluminates have been reported by von Barner, *et al.*, [18] and that of niobium by Ting, *et al.* [19]. In the case of tantalum, the mechanism for the reduction of Ta(V) involves the formation of low oxidation state cluster species such as $\text{Ta}_6\text{Cl}_{14}$, which, due to high stability and/or insolubility in the melt, prevent further reduction to the metal. Similarly, the mechanism for the reduction of Nb(V) in the chloroaluminate system involves the formation of the cluster Nb_3Cl_8 , which inhibits reduction to the metal. Analogous results with zirconium [20] and tungsten [21] suggest a general tendency of the chloroaluminate system to stabilize the formation of cluster species of refractory metals, and thus hinder the electrolytic formation of metal deposits in these melts.

Fluoride-containing chloroaluminate melts are a possible compromise between the use of fluoride melts, which require somewhat severe conditions, and low-temperature chloroaluminate melts. It was felt that the inclusion of fluoride into the chloroaluminate melts may sufficiently inhibit the formation of cluster species as to allow reduction to the metal.

Raman spectroscopy has proved to be a useful tool in the analysis of a wide variety of solutes in fluoride and chloroaluminate molten salts, as well as of the melts themselves. Gilbert, *et al.*, [22] reported the Raman spectra of chloroaluminate melts containing varied amounts of fluoride. These investigations indicated the existence of fluorochloroaluminate species of the form $\text{AlF}_x\text{Cl}_{4-x}^-$, with x dependent on the ratio (R) of fluoride to aluminum. Huglen, *et al.*, [23] characterized alkali chloroaluminate melts which contained TaCl_3 using Raman spectroscopy; these workers found that the formation of TaCl_6^- occurred readily in melts saturated with chloride.

Experimental

All chemicals were purified using the usual methods for chloroaluminate preparation. Aluminum chloride (Fluka, puriss) was vacuum distilled twice in Pyrex tubes; sodium chloride (Mallinckrodt, reagent grade) was dried under vacuum (< 50 mTorr) at 400°C for > 48 hours; sodium fluoride (Fluka, purum) was melted in a glassy carbon crucible and recrystallized by slow cooling; tantalum(V) chloride and niobium(V) chloride (Aesar, 99.9%) were sublimed in

evacuated, sealed pyrex tubes at 200 and 220 °C, respectively.

Sodium fluorochloroaluminate melts were prepared by combining NaF and NaAlCl₄ in the desired ratio and premelting this mixture in quartz tubes[22].

For the Raman studies, the samples were irradiated with either the 488.0 nm or the 514.5 nm line from a Coherent Model I100-15 Argon Ion laser. The scattered signals were acquired at 90° on a Jobin-Yvon Ramanor 2000M monochromator equipped with a cooled RCA CR31034 photomultiplier tube and a Pacific Precision Instruments Model 126 photon counter interfaced to an IBM PS/2 Model 55SX computer.

Electrochemical studies were conducted using a glassy carbon crucible in a stainless steel or nickel cell, or in sealed quartz cells. The differential thermal analysis studies were conducted using quartz cells and a DTA system built in-house. The points on the phase diagram were determined primarily from cooling curves.

RESULTS

Phase Diagram for NaAlCl₄-NaF: In order to establish the minimum working temperature for the sodium fluorochloroaluminate (NAFCAL) melts at various values of R, the phase equilibria of the system NaAlCl₄-NaF were investigated using differential thermal analysis. The approximate phase diagram for this system is given in Figure 1. An examination of the region through which the mixture is less than 75 mole percent in NaF ($R = F/Al < 3$) reveals three phase lines: The horizontal line at ≈152 °C is attributed to the melting of NaAlCl₄; the topmost line seen in this region is ascribed to the solubilization of NaCl in the melt; the middle line arises from the exothermic

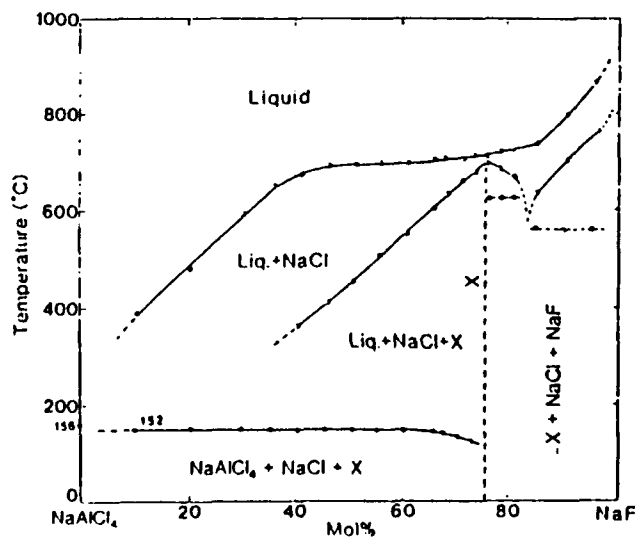
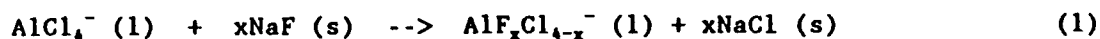


Figure 1. Phase diagram of the NaAlCl₄ - NaF system. The compound X refers to NaAlF₃Cl.

reaction (see equation 1) which results in the fluorochloroaluminate species. Two important conclusions to be drawn from this diagram are that at values of R less than three, all fluoride in the molten mixture is in the form of



fluorochloroaluminate, and that this fluoride-containing species is in the liquid state at fairly low temperatures when the fluoride concentration is low.

At 75 mole percent NaF ($R = 3.0$), the line for the exchange reaction between NaAlCl_4 and NaF reaches a maximum and begins to decline towards an apparent eutectic point at approximately 85 mole percent NaF. Such behavior indicates the formation of a compound between NaAlCl_4 and NaF; the fact that this occurs at $R = 3.0$ implies that the compound formed is NaAlF_3Cl .

Raman Spectroscopy of Ta(V) in Fluorochloroaluminates: Raman spectra of fluorochloroaluminate melts containing potassium heptafluorotantalate, K_2TaF_7 , have been obtained. A spectrum for a 0.28 molal solution of K_2TaF_7 in NAFCAL ($R = 1.6$) is shown in Figure 2a. The TaF_7^{2-} moiety is expected to exhibit a strong band at approximately 640 cm^{-1} [7,17]. However, that band is absent. Rather, below 850 cm^{-1} , this spectrum is similar to that which one would expect from NAFCAL ($R = 1.5$) in the absence of any solute[22]. Figure 2b shows a Raman spectrum of 0.26 m K_2TaF_7 in NAFCAL at higher fluoride concentration ($R = 2.5$).

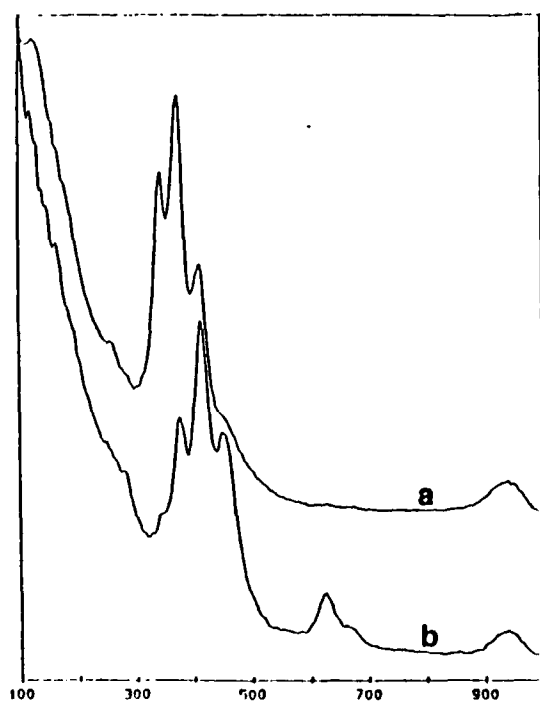


Figure 2. Raman spectra of NAFCAL solutions of K_2TaF_7 .

- a. 0.28 m K_2TaF_7 in NAFCAL ($R = 1.6$). Temperature - 810 °C.
- b. 0.26 m K_2TaF_7 in NAFCAL ($R = 2.5$). Temperature - 830 °C.

The differences between the spectra 2a and 2b at the higher R value are directly related to the increased concentration of the more highly fluorinated fluorochloroaluminate ions. Of significance is that the Raman spectra of K_2TaF_7 in basic sodium chloroaluminate melt (with no added NaF) resemble the Raman spectra of NAFCAL melts without K_2TaF_7 . The absence of spectral evidence for TaF_7^{2-} and the formation of fluorochloroaluminate species suggest that TaF_7^{2-} is exchanging fluoride for chloride from solvent species. These observations indicate that there is an exchange reaction in which the formation of Al-F bonds is favored over that of Ta-F bonds, even at R values greater than 1. However, the exact identity of the species formed is unknown. It is noted in Figure 2b that while the band positions are those expected for the various fluorochloroaluminate ions, the relative intensities among the 372, 411, and 452 cm^{-1} bands are different from those which have been reported previously for the composition with $R = 2.5$ [22]. Specifically, the band at 411 cm^{-1} is more intense in the presence of K_2TaF_7 . Huglen, *et al.*, [23] obtained the Raman spectra for $TaCl_5$ and $TaCl_6^-$ in acidic and basic chloroaluminate melts. The former species, which predominates in acidic melts, exhibits a band at 414 cm^{-1} (285 °C). The octahedral $TaCl_6^-$ ion, which is favored in basic melts, has a band at 392 cm^{-1} (215 °C). Thus, it is reasonable to assume that the increased height in the 411 cm^{-1} band is due to some chlorinated tantalum species. That complete exchange between fluoride and chloride is occurring to some extent is supported by the observation that if a portion of the melt tube is allowed to remain at room temperature while the solution is molten, a solid is readily collected in the cooler portion of the tube. The Raman spectrum of this solid agrees well with the Raman spectrum of $TaCl_5$ [24]. The appearance of a band at 935 cm^{-1} for K_2TaF_7 in NAFCAL suggests that some tantalum oxide species is also present in solution.

Electrochemistry of Ta(V) and Nb(V) in NAFCAL: The electrochemistry of Ta(V) in NAFCAL (low R) and $NaAlCl_4$ solutions has been studied at temperatures ranging from 160 to 630 °C using cyclic voltammetry and normal pulse voltammetry. Figure 3a shows a typical cyclic voltammogram of K_2TaF_7 in $NaAlCl_4$ at 630 °C. The reduction peak at 0.35 V is due to reduction of Ta(V); its shape indicates that it is composed of at least two waves nearly superimposed; the oxidation wave seen on the return sweep has the appearance of a stripping wave. Figures 3b and 3c show cyclic voltammograms obtained for the same system at 540 and 400 °C, respectively. It can be seen that, not only does the peak height decrease with temperature, but the slope of the reduction peak also decreases, causing the wave to appear broader; these

trends continue as the temperature is further decreased. If one calculates the parameter αn from E vs. $\log [(i_d - i)/i]$ plots (which were found to be linear for all temperatures studied) for experiments conducted at various temperatures, one finds that the value found at 630 °C is nearly 5 times that found at 160 °C. This implies that either the number of electrons involved in the charge transfer reaction increases, or that the charge transfer kinetics increases with temperature, or that both of these conditions are true. It has been noted from electrolysis experiments that the deposition of tantalum metal from these melts occurs more readily at higher temperatures. It is interesting to note that no differences are observed in the electrochemical results of experiments utilizing $TaCl_5$ from those conducted with K_2TaF_7 as solute; indeed, identical results are obtained when both species are added to the solution. This appears to support the proposed exchange of F^- and Cl^- between $AlF_xCl_{4-x}^-$ and TaF_7^{2-} .

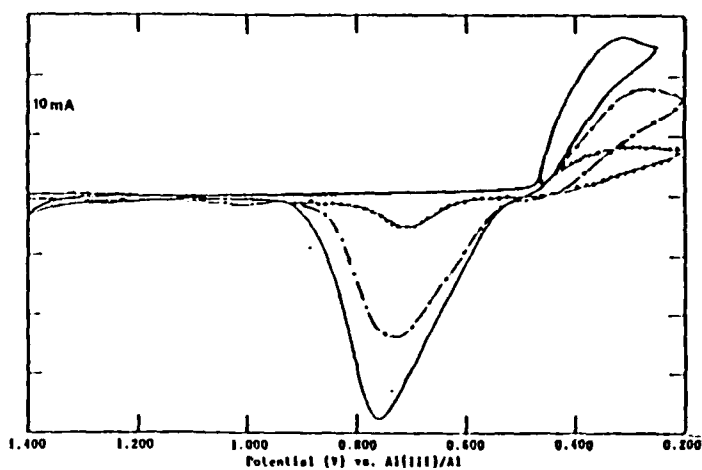


Figure 3. Cyclic voltammograms for Ta(V) in NAFCAL using a tungsten wire working electrode and an Al(III)/Al reference electrode.

- a. —————
Temperature = 630 °C.
b. -●-●-●-●-●-
Temperature = 540 °C.
c. ······
Temperature = 400 °C.

Investigation of the electrochemistry of Nb(V) in NAFCAL revealed similar results, with a sharp reduction peak, seemingly composed of more than one wave, observed at higher temperatures, and with the slope and peak height of this wave decreasing with temperature.

Electrolytic Deposition of Tantalum and Niobium from NAFCAL: Electrolysis experiments have been conducted to determine the feasibility of electrodepositing tantalum and niobium from NAFCAL, and to determine the optimum parameters for successful deposition. Photomicrography and ESCA (electron spectroscopy for chemical analysis) analyses of deposits obtained on nickel and stainless steel have shown that it is indeed possible to obtain electrodeposits of pure tantalum on these substrates. In the case of niobium,

it is likely that the deposit is an alloy of niobium and the substrate material.

Detailed analysis of a large number of tantalum electrolysis samples has shown that the optimum deposits were obtained using experimental parameters as follows:

Ratio, $R = [F^-]:[Al^{3+}]$: The best results are obtained when the value of R lies between 0.8 and 1.4.

Ta(V) Concentration: Of the range studied (3.3 - 25 weight percent), the best results were obtained in the range of 10 to 15 weight percent.

Current Density (I_0): A range from 8.0 to 170 mA/cm² was studied; the optimum range was found to be 10 to 50 mA/cm². Powdery deposits are formed at low I_0 , and high I_0 resulted in dendrite formation.

Temperature: A range of temperatures from 420 to 760 °C was studied; it was found that better quality deposits were produced at temperatures greater than 650 °C. At the lower temperatures, the deposits were powdery and nonmetallic.

References:

- 1) Mellors, G.W. and Senderoff, S.: J. Electrochem. Soc., 1965, 112, 266.
- 2) Senderoff, S., Mellors, G.W. and Reinhart, W.J.: *ibid.*, 1965, 112, 840.
- 3) Mellors, G.W. and Senderoff, S.: *ibid.*, 1966, 113, 60.
- 4) Mellors, G.W. and Senderoff, S.: *ibid.*, 1966, 113, 66.
- 5) Senderoff, S. and Mellors, G.W.: Science, 1966, 153, 1475.
- 6) Senderoff, S. and Mellors, G.W.: J. Electrochem. Soc., 1967, 114, 586.
- 7) Fordyce, J.S., and Baum, R.L.: J. Chem. Phys., 1966, 44, 1159.
- 8) Fordyce, J.S., and Baum, R.L.: *ibid.*, 1966, 44, 1166.
- 9) Decroly, C., Mukhtar, A. and Winand, R.: J. Electrochem. Soc., 1968, 115, 905.
- 10) Inman, D. and White, S.H.: J. Appl. Electrochem., 1978, 8, 375.
- 11) Ahmad, I., Spiak, W.A. and Janz, G.J.: *ibid.*, 1981, 11, 291.
- 12) Yoko, T. and Bailey, R.A.: Proc. First Int. Symp. Molten Salt Chem. and Tech., 1983, 111.
- 13) Qiao, Z. and Taxil, P.: J. Appl. Electrochem., 1985, 15, 259.
- 14) White, S.H. and Twardoch, U.M.: *ibid.*, 1987, 17, 225.
- 15) Capsimalis, G.P., Chen, E.S., Peterson, R.E. and Ahmad, I.: *ibid.*, 1987, 17, 253.
- 16) Taxil, P. and Mahenc, J.: *ibid.*, 1987, 17, 261.
- 17) von Barner, J.H., Christensen, E., Bjerrum, N.J. and Gilbert, B.: Inorg. Chem., 1991, 30, 561.
- 18) von Barner, J.H., McCurry, L.E., Jorgensen, C.A., Bjerrum, N.J. and Mamantov, G.: Submitted to Inorg. Chem., 1990.
- 19) Ting, G., Fung, K.W. and Mamantov, G.: J. Electrochem. Soc., 1976, 123, 624.
- 20) Gilbert, B., Mamantov, G. and Fung, K.W.: Inorg. Chem., 1975, 14, 1802.
- 21) Schoebrechts, J-S., Flowers, P.A., Hance, G.W. and Mamantov, G.: J. Electrochem. Soc., 1988, 135, 3057.
- 22) Gilbert, B., Williams, S.D. and Mamantov, G.: Inorg. Chem., 1988, 27, 2359.
- 23) Huglen, R., Poulsen, F.W., Mamantov, G. and Begun, G.M.: Inorg. Chem., 1979, 18, 2551.
- 24) Beattie, I.R. and Ozin, G.A.: J. Chem. Soc., A, 1969, 1691.

**Electrochemical Studies of Tantalum in
Fluorochloroaluminate Melts at 200 - 450°C**

G. S. Chen and G. Mamantov

Department of Chemistry,
University of Tennessee,
Knoxville, Tennessee 37996

We are interested in the electrochemistry of refractory metals such as niobium, tantalum and tungsten in alkali chloroaluminate and fluorochloroaluminate melts. Von Barner et al.(1) have recently reported on the electrochemical and spectroscopic studies of tantalum species in $\text{AlCl}_3\text{-NaCl}$ melts at 160 - 300°C. Tantalum (V) forms two different species, TaCl_6^- and TaCl_5 , in basic ($\text{AlCl}_3/\text{NaCl}$ mole ratio < 1) and moderately acidic $\text{AlCl}_3\text{-NaCl}$ melts (1,2). In addition, TaOCl_4^- is formed in basic melts in the presence of small amounts of oxide ions (1). It was concluded that the reduction of tantalum (V) in an acidic $\text{AlCl}_3\text{-NaCl}$ (51.49 mol%) at 175°C follows the reaction sequence, $\text{Ta}^{5+} + e = \text{Ta}^{4+}$, $2\text{Ta}^{4+} = \text{Ta}_2^{8+}$, $\text{Ta}_2^{8+} + 2e = \text{Ta}_2^{6+}$, $5\text{Ta}_2^{6+} = \text{Ta}_6^{14+} + 4\text{Ta}^{4+}$, resulting in the formation of one or more tantalum clusters(1,3). Formation of metallic tantalum was not observed in the electrolysis at 175°C in the sodium chloroaluminate melts.

McCurry(3) also investigated the electrochemical behavior of tantalum(V) in $\text{AlCl}_3\text{-NaCl}_{\text{sat}}$ melts in the presence of small amounts of oxide. These studies resulted in a voltammetric method employing tantalum(V) as a probe to determine dissolved oxide impurities in molten $\text{AlCl}_3\text{-NaCl}_{\text{sat}}$ (4).

Sodium fluorochloroaluminate melts are interesting media because the electrochemistry and spectroscopy of solutes can be examined over a large temperature range (from 200°C to 800°C or higher). The attack of pyrex and quartz cells by these melts is much smaller than that by alkali fluoride melts(5). The cathodic limit of the fluorochloroaluminate melts is found to occur at more negative potentials than that of sodium chloroaluminate melts at high temperatures. Although the $\text{NaAlCl}_4\text{-NaF}$ (90-10 mol%) system becomes completely molten only at 395°C(6), the liquid phase, which is saturated with NaCl, is a useful solvent at temperatures as low as 200°C. In this paper, we describe the electrochemical studies of tantalum(V) in the fluorochloroaluminate melts at 200 - 450°C.

$\text{AlCl}_3\text{-NaCl}_{\text{sat}}$ melts were prepared from purified aluminum chloride and vacuum dried sodium chloride. Any remaining base metal impurities in the melts were removed by adding aluminum metal (ASAR, 99.999%) in the process of preparing the melts. Sodium fluorochloroaluminate melts were prepared by mixing CCl_4 -treated $\text{AlCl}_3\text{-NaCl}_{\text{sat}}$ salts with high purity sodium fluoride (ASAR, puratronic, 99.99%) in a suitable ratio, followed by premelting this mixture in a quartz tube. It is very important to eliminate small amounts of oxide species in the melts since the presence of the oxide species will complicate the electrochemical behavior of Ta, Nb, and W in these melts(7-10). Oxide-free melts are easily obtained by treating the melts with carbon tetrachloride (11).

Several electrochemical techniques, including cyclic voltammetry, normal pulse voltammetry, square wave voltammetry and exhaustive electrolysis, were used to clarify the electrochemical behavior of tantalum species. *In situ* spectroscopic studies were also performed.

The results obtained from these various techniques show that the electrochemical reduction of tantalum(V) in the fluorochloroaluminate melts is critically dependent on the temperature. It is complicated by preceding and following chemical reactions. Fig. 1 shows typical net-current square wave voltammograms of tantalum(V) at a tungsten electrode at temperatures from 200°C to 450°C. Only one well-defined wave (Wave 1) is seen at 200°C. As the temperature was increased to 300°C or higher, a new wave (Wave 2) appeared; this wave became much better defined at temperatures higher than 350°C. This wave shifted to a more negative potential with temperature. Wave 3 was ill-defined at temperatures lower than 300°C; it became well-defined at higher temperatures. The third reduction wave for the reduction of tantalum (V) resulted in the formation of a tantalum cluster ($\text{Ta}_6\text{Cl}_{12}^{2+}$) in the temperature region of 200°C to 450°C. Metallic tantalum was also observed when the exhaustive electrolysis was performed at 450°C.

The details of the reduction process of tantalum(V) in this medium will be presented.

Acknowledgement

This work was supported by the Air Force Office of Scientific Research, Grant No. 88-0307.

References

- 1) J.H.von Barner, L.E. McCurry, C.A. Jørgensen, N.J. Bjerrum and G. Mamantov, *Inorg. Chem.*, **31**, 1034(1992).
- 2) R. Huglen, F.W. Poulsen, G. Mamantov and G.M. Begun, *Inorg. Chem.*, **19**, 2551(1979).
- 3) L.E. McCurry, Ph.D. Dissertation, University of Tennessee, 1978.
- 4) T.M. Laher, L.E. McCurry and G. Mamantov, *Anal. Chem.* **57**, 500(1985).
- 5) B. Gilbert, S.D. Williams and G. Mamantov, *Inorg. Chem.* **27**, 2359(1988).
- 6) N. Sato, K.D. Sienerth and G. Mamantov, unpublished results.
- 7) Ting, Ph.D. Dissertation, University of Tennessee, 1973.
- 8) H. Linga, Z. Stojek and R.A. Osteryoung, *J. Am. Chem. Soc.* **103**, 3754 (1981).
- 9) P.A. Barnard and C.L. Hussey, *J. Electrochem. Soc.*, **137**, 913(1990).
- 10) I. W. Sun, K. D. Sienerth and G. Mamantov, *J. Electrochem. Soc.*, **138**, 2825(1991).
- 11) G. S. Chen, I.W. Sun, K.D. Sienerth, A.G. Edwards and G. Mamantov, paper in preparation.

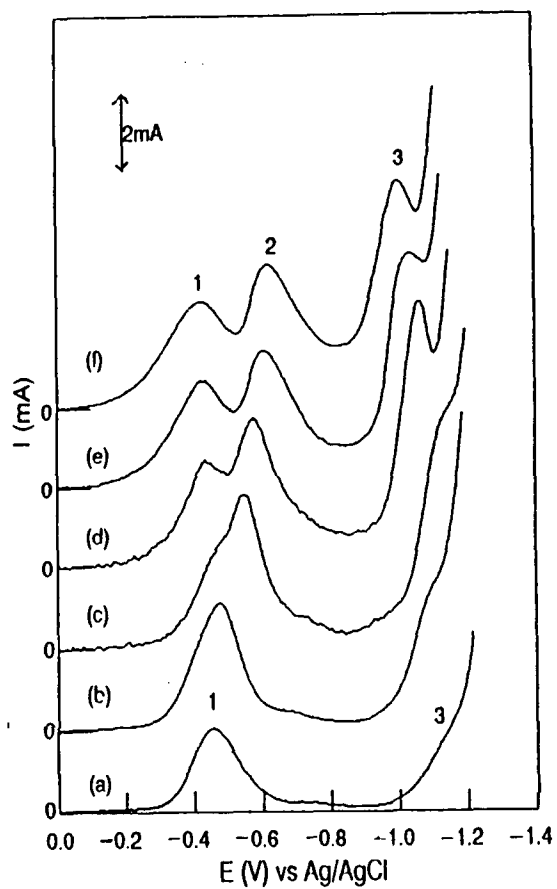


Fig.1 Net-current square wave voltammograms of tantalum(V) (37.6×10^{-3} mol/kg) in the NaAlCl_4 -NaF(90-10 mol%) melt at (a) 200°C, (b) 250°C, (c) 300°C, (d) 350°C, (e) 400°C and (f) 450°C. Tungsten electrode: 0.175 cm^2 ; step potential: 2 mV; pulse amplitude (E_{sw}): 25 mV; frequency: 10 Hz.

RECENT STUDIES OF THE ELECTROCHEMICAL
BEHAVIOR OF Nb(V) IN $\text{AlCl}_3\text{-NaCl}_{\text{SAT}}$
AND RELATED MELTS

K. D. Sienerth and G. Mamantov

Department of Chemistry
University of Tennessee
Knoxville, Tennessee 37996-1600

It is only fairly recently that the effect of oxide impurities on the electrochemical behavior of the refractory metals niobium and tantalum in molten halides has been realized. Polyakov and coworkers (1-3) found that the addition of oxide to alkali chloride-fluoride melts dramatically changes the voltammetric behavior observed in the reduction of both Nb(V) and Ta(V). Mamantov and coworkers (4) observed a wave due to the reduction of tantalum oxychloride in oxide-containing $\text{AlCl}_3\text{-NaCl}_{\text{sat}}$ melts; this wave had a peak potential approximately 0.2V more negative than that due to the reduction of tantalum chloride. Von Barner et al. (5) have recently reported on the electrochemical and spectroscopic studies of tantalum species in $\text{AlCl}_3\text{-NaCl}$ melts at 160-300°C. Evidence was presented for the formation of TaOCl_4^- in basic melts in the presence of small amounts of oxide ions (5). Hussey and coworkers (6-8) have published several papers on the effect of oxide on niobium and tantalum electrochemistry in the ambient temperature molten salt $\text{AlCl}_3\text{-1-methyl-3-ethylimidazolium chloride}$ ($\text{AlCl}_3\text{-MEIC}$).

Hussey and coworkers (6-8) have also reported on the use of phosgene to remove oxide from $\text{AlCl}_3\text{-MEIC}$. Our group has reported that this reagent is also effective in removing oxide from $\text{AlCl}_3\text{-NaCl}_{\text{sat}}$ (9). We have found recently that carbon tetrachloride undergoes a reaction with oxide in sodium chloroaluminate solutions resulting in the formation of CO_2 which is easily removed by evacuation (10).

The advent of effective methods for oxide removal from chloroaluminate melts has made it possible to study the electrochemical reduction of niobium and tantalum in these melts in the absence of interferences by oxide impurities.

Voltammetric studies of NbCl_5 in melts treated with CCl_4 or COCl_2 have revealed that previously reported results (11, 12), which had been interpreted in terms of the reduction of niobium chloride species, were in fact conducted in solutions quite high in oxide (≥ 50 mM). Figure 1 shows a cyclic voltammogram (CV) obtained for a solution of NbCl_5 in the $\text{AlCl}_3\text{-NaCl}_{\text{sat}}$ melt which had been treated with CCl_4 prior to use. The observed voltammetric response is different, especially with respect to the first wave, from that previously reported (11, 12). After an excess of oxide (in the form of Na_2CO_3) had been added to the solution, the CV (Figure 1) resembled that reported previously (12).

We have studied extensively the electrochemical behavior of Nb(V) in $\text{AlCl}_3\text{-NaCl}_{\text{sat}}$. It has been found that the initial reduction wave, which occurs at 0.12V vs. the Ag(I)/Ag reference electrode, is due to a one-electron reduction of Nb(V) to Nb(IV). The subsequent waves result in the further reduction of Nb(IV) to various

subvalent niobium chloride species. The stability of cluster species in this melt at temperatures below 200°C is probably the primary factor in the inability to obtain metallic deposits of the metal at low temperatures.

At increased temperatures, it has been possible to obtain deposits of niobium metal by constant current electrolysis. At temperatures higher than 500°C, smooth layers of niobium metal could be produced on tungsten and nickel cathodes, but the layers were very thin (probably less than 10 μm), and were coated with much thicker layers of insoluble niobium chloride cluster species.

It was anticipated that the addition of fluoride ions to the melt might serve to decrease the stability of the subvalent metal chloride species since fluoride-containing clusters are rare. However, even 10 mole percent of sodium fluoride in solution had no significant effect on the electrochemistry of Nb(V).

Acknowledgment

This research was supported by the Air Force Office of Scientific Research (Grant #88-0307).

References

1. V.I. Konstantinov, E.G. Polyakov and P.T. Stangrit, *Electrochim. Acta*, **23**, 713 (1979).
2. V.I. Konstantinov, E.G. Polyakov and P.T. Stangrit, *ibid.*, **26**, 445 (1981).
3. L.P. Polyakova, E.G. Polyakov, A.I. Sorokin and P.T. Stangrit, *J. Appl. Electrochem.*, **22**, 628 (1992).
4. T.M. Laher, L.E. McCurry and G. Mamantov, *Anal. Chem.*, **57**, 500 (1985).
5. J.H. von Barner, L.E. McCurry, C.A. Jørgensen, N.J. Bjerrum and G. Mamantov, *Inorg. Chem.*, **31**, 1034 (1992).
6. I-W. Sun, E.H. Ward and C.L. Hussey, *Inorg. Chem.*, **26**, 4309 (1987).
7. I-W. Sun and C.L. Hussey, *Inorg. Chem.*, **28**, 2731 (1989).
8. P.A. Barnard and C.L. Hussey, *J. Electrochem. Soc.*, **137**, 913 (1990).
9. I-W. Sun, K.D. Sienerth and G. Mamantov, *J. Electrochem. Soc.*, **138**, 2850 (1991).
10. G.S. Chen, I-W. Sun, K.D. Sienerth, A.G. Edwards, and G. Mamantov, paper in preparation.
11. G. Ting, Ph.D. Dissertation, University of Tennessee, Knoxville (1973).
12. G. Ting, K.W. Fung and G. Mamantov, *J. Electrochem. Soc.*, **123**, 624 (1976).

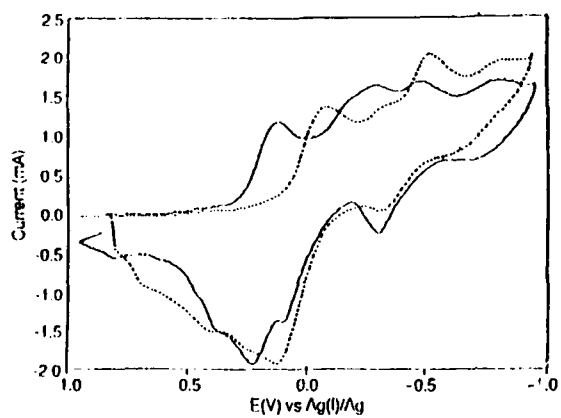


Fig.1 Cyclic voltammograms of Nb(V) obtained in $\text{AlCl}_3\text{-NaCl}$, using a tungsten wire (0.24 cm^2) working electrode. The Nb(V) concentration: $1.88 \times 10^{-2} \text{ M}$; temperature: 178°C , scan rate: 0.20 V/s .

- a. (—) Obtained in a melt treated with CCl_4 (no oxide).
- b. (---) Obtained in a melt containing excess oxide, added as Na_2CO_3 .

ELECTROCHEMICAL INVESTIGATIONS
IN BASIC ALKALI CHLOROALUMINATE MELTS

A Thesis
Presented for the
Master of Science
Degree
The University of Tennessee, Knoxville

Chaolan Hu

August 1991

ABSTRACT

Alkali chloroaluminate melts, such as the $\text{AlCl}_3/\text{NaCl}$ melt, have drawn considerable interest as aprotic media for chemical, electrochemical and various spectroscopic studies. These melts are characterized by relatively low melting points, large decomposition potentials, and a wide optical transparency range. The acid-base properties of these melts can be varied over a wide range by changing the melt composition.

The utility of ultramicroelectrodes for electrochemical studies in $\text{AlCl}_3/\text{NaCl}_{\text{sat}}$ melts has been demonstrated by using iron(III) chloride as a probe system. Cyclic voltammetric and normal pulse voltammetric results obtained at a tungsten disk ultramicroelectrode were compared to the results obtained at a conventional tungsten disk electrode. Several improvements resulting from the use of ultramicroelectrodes with respect to conventional electrodes were observed in this research.

The electrochemical and spectroscopic studies of $[\text{Bu}_4\text{N}]_2[\text{Re}_2\text{Cl}_8]$ and $\text{K}_2[\text{ReCl}_6]$ in the $\text{AlCl}_3/\text{NaCl}_{\text{sat}}$ melt are also reported in this thesis. UV-visible absorption spectroscopic studies reveal that $[\text{Re}_2\text{Cl}_8]^{2-}$ and $[\text{ReCl}_6]^{2-}$ are stable in the $\text{AlCl}_3/\text{NaCl}_{\text{sat}}$ melt. Cyclic voltammetry (CV), normal pulse voltammetry (NPV), and controlled potential electrolysis were used to study the reduction of these species. Cyclic voltammograms and normal pulse voltammograms exhibit two

reduction waves. The first reduction peak of $[\text{Re}_2\text{Cl}_8]^{2-}$ involves an EC mechanism in which $[\text{Re}_2\text{Cl}_8]^{2-}$ is first reduced to $[\text{Re}_2\text{Cl}_8]^{3-}$. The species $[\text{Re}_2\text{Cl}_8]^{3-}$ is not stable in this melt and is converted to some unknown species. Electrochemical and spectroscopic results suggest that the initial reduction of $[\text{ReCl}_6]^{2-}$ involves an ECEC mechanism in which $[\text{ReCl}_6]^{2-}$ is first reduced to $[\text{ReCl}_6]^{3-}$. This species is unstable in the melt and dimerizes to give $[\text{Re}_2\text{Cl}_8]^{2-}$, which has a reduction potential more positive than that of $[\text{ReCl}_6]^{2-}$, and therefore is immediately reduced to $[\text{Re}_2\text{Cl}_8]^{3-}$ which is converted to some unknown species. Finally, the addition of Re_3Cl_9 to the $\text{AlCl}_3/\text{NaCl}_{\text{sat}}$ melt produced $[\text{ReCl}_6]^{2-}$ and an unknown solid.

Journal of Organometallic Chemistry, 429 (1992) 119–134
Elsevier Sequoia S.A., Lausanne
JOM 22424

Spectroscopic investigations of catalytic iridium carbonyl species in sodium chloroaluminate melts

Louis J. Tortorelli ^a, Paul A. Flowers ^a, Brisco L. Harward ^a, Gleb Mamantov ^a
and Leon N. Klatt ^b

^a *Department of Chemistry, University of Tennessee, Knoxville, TN 37996-1600 (USA)*

^b *Analytical Chemistry Division, Oak Ridge National Laboratory, Oak Ridge, TN 37831-6142 (USA)*

(Received May 28, 1991)

Abstract

In situ spectroscopic studies of the iridium chemistry occurring during the catalytic hydrogenation of carbon monoxide employing $\text{IrCl}(\text{CO})_3$ and $\text{Ir}_4(\text{CO})_{12}$ in an aluminum chloride-sodium chloride (63:37 mole%) melt were performed. Infrared, UV-visible, Raman, and ^1H NMR data indicate that similar monomeric species are generated during catalysis. Infrared investigation of the introduction of $\text{IrCl}(\text{CO})_3$ into molten $\text{AlCl}_3:\text{NaCl}$ (63:37) under $\text{CO}:\text{H}_2$ (1:3 mole ratio) and the reaction between $\text{IrCl}(\text{CO})_3$ and carbon monoxide in an acidic melt suggest the initial formation of an iridium-carbonyl species followed by the generation of a hydridocarbonyl complex in the initial stage of the catalysis. Infrared data also indicate that the method of introduction for $\text{Ir}_4(\text{CO})_{12}$ into the $\text{AlCl}_3:\text{NaCl}$ medium under 1 atm of $\text{CO}:\text{H}_2$ (1:3 mole ratio) has a marked effect on the spectra observed. In an acidic melt $\text{IrCl}(\text{CO})_3$ reacts with hydrogen to form hydrogen chloride, methane and metallic iridium.

Introduction

The threat of low oil and natural gas reserves in the early 1970's initiated extensive investigations of hydrocarbon production via the reduction of carbon monoxide by hydrogen, i.e. the Fischer-Tropsch reaction. The Fischer-Tropsch process traditionally involves the use of heterogeneous catalysts [1–4] and yields straight-chain hydrocarbons along with alkenes and oxygenated compounds as primary products.

Interest in homogeneous Fischer-Tropsch catalysis has been stimulated in part by the potential for increased product selectivity [5,6] and milder reaction conditions [7]. For example, Thomas *et al.* [7] have observed the reduction of carbon monoxide to methane utilizing $\text{Os}_3(\text{CO})_{12}$ and $\text{Ir}_4(\text{CO})_{12}$ as the homogeneous catalyst precursors in organic solvents at 140°C and approximately 2 atm of

Correspondence to: Dr. G. Mamantov, Department of Chemistry, University of Tennessee, Knoxville, TN 37996-1600, USA.

pressure; unfortunately, slow reaction rates were observed. The authors also noted that "classic" mononuclear complexes, under identical reaction conditions, were catalytically inactive. Hydrogenation of carbon monoxide using soluble mononuclear complexes as catalysts has been demonstrated [8,9], but temperatures above 200°C and pressures between 200 and 1300 atm were required, and only oxygenated products were produced.

Investigations of chemical systems in molten salt media often show that the solvent plays an active role in the solute chemistry. This is frequently the case for chloroaluminate melts (mixtures of aluminum chloride with other chloride salts) where the Lewis acidity may be adjusted by varying the aluminum chloride concentration [10]. Chloroaluminate melts are termed acidic, neutral, or basic if the mole ratio of aluminum chloride to companion salt is greater than, equal to, or less than one, respectively.

Demitras and Muetterties [11] first reported on the catalytic activity of $\text{Ir}_3(\text{CO})_{12}$ under $\text{CO}:\text{H}_2$ (1–2 atm) in an acidic sodium chloroaluminate melt (160–180°C). In a subsequent study, Muetterties and coworkers [12] performed a more detailed analysis of this system, including infrared analysis of frozen catalyst-melt reaction mixtures obtained in Nujol mulls. For reaction times in excess of one hour, bands were observed at 2190, 2160, 2125, 2112, and 1630 cm^{-1} for the resultant iridium carbonyl species. Without the $\text{CO}:\text{H}_2$ fill gas, $\text{Ir}_4(\text{CO})_{12}$ decomposed as evidenced by the disappearance of all bands in the carbonyl stretching region.

Collman *et al.* [13] conducted a kinetic study of the same catalytic system under flow and recycle conditions, and also demonstrated that $\text{IrCl}(\text{CO})_3$ is active as a catalyst precursor. Different product distributions from those of Muetterties and coworkers [11,12] were obtained in this work, and it was concluded that a different active catalyst was produced. Although no spectra were shown, it was stated that a multiband pattern was observed in the 2000–2200 cm^{-1} region.

The major difference between the procedures employed by the two groups was the method of introduction of $\text{Ir}_4(\text{CO})_{12}$ into the melt. Muetterties and coworkers premixed the iridium complex with the frozen melt before heating (pre-melt addition), whereas Collman *et al.* added the iridium complex to the melt at 175°C (post-melt addition).

There are two interesting and potentially advantageous traits of this chloroaluminate melt-based catalytic system, namely (1) the melt apparently serves as a promoter allowing carbon monoxide reduction to occur at relatively low pressures and temperatures, and (2) oxygenated products are not generated. Presented herein are the results of *in situ* spectroscopic studies of molten sodium chloroaluminate solutions of $\text{IrCl}(\text{CO})_3$ and $\text{Ir}_4(\text{CO})_{12}$ under various atmospheres conducted with the hope of identifying the catalytically active species present in this chemical system. A preliminary account of this work has appeared in the Proceedings of a Symposium [14].

Experimental

Reagents. Dodecacarbonyltetrairidium, $\text{Ir}_4(\text{CO})_{12}$, and chlorotricarbonyliridium(I), $[\text{IrCl}(\text{CO})_3]_n$, were purchased from Strem Chemicals Inc. and used without further purification. Prepurified nitrogen (99.998%, MG Scientific Gases), high-

purity carbon monoxide (99.8%, Air Products), hydrogen (99.9%, Air Products), and deuterium (99% Linde Specialty Gases) were used as received. Tetramethylammonium bromide (TMAB) was obtained from Fluka Chemical and recrystallized from methanol three times. Anhydrous aluminum chloride (> 99%, Fluka Chemical) was purified by an extraction/distillation procedure similar to one described previously [15]. Sodium chloride (reagent grade, Mallinckrodt, Inc.) was vacuum-dried at 400°C for four days before use. The sodium chloroaluminate melts were prepared by fusing the appropriate quantities of aluminum chloride and sodium chloride in an evacuated sealed pyrex ampule at 175°C.

Instrumentation. Infrared spectra were acquired with a Digilab FTS-20E Fourier transform infrared spectrometer (Bio-Rad, Digilab Division) operating at an instrumental resolution of 4 cm⁻¹. The IR cell employed for all *in situ* measurements has been described previously [16]. Gas-phase IR spectra were obtained in a vacuum-tight cell equipped with KBr windows. Raman spectra were acquired using a Jobin-Yvon Ramanor 2000M spectrometer equipped with an Instruments S.A. Inc. Model 980015 controller and a Pacific Model 126 photometer. The argon-ion laser line at 514.5 nm from a Spectra Physics Model 171 laser was used to illuminate the sample. UV-visible spectra were recorded with a rapid-scanning spectrometer (RSS) system [17]. Raman and UV-visible cells were constructed from Pyrex and quartz according to previously reported designs [18]. Proton nuclear magnetic resonance spectra were recorded on JEOL FX90Q spectrometer operating at 89.55 MHz with tetramethylammonium bromide (TMAB) as the internal reference set to 3.21 ppm. All NMR spectra were obtained with the spectrometer operating on external lock. X-Ray photoelectron spectra were acquired with the Perkin-Elmer PHI 5100 ESCA System.

Procedure. Due to the moisture and air sensitivity of aluminum chloride, all manipulations involving melts were performed in a Vacuum Atmospheres glove box (moisture level < 2 ppm) with prepurified nitrogen as the filler gas. Reagent gases were added to the sample cells either prior to melting via a vacuum manifold (the pressure was measured at this point) or afterwards from a sealed Pyrex tube equipped with a break seal. Likewise, the iridium carbonyls were introduced to the chloroaluminate salts either prior to melting by simply mixing the two solids or afterwards by means of a FLICKET valve assembly (Ace Glass, Inc.).

Results

Spectra under nitrogen. A solution of IrCl(CO)₃ in a 63 mole percent (m/o) AlCl₃ melt at 175°C under 1 atm of nitrogen results in a clear yellow solution whose infrared spectrum exhibits the bands listed in Table 1. In a 49 m/o melt a significantly different infrared spectrum was observed; the observed bands are also listed in Table 1.

Previous investigations [12,13] have shown that Ir₄(CO)₁₂ is unstable in acidic sodium chloroaluminate melts in the absence of a significant pressure (> 0.1 atm) of carbon monoxide; under these conditions the cluster decarbonylates as evidenced by carbon monoxide evolution and precipitation of iridium metal [11].

For comparison purposes, the relevant infrared bands of IrCl(CO)₃ and Ir₄(CO)₁₂ in KBr pellets and of pure IrCl(CO)₃ studied by diffuse reflectance are also listed in Tables 1 and 2, respectively.

Table 1

CO stretching frequencies obtained from the IR spectra of $\text{IrCl}(\text{CO})_3$

$\text{IrCl}(\text{CO})_3$	$\nu(\text{CO}), \text{cm}^{-1}$ ^a
Pure solid (spectrum obtained by diffuse reflectance)	2143(m), 2132(s), 2100(s), 2090(s), 2050(s), 2025(m)
KBr	2143(m), 2132(s), 2100(s), 2090(s), 2059(s), 2024(m)
$\text{AlCl}_3:\text{NaCl}$ (63:37)- N_2	2178(m), 2168(w), 2143(m), 2125(s), 2107(m), 2085(w)
$\text{AlCl}_3:\text{NaCl}$ (49:51)- N_2	2170(w), 2153(w), 2126(w), 2087(s), 1985(s)
$\text{AlCl}_3:\text{NaCl}$ (63:37)-CO	2125(s)
$\text{AlCl}_3:\text{NaCl}$ (63:37)-CO: H_2 (pre-melt addition)	2230(w), 2187(m), 2157(s), 2125(m)
$\text{AlCl}_3:\text{NaCl}$ (63:37)-CO: D_2 (pre-melt addition)	2187(m), 2176(sh), 2157(s), 2125(m)
$\text{AlCl}_3:\text{NaCl}$ (63:37)-CO: H_2 (post-melt addition) $t = 0 \text{ h}$	2187(vw), 2178(vw), 2157(vw), 2168(vw), 2125(s), 2085(vw)
$\text{AlCl}_3:\text{NaCl}$ (63:37)- H_2	2125, 2107 (decay) 2178, 2168, 2157, 2143 (growth-decay) 2075(w), 2041(w) (growth)

^a s = strong, m = medium, w = weak, sh = shoulder.

Spectra under carbon monoxide. Infrared spectra of $\text{IrCl}(\text{CO})_3$ in a 63 m/o melt under 1 atm of carbon monoxide at 150°C exhibit a single intense band at 2125 cm^{-1} . The intensity of this band remained constant over the 24 h period examined, indicating the presence of a stable iridium species. The infrared spectrum of $\text{IrCl}(\text{CO})_3$ in a 49 m/o melt under 1 atm carbon monoxide was similar to that obtained under nitrogen.

The initial infrared spectrum of $\text{Ir}_4(\text{CO})_{12}$ in a 63 m/o melt under 1 atm of carbon monoxide at 150°C exhibited bands at the frequencies listed in Table 2. After 3–4 h, the band at 2143 cm^{-1} disappeared and the intensity of the band at 2125 cm^{-1} increased. There were no differences in the infrared spectra obtained if the solution was stirred manually or if it was quiescent.

Solutions of $\text{IrCl}(\text{CO})_3$ and $\text{Ir}_4(\text{CO})_{12}$ in a 63 m/o melt under 1 atm of carbon monoxide at 150°C yielded similar UV-visible spectra with maxima at 278, 326, and 430 nm. The intensity of these bands increased with time; however, the rate of growth was slower for $\text{Ir}_4(\text{CO})_{12}$. After 10 h the ratio of the molar absorptivities of these bands for the solutions of the cluster and the monomer was 4:1, indicating that the iridium cluster reacted to form a mononuclear complex. The rate of this

Table 2
CO stretching frequencies obtained from the IR spectra of $\text{Ir}_3(\text{CO})_{12}$

$\text{Ir}_3(\text{CO})_{12}$	$\nu(\text{CO}), \text{cm}^{-1}$		
KBr	2112(w), 2090(wsh), 2056(s), 2023(m), 2006(wsh)		
$\text{AlCl}_3:\text{NaCl}$ (63:37)-CO, $t = 0$ h	2157(w), 2143(s), 2125(m), 2107(sh), 2083(w)		
$\text{AlCl}_3:\text{NaCl}$ (63:37)-CO, $t = 4$ h	2156(w), 2125(s), 2110(sh), 2083(w)		
$\text{AlCl}_3:\text{NaCl}$ (63:37)-CO: H_2 (Pre-melt addition)	$t = 1$ h	$t = 10$ h	$t = 24$ h
	2187(m)	2187(m)	2187(w) 2178(s) 2168(sh) 2157(m) 2143(s) 2132(m)
	2157(s)	2157(s)	
	2125(m)	2125(m) 2114(m)	
	2107(m) 2085(w)	2107(sh)	2107(w)
		1656(w)	1656(m)
$\text{AlCl}_3:\text{NaCl-CO:D}_2$ (63:37) (Pre-melt addition)	$t = 1$ h	$t = 10$ h	$t = 24$ h
			2182(s)
	2176(w)	2178(m) 2168(vw)	2168(w)
	2157(m)	2157(s)	
			2143(s)
	2125(s)	2131(s)	2125(m)
	2107(s)	2107(m)	2107(m)
	2085(m)		
		1639(w)	1639(m)
$\text{AlCl}_3:\text{NaCl-(63:37)}$ CO: H_2 , $t = 0$ h (Post-melt addition)	2164(sh), 2157(w), 2140(s), 2134(s), 2125(s), 2105(m), 2085(sh), 2043(vw)		
$\text{AlCl}_3:\text{NaCl-(63:37)}$ CO: H_2 , $t = 4$ h (Post-melt addition)	2187(sh), 2180(m), 2170(sh), 2154(m) 2143(m), 2125(s), 2107(s), 2085(m), 2043(w)		
$\text{AlCl}_3:\text{NaCl-(63:37)}$ CO: H_2 , $t = 9$ h (Post-melt addition)	2230(w), 2187(m), 2157(s), 2125(m)		

" s = strong, m = medium, w = weak, vw = very weak, sh = shoulder.

conversion was shown to follow first-order kinetics. An average rate constant of $1.32 \pm 0.26 \times 10^{-4} \text{ s}^{-1}$ was calculated from the data obtained using the three UV-visible bands.

Raman spectra of $\text{Ir}_3(\text{CO})_{12}$ in a 63 m/o melt (post-melt addition) under 1 atm carbon monoxide at 150°C exhibited a weak band at 202 cm^{-1} , which disappeared within one hour after introduction of the cluster to the melt. This band is within the region expected for a metal-metal stretch [19], and its dependence upon the

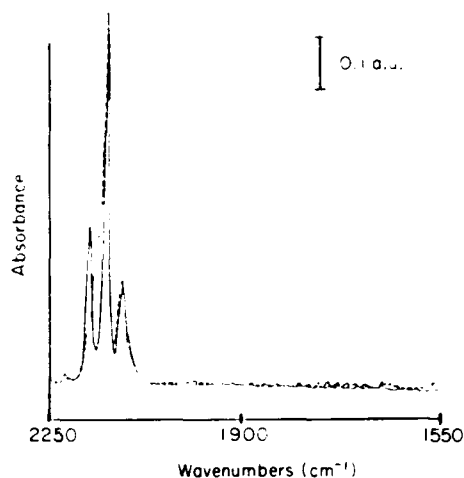


Fig. 1. Infrared spectra of $\text{IrCl}(\text{CO})_3$ in 63 m/o AlCl_3 melts under 1 atm of $\text{CO}:\text{H}_2$ (solid curve) and $\text{CO}:\text{D}_2$ (dashed curve); $[\text{IrCl}(\text{CO})_3] = 8 \text{ m.M.}$ 175°C. Mole ratio of $\text{CO}_{\text{gas}}:\text{IrCl}(\text{CO})_3 > 4.$

polarization state of the exciting radiation suggests that it is a symmetric vibration. Under identical conditions, this band was not observed with $\text{IrCl}(\text{CO})_3$.

Spectra under carbon monoxide:hydrogen. A solution of $\text{IrCl}(\text{CO})_3$ (pre-melt addition) in a 63 m/o melt under 1 atm $\text{CO}:\text{H}_2$ (1:3 mole ratio) was clear and yellow in color. The infrared spectrum, shown in Fig. 1, exhibited bands at the frequencies listed in Table 1. The intensities of these infrared bands were essentially constant over the 24 h period examined. This behavior was also observed upon addition of $\text{CO}:\text{H}_2$ to a solution containing $\text{IrCl}(\text{CO})_3$ initially under a carbon monoxide atmosphere.

The infrared spectrum observed immediately after the addition of $\text{IrCl}(\text{CO})_3$ (post-melt addition) to a 63 m/o melt under 1 atm of $\text{CO}:\text{H}_2$ at 170°C exhibited the bands listed in Table 1. Between 2.5 and 6 h the intensity of the band at 2125 cm^{-1} decreased while the intensity of the bands at 2187 and 2157 cm^{-1} increased. After 6 h the intensities of these bands remained essentially constant. Five days later the intensity of the 2125 cm^{-1} band decreased while the 2187 and 2157 cm^{-1} bands increased.

A solution of $\text{Ir}_3(\text{CO})_{12}$ (pre-melt addition) in a 63 m/o melt under 1 atm of $\text{CO}:\text{H}_2$ (1:3 mole ratio) at 175°C is clear and yellow in color. The infrared spectrum of a 2 m.M solution, shown in Fig. 2, exhibited bands, listed in Table 2, whose relative intensities changed over the course of a 24 h period, indicating the presence of several iridium carbonyl species of different stabilities. About 1 h after melting, bands were observed at 2187 , 2157 , 2125 , 2107 and 2085 cm^{-1} . At 10 h the intensities of the 2187 and 2157 cm^{-1} bands increased considerably relative to the other bands while the intensities of the 2107 and 2085 cm^{-1} bands decreased; a very weak band was observed at 1656 cm^{-1} . After 24 h the intensities of the 2187 and 2157 cm^{-1} bands started to decrease, the 1656 cm^{-1} band grew substantially, and new and intense features were observed at 2178 and 2143 cm^{-1} .

The dynamic behavior of $\text{Ir}_3(\text{CO})_{12}$ is illustrated in Fig. 3, which shows the variation in the observed absorbance for several of the prominent spectral features

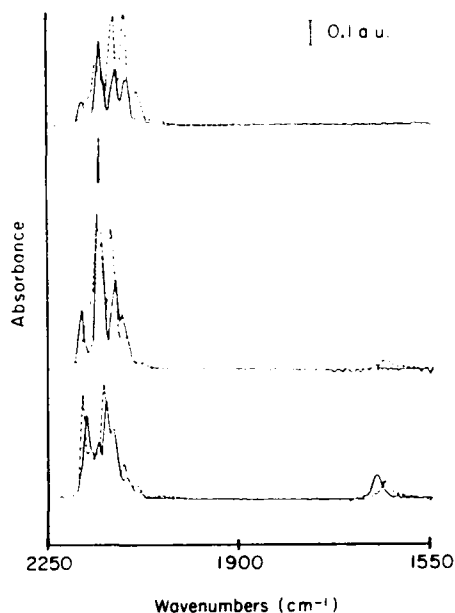


Fig. 2. Infrared spectra of $\text{Ir}_3(\text{CO})_{12}$ in 63 m/o AlCl_3 melts (pre-melt addition) under 1 atm of $\text{CO}:\text{H}_2$ (solid curve) and $\text{CO}:\text{D}_2$ (dashed curve) obtained *ca.* 1 h (upper), 10 h (middle), and 24 h (lower) after melting; $[\text{Ir}_3(\text{CO})_{12}] = 2 \text{ mM}$, 175°C .

as a function of time. Essentially three different responses are observed, *i.e.*, decay (2125, 2107 and 2085 cm^{-1} bands), growth (2178, 2143, and 1656 cm^{-1} bands), and growth followed by decay (2187 and 2157 cm^{-1} bands). For an 8 mM solution of $\text{Ir}_3(\text{CO})_{12}$ the intensities of the 2125, 2107 and 2085 cm^{-1} bands steadily increased until reaching a maximum value at about 18 h; the 1656 cm^{-1} band appeared only as a weak transient feature, disappearing entirely by the end of the 24 h period examined.

When $\text{Ir}_3(\text{CO})_{12}$ is added to a 63 m/o melt at 170°C (post-melt addition) under 1 atm of $\text{CO}:\text{H}_2$ (1:3 mole ratio), different dynamics of the infrared spectral features were observed. The bands observed as a function of time are listed in Table 2. After about 9 h, bands at 2230, 2187, 2157 and 2125 cm^{-1} were observed. The last spectrum, taken after 41 hours, was very similar to the spectrum shown in Fig. 1.

An interesting result from the infrared studies was the observed growth of melt oxide bands [20], *i.e.*, solvated AlOCl , at 791 and 691 cm^{-1} as a function of time. Figure 4 shows the increase in absorbance for the 791 cm^{-1} band for the solutions containing $\text{IrCl}(\text{CO})_3$ and $\text{Ir}_3(\text{CO})_{12}$. These results support previous reports [12,13] that the melt serves as an oxide "sink" during the course of the reaction, consuming any intermediate oxygenated products (including water) via reaction with AlCl_3 . Figure 4 also points to a slower rate of catalysis exhibited by the monomer relative to the cluster species; this behavior has been previously reported [13].

In the UV-visible spectral region solutions of $\text{IrCl}(\text{CO})_3$ in 63 m/o melt under 1 atm of $\text{CO}:\text{H}_2$ exhibited absorption maxima at 272, 322, 406, and 430 nm, which

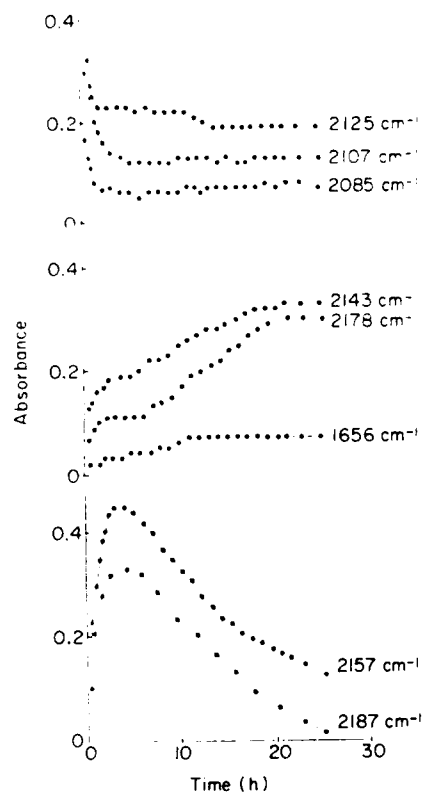


Fig. 3. Plots of absorbance versus time after melting for several prominent features from the spectra for the CO:H₂ system shown in Fig. 2.

increased in intensity as a function of time. The short wavelength region (< 250 nm) was characterized by a rapidly increasing absorption. The position and relative intensities of the bands at 272, 322, and 430 nm were very similar to the spectrum

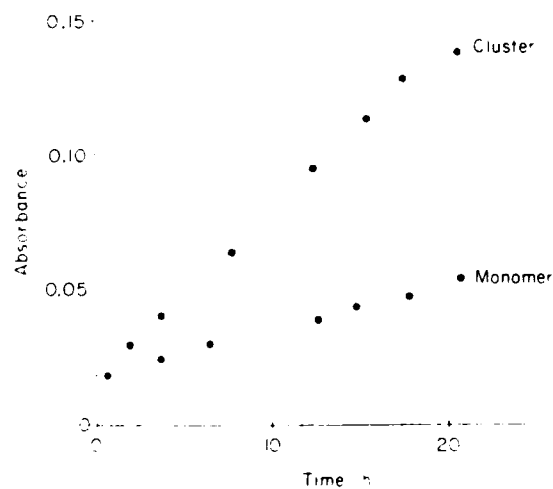


Fig. 4. Plots of absorbance at 791 cm⁻¹ versus time after melting for 2 mM Ir₃(CO)₁₂ (upper curve) and 8 mM IrCl(CO)₃ (lower curve) in 63 m² AlCl₃ melts under 1 atm CO:H₂.

obtained under carbon monoxide. Under identical conditions, similar results were obtained for solutions of $\text{Ir}_3(\text{CO})_{12}$.

The Raman spectrum of $\text{Ir}_4(\text{CO})_{12}$ in 63 m/o melt (post-melt addition) under 1 atm of $\text{CO}:\text{H}_2$ (1:3 mole ratio) at 150°C showed the same weak, transient band at 202 cm^{-1} as was observed under a carbon monoxide atmosphere. Again, this band was absent from the spectrum of $\text{IrCl}(\text{CO})_3$ under identical conditions.

^1H NMR spectra of $\text{IrCl}(\text{CO})_3$ (pre-melt addition) in a 63 m/o melt under 1 atm of $\text{CO}:\text{H}_2$ (1:3 mole ratio) at 130°C exhibited one major peak at -10.7 ppm vs. TMAB (internal reference, 3.21 ppm vs. TMS [21]) over the 36 h time period examined: this feature was observed immediately after melting. Two much weaker proton resonances at -19.5 (0.9% the intensity of the peak at -10.7 ppm) and $+5.4$ ppm (1.3% the intensity of the peak at -10.7 ppm) appeared about 2 h after melting. No significant change in the intensity of these resonances was observed throughout the experiment.

^1H NMR spectra of $\text{Ir}_4(\text{CO})_{12}$ in a 63 m/o melt (pre-melt addition) under 1 atm of $\text{CO}:\text{H}_2$ at 130°C exhibited a major resonance at -10.7 ppm, which appeared roughly 1.5 h after melting and remained throughout the 24 h period the reaction was monitored. Weaker proton resonances were observed at -19.5 and $+1.4$ ppm. The peak at $+1.4$ ppm, first observed about 3 h after melting, was initially flanked by two other resonances at $+0.9$ and $+0.3$ ppm which disappeared after 4 h. The relative intensities of the two weaker features at -19.5 and $+1.4$ ppm increased roughly twofold during the 24 h reaction period. Toward the end of the experiment a proton resonance appeared at $+5.3$ ppm (28% the intensity of the peak at -10.7 ppm). When the ^1H NMR spectra of $\text{Ir}_4(\text{CO})_{12}$ were acquired with TMAB as an external reference, an additional peak at $+3.6$ ppm was observed about 5 h after melting. Spectral interference from the TMAB prevented the observation of this resonance when TMAB was used as an internal reference. During the course of the experiment, the intensity of the resonance at $+3.6$ ppm increased while the intensity of the major resonance at -10.7 ppm decreased.

A ^1H NMR spectrum of a 63 m/o AlCl_3 melt under hydrogen chloride atmosphere at 130°C exhibited a proton resonance at $+1.6$ ppm.

Spectra under carbon monoxide: deuterium. As the catalytically active species in Fischer-Tropsch systems are frequently hydridocarbonyl complexes, the experiments performed under $\text{CO}:\text{H}_2$ were repeated under $\text{CO}:\text{D}_2$. Such isotopic substitution has long been employed in the study of transition metal hydridocarbonyl species [22].

A solution of $\text{IrCl}(\text{CO})_3$ (pre-melt addition) under 1 atm of $\text{CO}:\text{D}_2$ (1:3 mole ratio) yielded an infrared spectrum which remained unchanged for the 24 h period examined (see Table 1 and Fig. 1). A solution of $\text{Ir}_4(\text{CO})_{12}$ under similar conditions exhibited transient behavior similar to that observed under $\text{CO}:\text{H}_2$ (see Table 2 and Fig. 2). Frequency shifts relative to the hydrogen systems were observed for some of the carbonyl bands in each of the mixtures, suggesting that the species produced under the employed conditions are hydrido- (or deuterido-) carbonyls. Such frequency shifts are a result of resonance interaction between the C-O and Ir-H vibrational states.

Reaction of $\text{IrCl}(\text{CO})_3$ with hydrogen. The reaction of $\text{IrCl}(\text{CO})_3$ with hydrogen in a 63 m/o melt at 175°C was also studied. After introduction of hydrogen to a solution initially under nitrogen, the infrared spectra exhibited a decay of bands at

2125 and 2107 cm^{-1} , growth followed by the decay of bands at 2178, 2168, and 2143 cm^{-1} , appearance of two weak bands at 2075 and 2041 cm^{-1} , and a new band at 2157 cm^{-1} which appeared upon introduction of the hydrogen and then totally decayed. The infrared spectra also revealed the growth of melt oxide bands at 691 and 791 cm^{-1} as the reaction proceeded. During the course of the reaction, the solution changed color from a clear, bright yellow to cloudy gray. Upon termination of the reaction, denoted by the formation of the cloudy gray solution, a bright silvery substance formed on the glass walls of the reaction vessel. X-Ray photoelectron spectroscopic analysis revealed this precipitate to be metallic iridium. Infrared analysis of the gas phase above the reaction mixture showed the presence of hydrogen chloride and methane.

Discussion

Spectra under nitrogen. The increase in the carbonyl stretching frequencies observed for $\text{IrCl}(\text{CO})_3$ in an $\text{AlCl}_3:\text{NaCl}$ melt under a nitrogen atmosphere relative to those observed for the pure solid or in KBr (see Table 1) indicates a reduction in the amount of electron density at the iridium metal center. This reduced electron density results in decreased back-bonding between the iridium and the π^* orbitals of the carbonyl ligand, hence a stronger C–O bond and a higher stretching frequency. This reduction in electron density at the metal center could result from an increase in the oxidation state of iridium and/or the formation of a Lewis acid adduct with aluminum chloride. Adduct formation could occur at the chloride ligand, the oxygen atoms of the carbonyl ligands, or the iridium atom itself [23]. Adducts in which the aluminum atom of aluminum chloride coordinates directly to the metal center of a carbonyl complex typically result in increases of 65–125 cm^{-1} in the carbonyl stretching frequencies, while adducts involving coordination through the chloride ligand generally show increases of about 20 cm^{-1} [23,24]. A Lewis-acid adduct in which the aluminum chloride coordinates to the oxygen atom of a terminal carbonyl ligand has been discarded as a possibility in this case since such adducts exhibit decreases in the stretching frequencies of the complexed carbonyl ligand [23,25].

Thus, the infrared results suggest the formation of a solvated species, $\text{IrCl}(\text{CO})_3\text{L}_n$ ($\text{L} = \text{AlCl}_3$), in acidic melts under a nitrogen atmosphere.

Spectra under carbon monoxide. As noted earlier, $\text{Ir}_4(\text{CO})_{12}$ decomposes to iridium metal in an acidic sodium chloroaluminate melt under an inert atmosphere; however, under a carbon monoxide atmosphere, soluble iridium complexes are generated. Infrared spectra of both the cluster and the monomer in acidic melts under carbon monoxide exhibit a strong terminal carbonyl band at 2125 cm^{-1} , suggesting that the same complex is generated from both precursors. This contention is also supported by the UV-visible spectroscopic data. The additional features observed in the infrared spectra of the cluster suggest the formation of at least one other iridium carbonyl complex. The delay in the appearance of the three bands in the UV-visible spectra and in the single major feature in the infrared spectra exhibited by the cluster system indicates that $\text{Ir}_4(\text{CO})_{12}$ is experiencing an additional reaction in the melt before generating the final product *i.e.*, fragmentation to a mononuclear complex. Such a reaction is supported by the observed 4 : 1

ratio of the molar absorptivities for $\text{Ir}_4(\text{CO})_{12}$ vs. $\text{IrCl}(\text{CO})_3$ obtained from the UV-visible measurements and the transient band at 202 cm^{-1} in the Raman spectrum of the cluster under carbon monoxide.

Possible structures for an iridium-carbonyl complex that exhibits one carbonyl stretching frequency in its infrared spectrum are $\text{Ir}(\text{CO})_6^{3+}$, $\text{trans-Ir}(\text{CO})_4\text{L}_2^-$ ($\text{L} = \text{AlCl}_3$), $\text{Ir}(\text{CO})_4$, $\text{Ir}(\text{CO})_3\text{L}_2$ (trigonal bipyramid), and $\text{trans-Ir}(\text{CO})_2\text{X}_2\text{L}_2$ [26,27a]. The most likely structure for the iridium complex generated under carbon monoxide, given the spectroscopic data above, is $\text{trans-Ir}(\text{CO})_4\text{L}_2^-$. It is worth noting that Ru^{I} and Ir^{I} square planar complexes form similar adducts with boron Lewis acids [27b]. All of the possible iridium-carbonyl complexes containing three or fewer carbonyl ligands are ruled out since such a species should have been generated in the acidic melt under nitrogen. The possibility of forming either $\text{Ir}(\text{CO})_6^{3+}$ or $\text{Ir}(\text{CO})_4^-$ is likewise discounted since these species would require that the iridium atom undergo a two-electron oxidation or reduction, respectively. Also, the carbonyl stretching frequency for $\text{Ir}(\text{CO})_4^-$, reported at 1895 cm^{-1} [28], would be expected to occur at a frequency lower than 2125 cm^{-1} even if a Lewis acid adduct was formed with the solvent. The role of aluminum chloride in the above reaction is evident from the data obtained from an identical reaction performed in a sodium chloride saturated melt. As mentioned in the Results section, no reaction was observed when carbon monoxide was added to a basic melt solution containing $\text{IrCl}(\text{CO})_3$ originally under a nitrogen atmosphere.

Spectra under $\text{CO}:\text{H}_2$, D_2 . In a previous report by Collman *et al.* [13], it was stated that a similar iridium complex is generated from the $\text{IrCl}(\text{CO})_3$ and $\text{Ir}_4(\text{CO})_{12}$ precursors in the chloroaluminate Fischer-Tropsch system. This has been further substantiated by *in situ* IR, NMR and UV-visible spectroscopy in this work; however, the greater number of peaks observed in the IR (pre-melt addition) and NMR spectra for the cluster relative to the monomer indicate that additional iridium complexes are generated in the cluster system. These additional iridium complexes are generated upon melting when $\text{Ir}_4(\text{CO})_{12}$ is premixed with the frozen melt.

The experiments involving the introduction of $\text{IrCl}(\text{CO})_3$ to an acidic melt at 170°C under $\text{CO}:\text{H}_2$ suggest that the carbonyl bands located at 2187, 2157, and 2125 cm^{-1} may be attributed to two different complexes. One complex is responsible for the band at 2125 cm^{-1} , which is generated from the reaction between $\text{IrCl}(\text{CO})_3$ and carbon monoxide and is the same complex formed under a carbon monoxide atmosphere in the melt. This complex then reacts with hydrogen to generate a complex that exhibits carbonyl bands at 2187 and 2157 cm^{-1} .

When $\text{Ir}_4(\text{CO})_{12}$ is introduced into the melt at 170°C , it appears that a reaction occurs between the cluster and carbon monoxide and/or hydrogen. This interaction could be responsible for the stoichiometric amount of methane generated in the initial segment of the reaction as observed by Collman *et al.* [13]. The eventual formation of the iridium complexes that give rise to infrared bands at 2187, 2157, and 2125 cm^{-1} supports the claim by Collman *et al.* [13] that similar iridium complexes are generated in the Fischer-Tropsch reaction.

The reaction mixtures under $\text{CO}:\text{H}_2$ or $\text{CO}:\text{D}_2$ which utilize $\text{Ir}_4(\text{CO})_{12}$ as the catalyst precursor (pre-melt addition) represent complex and dynamic chemical systems as shown by previous reports [12,13] and the data presented here. Based on the observed time dependent responses, at least four different iridium carbonyl

species (one for each type of response) appear to be produced under these conditions (see Fig. 3). For at least two of these species, frequency shifts are observed upon substituting deuterium for hydrogen in the fill gas mixtures, indicating that the complexes produced contain hydride (or deuteride) ligands. In a hydridocarbonyl complex, resonance interaction between the $\nu(\text{CO})$ and $\nu(\text{IrH})$ vibrational levels may occur if these states are of similar energy and symmetry [29].

The species initially produced from the oxidative fragmentation of $\text{Ir}_4(\text{CO})_{12}$ which decays with time exhibited infrared bands at 2125, 2107, and 2085 cm^{-1} under both $\text{CO}:\text{H}_2$ and $\text{CO}:\text{D}_2$ gas mixtures (these bands were observed as constant spectral features for solutions of the cluster under carbon monoxide). This complex, termed species **A**, apparently does not contain a hydride (or deuteride) ligand.

Another species, termed **B**, which is also produced from $\text{Ir}_4(\text{CO})_{12}$ under $\text{CO}:\text{H}_2$ and then decays during the 24 h period, gave strong bands at 2187 and 2157 cm^{-1} ; under $\text{CO}:\text{D}_2$, this complex exhibited bands at 2176 and 2157 cm^{-1} .

Species produced from $\text{Ir}_4(\text{CO})_{12}$ under $\text{CO}:\text{H}_2$ which are gradually generated over the 24 h period examined give rise to bands at 2178, 2143, and 1656 cm^{-1} ; under $\text{CO}:\text{D}_2$, these species exhibit bands at 2182, 2143, and 1639 cm^{-1} . The curves presented in Fig. 3 suggest that two different carbonyl complexes are produced, one species **C**₁, represented by the two higher frequency bands and the other, species **C**₂, by the low frequency band (*i.e.*, at 10 h, the intensity of the 1656 cm^{-1} feature had stabilized; both 2178 and 2143 cm^{-1} bands increased continually over the 24 h period). Since no bands were observed to shift from the 1900–2200 cm^{-1} region to the 1300–1600 cm^{-1} region upon substituting deuterium for hydrogen [29], no Ir–H or Ir–D bands could be assigned. Failure to observe metal hydride or deuteride infrared bands is a fairly common occurrence [29,30]. The shifts in the carbonyl stretching frequencies upon deuteration, however, offer indirect evidence that the species do contain hydride (or deuteride) ligands. More direct evidence for the existence of hydridocarbonyl species is obtained from the ¹H NMR spectra (see below). The low-frequency IR bands at 1656 and 1639 cm^{-1} exhibited by $\text{Ir}_4(\text{CO})_{12}$ under $\text{CO}:\text{H}_2$ and $\text{CO}:\text{D}_2$, respectively, suggest that a polynuclear iridium complex is formed since carbonyl frequencies in this region are characteristic of bridging carbonyl-Lewis acid adducts [31]. The shift which occurs upon deuteration in this case is a result of resonance interaction between the $\nu(\text{IrD})$ and the bridging $\nu(\text{CO})$ levels. Although no bands were observed in the C–H stretching region (2800–3200 cm^{-1}), the possibility that these low frequency (*ca.* 1650 cm^{-1}) features are due to carbonyl stretching of a formyl group produced by insertion of carbon monoxide between the metal and a hydride (or deuteride) ligand cannot be excluded [13].

The major spectral changes resulting from deuterium substitution in the $\text{IrCl}(\text{CO})_3$ system were the decrease in relative intensity of the highest frequency band at 2187 cm^{-1} and the appearance of a shoulder on the 2157 cm^{-1} band at about 2176 cm^{-1} (Fig. 1). This may likewise be interpreted as a shift of one of two closely placed features around 2187 to 2176 cm^{-1} ; this is the same behavior as observed for the cluster system at 10 h (pre-melt addition). The presence of additional bands observed for the cluster system (*e.g.*, at 2114 cm^{-1}), indicates the formation of additional carbonyl species upon melting when the cluster is pre-mixed with the frozen melt.

The infrared spectra of $\text{Ir}_4(\text{CO})_{12}$ solutions (pre-melt addition) under $\text{CO}:\text{H}_2$ and $\text{CO}:\text{D}_2$ at long reaction times have several features in common with the spectrum of $\text{IrCl}(\text{CO})_3$ under nitrogen. Although the spectra for the cluster system contain additional bands (e.g., the bridging carbonyl features), there appears to be a significant spectral contribution from a species similar to that which results from the monomer under nitrogen, most noticeably at 2143 cm^{-1} . This may reflect production of this species from other hydride (or deuteride) complexes as the fill gas is depleted during the course of the reaction. Based on the results of experiments in which $\text{CO}:\text{H}_2$ was added to solutions initially under nitrogen, it appears that regeneration of the alleged catalyst may be accomplished by simply replenishing the fill gas. In cases where carbon monoxide is the limiting reagent, however, it seems likely that the excess hydrogen will react with the monomeric iridium carbonyl complex in the manner observed for solutions of $\text{IrCl}(\text{CO})_3$ under hydrogen, generating methane, hydrogen chloride, and metallic iridium.

By comparison (pre-melt addition experiments), the reaction mixture utilizing $\text{IrCl}(\text{CO})_3$ as the catalyst precursor resulted in a much simpler system containing an iridium carbonyl species which was relatively stable over the 24 h period examined. The greater stability of the monomer relative to the cluster system may be due to the relatively higher pressures of reactant gases present in the former system throughout the time period examined. The $\text{CO}:\text{H}_2$ or $\text{CO}:\text{D}_2$ pressure is expected to be greater at any given time during the reaction for the monomer system because (a) $\text{Ir}_4(\text{CO})_{12}$ rapidly consumes a stoichiometric amount of reactants (*i.e.*, carbon monoxide and hydrogen or deuterium) as it decomposes at the onset of the reaction, and (b) the reaction rate for the $\text{IrCl}(\text{CO})_3$ system is about 20% slower than that of the cluster [13]. Thus after 24 h, the cluster system has depleted the fill gas pressure to levels where the catalytic iridium species become unstable; the monomer system, however, has consumed less of the fill gas at this point and is still in the "steady state" regime of reactant concentration. This behavior is illustrated in Fig. 4; the cluster system clearly exhibits a more rapid rate of reaction.

The indirect evidence for the generation of an iridium-hydride complex obtained from the infrared studies is substantiated by the ^1H NMR data. The proton resonance at -10.7 ppm observed in the ^1H NMR spectra of the monomer and cluster suggests that both iridium precursors generate a similar complex in the acidic melt under $\text{CO}:\text{H}_2$, possibly $\text{HIr}(\text{CO})_3(\text{AlCl}_3)_2$. The presence of other proton resonances observed for the cluster precursor likewise supports the contention that other hydrogen-containing iridium species are generated (the peak observed at $+1.6$ ppm for a sample of pure melt under a hydrogen chloride atmosphere precludes assignment of any observed proton resonances to dissolved hydrogen chloride). These other major proton resonances observed in the ^1H NMR spectra for $\text{Ir}_4(\text{CO})_{12}$ are a result of the additional iridium complexes generated when $\text{Ir}_4(\text{CO})_{12}$ is premixed with the frozen melt. The other proton resonances may be a result of formyl- or alkyl-Ir protons.

It has been noted that the transient characteristics of infrared spectra for an 8 mM solution of $\text{Ir}_4(\text{CO})_{12}$ under $\text{CO}:\text{H}_2$ differed from those of a 2 mM solution. This observation suggests that different species (or different relative concentrations of two or more species) are produced from different initial concentrations of $\text{Ir}_4(\text{CO})_{12}$. This behavior together with the different results obtained depending on

the method of addition of the iridium complex into the melt is consistent with the observed discrepancies between the works of Collman *et al.* [13] and Muetterties and coworkers [11,12], in which the initial cluster concentrations were about 2 (post-melt addition) and 8 mM (pre-melt addition), respectively, and supports the assertion [13] that different catalytic species were produced by the two groups.

Conclusion

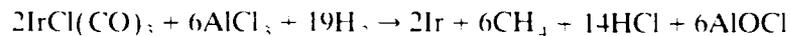
The spectroscopic data reported here show that both iridium complexes generate the same active catalyst when added to the melt and that the method of introduction to the melt has a profound effect on the infrared spectra obtained for the cluster system. As indicated in the Discussion section, the following reaction scheme for $\text{Ir}_4(\text{CO})_{12}$ in the presence of carbon monoxide and hydrogen in the acidic melt (pre-melt addition) is proposed.

- (a) Rapid oxidative fragmentation of $\text{Ir}_4(\text{CO})_{12}$ to yield a complex that has infrared bands at 2125, 2107, and 2085 cm^{-1} (species **A**).
- (b) Production and then depletion of a complex with infrared bands at 2187 and 2157 cm^{-1} (species **B**) from species **A**.
- (c) Gradual production of two complexes, one with infrared bands at 2178 and 2143 cm^{-1} (species C_1) and the other with a band at 1656 cm^{-1} (species C_2) from species **B**.

By comparison to analogous studies [32], it seems likely that species **B** represents the catalytically active species in this medium. As the reaction proceeds and the fill gas is depleted, this species becomes unstable and is converted to different complexes, species C_1 and C_2 . Based upon the observed frequency shifts accompanying deuterium substitution, it appears that species **B**, C_1 , and C_2 are all hydridocarbonyl complexes.

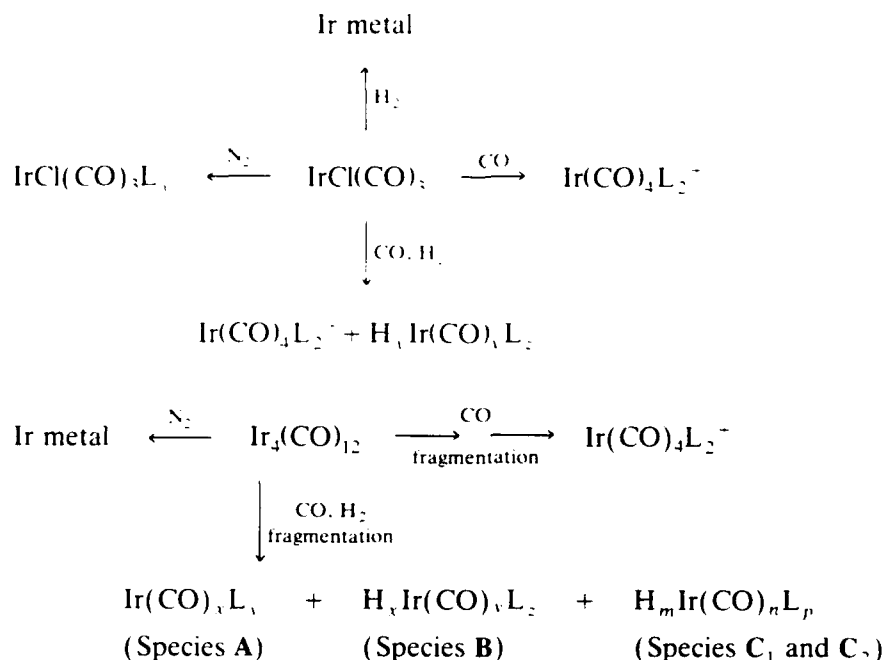
It is clear that the $\text{Ir}_4(\text{CO})_{12}$ precursor, in the premixed experiments, generates other iridium complexes in addition to those produced from $\text{IrCl}(\text{CO})_3$. It also appears that these additional species may exhibit catalytic activity and may be responsible for the discrepancies in the product distribution observed by Muetterties [11] and Collman [13].

The proposed reaction between $\text{IrCl}(\text{CO})_3$ and hydrogen in the acidic melt is:



This reaction presumably is the fate of the iridium carbonyl catalyst at the end of the reaction carried out in the presence of excess hydrogen. When performed under an excess of carbon monoxide, the iridium-carbonyl complex that gives rise to the infrared band at 2125 cm^{-1} is generated at the end of the process. This complex can then regenerate the catalyst when the synthesis gas is reintroduced into the system.

The proposed reaction schemes for the "post-melt addition" for both $\text{IrCl}(\text{CO})_3$ and $\text{Ir}_4(\text{CO})_{12}$ in an acidic melt under different atmospheres are given below ($\text{L} = \text{AlCl}_3$):



Unambiguous identification of the active catalyst in this system would have been greatly aided if the far infrared region ($< 600 \text{ cm}^{-1}$) had been accessible. Unfortunately, strong solvent absorptions in this region prevented observation of the iridium–ligand vibrations. An attempt was made to use a shorter path length cell which brought the solvent absorptions on scale, but such a short path length prevented observations of the relatively weak metal–ligand bands. Many attempts at isolation of the iridium complexes from the melt were unsuccessful (*e.g.*, distillation and extraction) and indicated these species to be stable only under the employed reaction conditions.

Finally, it should be noted that Collman *et al.* have pointed out the limited technological importance of a catalytic process which consumes aluminum chloride [13]. Nonetheless, the chloroaluminate-based system described herein represents a unique example of the homogeneous Fischer–Tropsch reaction which may serve as a model for more practical catalytic systems. Such systems may include the regeneration of anhydrous aluminum chloride from aluminum oxychloride and related species [33,34].

Acknowledgements

This work was supported in part by Grants 85-08321 and 88-0307 from the Air Force Office of Scientific Research and in part by the U.S. Department of Energy, Office of Energy Research, under contract DE-AC05-84OR21400 with Martin Marietta Energy Systems, Inc. B.L. Harward acknowledges support from the Laboratory Graduate Participation Program administered by the Oak Ridge Associated Universities for the U.S. Department of Energy. The authors acknowledge D. Trimble for obtaining the Raman spectra, and helpful discussions with G.P. Smith, C.E. Barnes, R.M. Pagni, and C. Woods. We are grateful to a reviewer for helpful suggestions for the interpretation of some of the results.

References

- 1 P. Sabatier and J.B. Senderens, C.R. Acad. Sci., 134 (1902) 514.
- 2 H.H. Storch, N. Golumbic and R.B. Anderson, Fischer Tropsch and Related Synthesis, Wiley, New York, 1951.
- 3 (a) C.M. Bartish and G.M. Drissel, Kirk-Othmer Encl. Technol., Wiley, New York, Vol. 4, 3rd ed., 1978, p. 778; (b) G.A. Mills and J.A. Cusumano, *ibid.*, Vol. 5, 3rd ed., 1978, p. 45.
- 4 G. Henrici-Olive and S. Olive, Angew. Chem., Int. Ed., Engl. 15 (1976) 136.
- 5 G.N. Schrauzer (ed.), Transition Metals in Homogeneous Catalysis, Marcel Dekker, New York, 1971.
- 6 J.S. Bradley, J. Am. Chem. Soc., 101 (1979) 7419.
- 7 M.G. Thomas, B.F. Beier and E.L. Muetterties, J. Am. Chem. Soc., 98 (1976) 1296.
- 8 J.W. Rathke and H.M. Feder, J. Am. Chem. Soc., 100 (1978) 3623.
- 9 B.D. Dombek, J. Am. Chem. Soc., 103 (1981) 6508.
- 10 G. Mamantov and R.A. Osteryoung, in G. Mamantov (Ed.), Characterization of Solutes in Nonaqueous Solvents, Plenum Press, New York, 1978.
- 11 G.C. Demitras and E.L. Muetterties, J. Am. Chem. Soc., 99 (1977) 2796.
- 12 H-K. Wang, H.W. Choi and E.L. Muetterties, Inorg. Chem., 20 (1981) 2661.
- 13 J.P. Collman, J.I. Brauman, G. Tustin and G.S. Wann III, J. Am. Chem. Soc., 105 (1983) 3913.
- 14 G. Mamantov, L.J. Tortorelli, P.A. Flowers, B.L. Harward, D.S. Trimble, E.M. Hondrogiannis, J.E. Coffield, A.G. Edwards and L.N. Klatt, in C.L. Hussey, S.N. Flengas, J.S. Wilkes and Y. Ito (Eds.), Proceedings of the Seventh International Symposium on Molten Salts, The Electrochemical Society, Inc., Pennington, NJ, 1990, pp. 794-804.
- 15 R. Marassi, J.Q. Chambers and G. Mamantov, J. Electroanal. Chem., 69 (1976) 345.
- 16 P.A. Flowers and G. Mamantov, Anal. Chem., 61 (1989) 190.
- 17 L.N. Klatt, J. Chromatogr. Sci., 17 (1979) 225.
- 18 V.E. Norvell, G. Mamantov, in D.G. Lovering and R.J. Gale (Eds.), Molten Salt Techniques, Vol. 1, Plenum Press, New York, 1983, Chap. 7.
- 19 F.A. Cotton and R.A. Walton, Multiple Bonds Between Metal Atoms, John Wiley & Sons, New York, 1982, Chap. 8.
- 20 P.A. Flowers and G. Mamantov, Anal. Chem., 59 (1987) 1062.
- 21 Nuclear Magnetic Resonance Spectra, Sadtler Research Laboratories, Inc., Philadelphia, PA, (1966) 6820M.
- 22 H.D. Kesz and R.B. Saillant, Chem. Rev., 72 (1972) 231.
- 23 B.V. Lokshin, E.B. Rusach, Z.P. Valueva, A.G. Ginzburg and N.E. Kolobova, J. Organomet. Chem., 102 (1975) 535.
- 24 K.D. Karlin, B.F.G. Johnson and J. Lewis, J. Organomet. Chem., 160 (1978) C21; B.F.G. Johnson, K.D. Karlin and J. Lewis, *ibid.*, 174 (1979) C29.
- 25 S.B. Butts, S.H. Strauss, E.M. Holt, R.E. Stimson, N.W. Alcock and D.F. Shriver, J. Am. Chem. Soc., 102 (1980) 5093.
- 26 C.M. Lukehart, Fundamental Transition Metal Organometallic Chemistry, Brooks / Cole, Monterey, CA, 1985, p. 80.
- 27 (a) F.A. Cotton and G. Wilkinson, Advanced Inorganic Chemistry: A Comprehensive Text, 5th ed., John Wiley & Sons, New York, 1988, pp. 901-917; (b) D.F. Shriver, Accounts Chem. Res., 3 (1970) 231.
- 28 J.L. Vidal and W.E. Walker, Inorg. Chem., 20 (1981) 249.
- 29 G.I. Geotroy and J.R. Lehman, Adv. Inorg. Chem. Radiochem., 20 (1977) 190.
- 30 M.Y. Darenbourg and C.E. Ash, Adv. Organomet. Chem., 27 (1987) 1.
- 31 (a) A. Alch, N.J. Nelson, D. Strobe and D.F. Shriver, Inorg. Chem., 11 (1972) 2976; (b) J.S. Kristoff, D.F. Shriver, *ibid.*, 13 (1974) 499.
- 32 R. Whyman, J. Organomet. Chem., 94 (1975) 303.
- 33 (a) C.B. Mamantov, T.M. Laher, R.P. Walton and G. Mamantov, in H.O. Bohner (Ed.), Light Metals 1985, The Metallurgical Society of AIME, 1985, pp. 519-528; (b) G. Mamantov and C.B. Mamantov, U.S. Patent 4, 493, 784, January 15, 1985.
- 34 J.W. Sun, K.D. Stenrath and G. Mamantov, J. Electrochem. Soc., 138 (1991) 2850.

ELECTROCHEMICAL STUDIES OF CALCIUM CHLORIDE-BASED
MOLTEN SALT SYSTEMS

A Thesis
Presented for the
Master of Science Degree
The University of Tennessee, Knoxville

Thomas P. Blanchard, Jr.

December 1992

ABSTRACT

Conductance and EMF studies of CaCl_2 -based melts were performed in the temperature range $790^\circ\text{C} - 990^\circ\text{C}$. Conductivity data collected using magnesia tubes and capillaries showed deviations from the data recommended by the National Bureau of Standards. These deviations are attributed to the slow dissolution of magnesia by the CaCl_2 - CaO melt. Conductivity data for molten CaCl_2 using a pyrolytic boron nitride capillary were in reasonable agreement with the recommended data; however, undissolved CaO in CaCl_2 may have caused blockage of the pyrolytic boron nitride capillary, resulting in fluctuations in the measured resistance. The utility of the AgCl/Ag reference electrode in CaCl_2 - AgCl and CaCl_2 - CaO - AgCl melts, using asbestos diaphragms and Vycor glass as reference half-cell membranes, was also investigated. Nernstian behavior was observed using both types of reference half-cell membranes in CaCl_2 - AgCl melts. The AgCl/Ag reference electrode also exhibited Nernstian behavior in CaCl_2 - CaO - AgCl melts using a Vycor reference half-cell membrane and a magnesia crucible.



First Observation of Electrochemiluminescence in Molten Salt Solutions

G. Mamantov,* K. D. Sienerth,** C. W. Lee, and J. E. Coffield

Department of Chemistry, University of Tennessee, Knoxville, Tennessee 37996-1600

S. D. Williams

Department of Chemistry, Appalachian State University, Boone, North Carolina 28608

ABSTRACT

The electrochemical oxidation and reduction of perylene in a neutral aluminum chloride—1,2-dimethyl-3-propyl-1H-imidazolium chloride (DMPIC) melt results in the formation of radical cations and anions of perylene at or near the electrode. An annihilation reaction between the radical ions of perylene, produced consecutively, results in electrochemiluminescence.

We have recently reported on the electrochemical reduction of perylene (PE) dissolved in mixtures of aluminum chloride and 1-ethyl-3-methyl-1H-imidazolium chloride (EMIC) as well as 1,2-dimethyl-3-propyl-1H-imidazolium chloride (DMPIC) (1). In basic AlCl_3 -EMIC melt (<50 mol% AlCl_3), both the radical anion and dianion of PE are produced at -1.83 and -2.17 V vs. Al(III)/Al in a 2:1 AlCl_3 -EMIC melt. The oxidation of PE cannot be observed in a basic melt because it is obscured by the oxidation of Cl^- ions present in large excess. The oxidation of PE was studied in the acidic AlCl_3 -EMIC (67 mol% AlCl_3) melt by Zingg (2, 3), who observed a single oxidation wave at a glassy carbon (GC) electrode at 0.83 V. Zingg concluded from coulometric and UV-visible spectrophotometric measurements that a precipitate consisting of both oxidized and unoxidized PE was formed on the electrode. The formation of the radical cation and the dication of PE in molten SbCl_5 was previously reported by Sorlie *et al.* (4). In the present study a neutral AlCl_3 -DMPIC melt was used to provide the maximum potential window (5, 6) in order to observe both the reduction and the oxidation of PE in the same melt. Electrochemiluminescence (ECL) has been observed for perylene in organic solvents, and includes a long wavelength component that has been attributed to perylene decomposition products (7) or perylene excimers (8).

Experimental

Preparation and purification of materials.—Salts and melts were prepared as reported elsewhere (9, 10). Electrochemical studies were conducted under nitrogen in a Vacuum Atmospheres drybox; the water level was below 2 ppm. Some ECL studies were conducted outside the drybox using a cell prepared from a 1 cm quartz cuvette and sealed with Teflon tape. Perylene (Aldrich Gold Label, 99%) was recrystallized from 100% ethanol. Spectroscopic and electrochemical measurements were carried out at ambient temperature.

Electrodes.—For the electrochemical studies, the reference electrode was an aluminum wire in a 2:1 AlCl_3 :DMPIC melt separated from the bulk by a fine Pyrex frit. The counter electrode was a tungsten coil in the same melt as the bulk, separated by a coarse Pyrex frit. The working electrode was either a tungsten wire or a glassy carbon disk or rod. For ECL measurements the reference electrode was an aluminum wire, the counter electrode a tungsten coil, and the working electrode was a platinum wire grid. These electrodes were in contact with the bulk solution.

Apparatus.—A PAR 175 Universal programmer linked to a PAR Model 175 Polarographic Analyzer and a Houston Instruments Omnigraphic 2000 X-Y recorder were used for cyclic voltammetric studies and ECL studies. The ECL spectrum was measured with an Instruments SA Ramanor 2000 spectrometer equipped with a cooled photomultiplier tube (PMT), a photon counting photometer, and an IBM PS/2 Model 50 interface. The spectrometer response was calibrated by a method similar to that described by Stair, *et al.* (11). The ECL spectrum has

been corrected for the wavelength dependence of the spectrometer response.

Results and Discussion

Cyclic voltammograms of the melt were featureless, with cathodic and anodic limits of approximately -2.50 and 2.30 V, respectively. The background current was lower than that reported by Gifford and Palmissano (5).

Electrochemical reduction of PE.—Voltammograms obtained with a 7.2 mM PE solution at tungsten and glassy carbon electrodes exhibited two reduction peaks at -1.83 and -2.30 V, which is consistent with the results of Coffield, *et al.* (1), for the reduction of PE to the radical anion and dianion, respectively.

Electrochemical oxidation of PE.—Cyclic voltammetry of the 7.2 mM PE solution at tungsten exhibited two oxidation waves with peak potentials at 0.90 and 1.67 V (Fig. 1). The behavior demonstrated in Fig. 1 is consistent with that observed by Zingg (2, 3), in the acidic AlCl_3 -EMIC melt; the first oxidation wave is attributed to the deposition of a film partially consisting of oxidized PE. Upon reversal of the potential sweep after the first wave, a stripping wave was observed. Sweeping to a more positive potential resulted in the voltammogram shown in Fig. 1. The second oxidation wave appeared to be totally irreversible, and further study will be required to determine the processes involved.

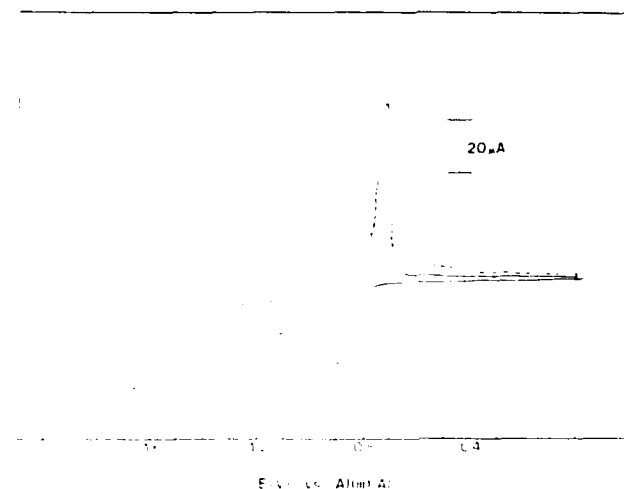


Fig. 1. Cyclic voltammograms at a tungsten wire electrode of a 7.2 mM solution of PE in neutral AlCl_3 -DMPIC at ambient temperature: (a, —) potential sweep reversed after the first oxidation wave, and (b, —) after the second wave. The peak potentials are reported vs. Al(III)/Al in a 2:1 AlCl_3 -DMPIC melt. The sweep rate is 0.10 V/s.

* Electrochemical Society Active Member
** Electrochemical Society Student Member

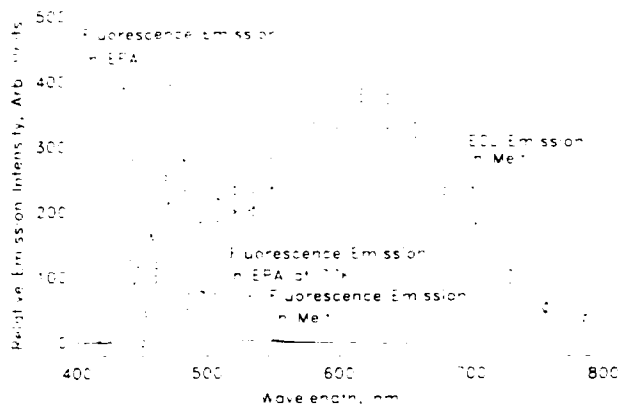


Fig. 2. Fluorescence and ECL emission spectra of perylene. ECL spectrum is for a 7 mM solution in neutral AlCl_3 -DMPIC melt at room temperature. Fluorescence spectra are for a 0.03 mM solution in EPA (mixture of ethyl ether, isopentane, and ethanol) at room temperature, and as a frozen glass at 77K; and a 0.005 mM solution in AlCl_3 -DMPIC melt at room temperature. From the photon count rate and spectrometer design it may be estimated that the ECL produces not more than about 3×10^4 photons $\text{s}^{-1} \text{nm}^{-1}$ in the direction of observation.

Electrochemiluminescence studies.—The annihilation reaction between electrochemically generated PE radical ions was studied by programming the potentiostat to continuously pulse between 50 mV negative of the first reduction peak and 50 mV positive of the first oxidation peak. The working electrode was observed during these cycles. Its surface was darkened during the oxidation half-cycle, and was restored to a clean appearance during the reduction half-cycle. Light emission was observed at the working electrode surface; light pulses were in synchronization with the potential pulses. The initial experiments used a square wave program with 2 s at each potential. The emission appeared to be brighter with a glassy carbon rod rather than with a tungsten wire; this may be due to its larger surface area. The emission was still more intense with a platinum gauze working electrode. The intensity of the emission appeared to decrease as the pulse rate was increased.

The ECL spectrum of a 7 mM PE solution was measured by focusing the image of the platinum gauze electrode on the entrance slit of the spectrometer, opening the slits (10 nm band-pass), and operating the photometer at 1000 cps full scale. The laboratory was darkened during the measurements. Since the working electrode was discolored during the oxidation (as was noted by Werner *et al.* (7)), an asymmetric pulse sequence was used to clean the electrode by holding it at a reducing potential for a longer period than for the oxidation. Under these conditions, the photometer registered brief pulses of light that varied in intensity by about 30%. Light pulses were not detected when the PMT shutter was closed, nor was light observed with a 3 mM PE solution. Nine pulses were averaged and integrated to give the emission intensity at each wavelength. The intensity of the ECL emission decreased as the spectrum was measured; this was compensated for by measuring the intensity at one wavelength several times during the experiment. The resulting spectrum is shown in Fig. 2. This figure also shows the fluorescence spectrum of PE in an organic solvent, at room temperature and as a frozen glass, and in the melt. Comparison with the ECL spectrum shows that the ECL spectrum includes the fluorescence spectrum (strongly attenuated by self-absorption in the rather concentrated solution), as well as a long wavelength component. These results are consistent with PE ECL measurements in conventional solvents (7, 8).

The PE ECL system described here may be energy deficient, the excited singlet energy is 2.77 eV (based on the O-O band in the melt fluorescence spectrum (13)) and the electrochemical energy input (12) is 2.73 ± 0.1 eV. Thus, the ECL may involve a

triplet intermediate (12), however, direct singlet excitation cannot be excluded. Feldberg (14) has suggested that in cases where both radical ions are in solution, the slope of an appropriate intensity versus time plot may indicate triplet intermediates. This is a plot of the log of the intensity vs. $(t_r/t_i)^2$, where, for our experiments, t_r is the duration of the reduction step and t_i is the time after oxidation begins. For reduction times varying from 1-10 s our data resulted in the value of -4 ± 2 for the average slope. This value is somewhat larger in magnitude than predicted for triplet intermediates (14), but is similar to that reported by Grabner and Brauer (8). The difference between the expected and measured slopes may be due to the formation of a film during oxidation in our experiments; this situation is not treated in the Feldberg model. Grabner and Brauer (8) concluded from such slopes that the ECL in conventional solvents involved triplet intermediates; in our solvent, the PE excited singlet energy is lower and we cannot rule out the possibility that direct singlet excitation occurs in the melt.

Conclusion

We have observed for the first time electrochemiluminescence in a molten salt solvent, that of perylene, in a neutral AlCl_3 -DMPIC melt. We have shown that in this melt perylene can be oxidized in two steps. Our results are consistent with ECL measurements for perylene in conventional solvents; the long wavelength component included in the ECL spectrum indicates that the emission is more complex than simple radiative relaxation of the PE singlet.

Acknowledgments

This research was supported by the University of Tennessee Science Alliance program and the Air Force Office of Scientific Research (Grant # 88-0307).

Manuscript submitted Dec. 2, 1991; revised manuscript received March 23, 1992.

The University of Tennessee assisted in meeting the publication costs of this letter.

REFERENCES

- J. E. Coffield, G. Mamantov, S. P. Zingg, G. P. Smith, and A. C. Buchanan, III, *This Journal*, **139**, 355 (1992).
- S. P. Zingg, private communication.
- J. E. Coffield, S. P. Zingg, K. D. Sienerth, S. Williams, C. Lee, G. Mamantov, and G. P. Smith, *Materials Science Forum*, **73-75**, 595 (1991).
- M. Sorlie, G. P. Smith, V. E. Norvell, G. Mamantov, and L. N. Klatt, *This Journal*, **128**, 333 (1981).
- P. R. Gifford and J. B. Palmissano, *ibid.*, **134**, 610 (1987).
- R. A. Osteryoung in "Molten Salt Chemistry," G. Mamantov and R. Marassi, Editors, p. 329, D. Reidel Publishing Company, Dordrecht (1986).
- T. C. Werner, J. Chang, and D. M. Hercules, *J. Amer. Chem. Soc.*, **92**, 5560 (1970).
- E. W. Grabner and E. Brauer, *Ber. Bunsen-Gesellschaft*, **76**, 111 (1972).
- R. Marassi, J. Q. Chambers, and G. Mamantov, *J. Electroanal. Chem. Interfacial Electrochem.*, **69**, 345 (1976).
- J. E. Coffield, G. Mamantov, S. P. Zingg, and G. P. Smith, *This Journal*, **138**, 2543 (1991).
- R. Stair, W. E. Schneider, and J. K. Jackson, *Applied Optics*, **2**, 1151 (1963).
- L. R. Faulkner and R. S. Glass, in "Chemical and Biological Generation of Excited States," W. Adam and G. Cilento, Editors, p. 191, Academic Press, New York (1982).
- The band head (O-O band) in the fluorescence of the frozen solution is within 1 nm of the maximum in the room temperature emission; assuming that the same behavior will occur in the melt, the melt O-O band will be at 447 nm (the maximum in the melt fluorescence). This gives an excited singlet energy of 2.77 eV.
- S. W. Feldberg, *J. Amer. Chem. Soc.*, **88**, 390 (1966). *J. Phys. Chem.*, **70**, 3928 (1966).